WAVE INDUCED OSCILLATIONS IN HARBORS: THE SOLUTION FOR A RECTANGULAR HARBOR CONNECTED TO THE OPEN-SEA

by

A. T. Ippen and Y. Goda

HYDRODYNAMICS LABORATORY

Report No. 59

Prepared Under

Contract No. Nonr-1841(59), NR-062-228
Office of Naval Research
U. S. Department of the Navy
Washington, D. C.

July, 1963

MIT

DEPARTMENT OF CIVIL ENGINEERING

SCHOOL OF ENGINEERING
MASSACHUSETTS INSTITUTE OF TECHNOLOGY
Cambridge 39, Massachusetts

R 63-36

HYDRODYNAMICS LABORATORY
Department of Civil Engineering
Massachusetts Institute of Technology

WAVE INDUCED OSCILLATIONS IN HARBORS: THE SOLUTION FOR A RECTANGULAR HARBOR CONNECTED TO THE OPEN-SEA

by

A. T. Ippen and Y. Goda

July 1963

Report No. 59

Prepared Under
Contract No. Nonr-1841(59), NR-062-228
Office of Naval Research
U. S. Department of the Navy
Washington, D. C.

ACKNOWLEDGEMENT

The work presented in this study was carried out at the Hydrodynamics Laboratory of the Department of Civil Engineering at the Massachusetts Institute of Technology. It was sponsored by the Office of Naval Research, U. S. Department of the Navy, under Contract Nonr - 1841(59). Administration of the contract was by the Division of Sponsored Research of the Massachusetts Institute of Technology under D.S.R. 8228.

The study was under the direction of Dr. Arthur T. Ippen, Professor of Hydraulics. Mr. Yoshimi Goda, carried out the analytical and experimental program. Mr. Qais N. Fattah gave assistance for the experimental study. The contribution to the initial phase of the analytical study by Dr. Louis N. Howard, Associate Professor of Mathematics, is deeply appreciated. An IBM 7090 digital computer was available for the numerical evaluation of most theoretical solutions through the M.I.T. Computation Center.

ABSTRACT

The determination of an amplification factor for a given harbor and a given wave period is an important problem concerning long period oscillations in harbors. The present study presents a means of computing the response of a rectangular harbor to the excitation by incident waves. With the aid of a digital computer, the complete response curve can be computed for any rectangular harbor. The results of experiments on model harbors have confirmed the validity of the computation. Experimental response curves, however, do not show the marked increase of the amplification factor at resonance with a narrowing of the harbor entrance, because of energy dissipation in a model harbor. The analysis of the response factor for waves with a continuous power spectrum also suggests that a narrowing of the entrance will lead to a reduction in the amplitude of long period oscillations in actual harbors, because of increasing sharpness of the response curves and the presence of energy dissipation mechanisms in harbors. Hence, the problem of the harbor paradox presented by Miles and Munk does not exist in actual harbors.

In addition to the above resonant characteristics, a study was conducted on the minimum effectiveness of wave absorbers and filters to simulate the open-sea conditions in a wave basin of finite dimensions. A reflection coefficient less than 0.2 is recommended for wave absorbers and filters. The importance of the basin size is also discussed.

TABLE OF CONTENTS

		Page
I.	INTRODUCTION	1
	1.1 Nature of the Problem	1
	1.2 Theoretical Aspects of the Problem	2
	1.3 Simulation of the Open-Sea Conditions for Model Experiments	4
II.	THEORY OF WAVE INDUCED OSCILLATION IN A RECTANGULAR HARBOR	5
	2.1 Solution of Wave Induced Oscillation in the Ideal Fluid	5
	2.1.1 Method of Analysis - Separation of Two Regions Outside and Inside the Harbor	5
	2.1.2 Wave Pattern Outside the Harbor	9
	2.1.3 Wave Pattern Inside the Harbor	11
	2.1.4 Evaluation of the Amplification Factor	15
	2.1.5 Some Characteristics of the Amplification Factor	19
	2.1.6 Resonant Characteristics of a Fully Open Harbor	21
	2.2 Effect of Energy Dissipation in Harbors on Resonant Characteristics	23
III.	EXPERIMENTAL EQUIPMENT AND PROCEDURES	30
	3.1 Adoption of Deep Water Waves for the Experimental Study	30
	3.2 Wave Basin and Model Harbor	32
	3.3 Wave Energy Dissipators	35
	3.4 Measurements of Wave Heights and Determination of Amplification Factor	38
IV.	RESULTS OF EXPERIMENTS AND NUMERICAL ANALYSES	39
	4.1 Approach to the Open-Sea Conditions	39
	4.1.1 Criteria for the Open-Sea Conditions	39
	4.1.2 Effect of Wave-Energy-Dissipator Efficiency on the Simulation of the Open-Sea Conditions	40
	4.1.3 Effect of Wave Basin Size on the Simulation of the Open-Sea Conditions	44
	4.2 Resonant Characteristics of Fully Open Rectangular Harbor	47
	4.2.1 Geometry Response of Fully Open Harbor	47
	4.2.2 Frequency Response of Fully Open Harbor	52

TABLE OF CONTENTS (Continued)

	Page
4.3 Resonant Characteristics of Partially Open Symmetrical Harbors	54
4.3.1 Numerical Analysis	54
4.3.2 Comparison of the Theory with the Experiments	59
4.4 Resonant Characteristics of Asymmetric Harbor	63
V. DISCUSSION OF HARBOR PARADOX	68
5.1 Sharpness of Response Curve Near Resonant Points	68
5.2 Response to Waves with Continuous Power Spectrum	70
5.3 Scale Effect in Model Experiments	73
5.4 Possibility of Harbor Paradox	74
VI. CONCLUSIONS	75
VII. RECOMMENDATIONS FOR FURTHER STUDY	76
VIII. REFERENCES	78
APPENDIX	81
A. Evaluations of Radiation Functions $\mathcal{Y}_1$ and $\mathcal{Y}_2$	81
B. FORTRAN Program for Computation of Amplification Factor	88

LIST OF FIGURES AND TABLES

Figure No.		Page
1.	Definition Sketch of the Model Harbor	6
2.	Radiation Functions, ψ_1 and ψ_2, versus Relative Half-Opening, kd	17
3.	Sketches of a Symmetrical and an Asymmetric Harbor	21
4.	Frequency Response Curves of Fully Open Harbors with and without Energy Dissipation	27
5.	Effect of Energy Dissipation on Resonant Characteristics of Fully Open Harbor (Fundamental Mode)	28
6.	Experimental Apparatus	33
7.	Detail of Model Harbor Arrangement	34
8.	Test Section of Wave Energy Dissipator (No. 4)	34
9.	Transmission and Reflection Coefficients of Wave Filters versus Incident Wave Steepness	36
10.	Arrangements of Wave Energy Dissipators	40
11-a.	Geometry Response of Test Harbor, Dissipators No. 5	41
11-b.	Geometry Response of Test Harbor, No Dissipator and Dissipators No. 6	41
12.	Variation of Resonant Characteristics due to Change in Effectiveness of Energy Dissipator	42
13.	Geometry Response of Test Harbor: Effect of Main Basin Size on Simulation of the Open-Sea Conditions	45
14.	Transversal Wave Envelopes in Narrow and Wide Main Basins (T = 0.6 sec.)	46
15.	Typical Geometry Responses of Fully Open Harbors	48
16.	Resonant Characteristics of Fully Open Harbor with Varying Length	50
17.	Path-Line Patterns, Fully Open Harbor	51

LIST OF FIGURES AND TABLES (Continued)

Figure No.		Page
18.	Frequency Response of a Fully Open Harbor and Variation of Outside Standing Wave Height with Wave Period	53
19.	Theoretical Frequency Response Curves of Symmetrical Harbors	55
20.	Resonant Length and Amplification Factor of a Symmetrical Rectangular Harbor	56
21.	Frequency Response of a Narrow Harbor, Fully Open and Partially Open	58
22.	Frequency Responses of Square Harbors with Partial Openings	60
23.	Frequency Response of a Wide Harbor with a Partial Opening	61
24.	Path-Line Patterns, Partially Open Harbor	62
25.	Theoretical Frequency Response Curves of Asymmetric Harbors	64
26.	Frequency Response of an Asymmetric Harbor	67
27.	Effect of Entrance Location on Transversal Resonant Oscillation of Odd Mode	67
A-1.	FORTRAN Programs for Radiation Functions ψ_1 and ψ_2	83
A-2.	Definition Sketch of Integration Range for ψ_2	87
B-1.	FORTRAN Program for Computation of Frequency Response of Asymmetric Harbor	90

Table No.		
1.	Dissipator Spacing Arrangement	35
2.	Comparison of Q with $R_{Res}(2b/\ell = 0.2)$	69
3.	Root-Mean-Square Response Factors of Symmetrical Harbors	72
B-1.	Conversion Table of Major FORTRAN Names to Symbols in Text	89

LIST OF SYMBOLS*

a = amplitude of outside standing wave

A = amplitude of oscillation inside harbor

b = harbor half-width

c = constant representing some magnitude of oscillating flow at the entrance

d = harbor half-opening-width

$f(x,y)$ = wave pattern function

$F(u,y)$ = Fourier transform of $f(x,y)$

h = water depth

H = wave height

k = wave number, $2\pi/\lambda$

K_T = transmission coefficient

K_R = reflection coefficient

ℓ = harbor length

m = integer referring number of transversal nodal lines, 0,1,2,..

n = integer referring number of longitudinal nodal lines,0,1,2,..

Q = measure of sharpness of response curve near resonance

R = amplification factor at a corner of the back wall of harbor

$_{Res}$ = subscript referring to a value at resonance

t = time

T = wave period

x = horizontal coordinate measured from the center of the harbor entrance and parallel to the coast line

y = horizontal coordinate measured from the center of the harbor entrance and perpendicular to the coast line

z = vertical coordinate measured upward from the mean-water level

γ = Euler's constant, 0.5772....

ε = relative location of entrance

---

*Note: Only the most commonly used symbols and definitions are listed here. Symbols and definitions which are not generally used throughout are defined only where they are used.

LIST OF SYMBOLS (Continued)

η = water surface elevation

λ = wave length

σ = angular frequency, $2\pi/T$

ϕ = velocity potential

ψ = radiation functions

ω = phase angle between outside standing wave and inside oscillation

I. INTRODUCTION

1.1 Nature of the Problem

A resonant phenomenon is always a fascinating subject of study. It also has a close relation to our daily life; a pipe organ originates its sounds through resonant vibrations of air in pipes: radio waves are transmitted and received with resonated circuits. A resonance may be dangerous, too; engineers have been very cautious not to match the natural frequencies of the structures which they design with the frequency of exterior oscillation. One of the troublesome examples and the subject of the present study is "long period oscillations in ports". Although the problem of the long period oscillations is limited to a small number of ports in the world, the troubles are so serious in specific harbors that the problem was discussed specially in the XIXth International Navigation Congress in London in 1957. At this congress, Joosting [1957] showed that in the Table Bay Harbor, Cape Town, the long period oscillations with amplitude larger than 3.5 in. had been observed for four days in the average per month in the summer seasons during the period 1941-1955.

What makes a long period oscillation intolerable for a harbor is the fact that it forces moored ships to move to-and-fro from their berthing positions, thus causing breaking of mooring lines, damages on fenders and piers, and in some cases collisions of ships with each other. In addition, the oscillation may produce strong currents up to several knots at the harbor entrance and carry ships out of control (Wilson[1960]). These long period oscillations, usually of the order of minutes, are not necessarily of large amplitude. On the contrary, they are usually only a few feet high or less. Knapp and Vanoni [1945] have stated for the Naval Operation Base, Terminal Island, California:

> In each case where a surge was reported, the height of the three-minute waves exceeded 0.1 ft. Apparently this height is in the neighborhood of the critical height beyond which damaging motion can be expected.

This is primarily due to the long periodicity of such oscillations. If a standing wave height of 2 ft. with a period of 3 minutes is observed at an anti-node of a rectangular harbor with a depth of 40 ft., a small float at a nodal zone is likely to move in oscillation over a distance of 51 ft.

The more serious factor involved in the problem, beyond the substantial damages on berthing facilities and ships, is the invisible loss in the harbor and ship operations. Once a long period oscillation is developed in a harbor and damages are reported, no cargo-handling operation is possible. The ships in the harbor may have to stay there a day or several days longer than their schedules. If the high operational cost of a freighter is considered, it is quickly realized that

the existence of such long period waves will greatly diminish the potential value of a specific harbor.

The arguments on the origin of the long period oscillations in harbors have not been settled. Surf-beats, passages of atmospheric jumps, or sudden shifts in the winds are reported to be responsible at certain instances for such oscillations (see Wilson [1957] for a detailed discussion). However, many investigators seem to be in agreement that the predominant mechanism of long period oscillations in harbors is the excitation through the harbor entrance by incoming long period waves. The existence of long period waves in the ocean has been proved by many records of wave spectra which show a wide frequency range of ocean waves up to several hours in period (Miles and Munks [1961]). Although these ocean waves of long periods are very low in heights and are completely invisible, an oscillation of appreciable height can be developed in a harbor through the resonance mechanism if the energy of incoming waves is concentrated in a narrow frequency range around one of the harbor's natural frequencies.

1.2 Theoretical Aspects of the Problem

Accepting the problem as a resonant oscillation excited by incident waves, one will ask what are the natural frequencies of a given harbor basin. The question cannot be answered readily, even for a rectangular harbor which seems to be the simplest case. A fully open rectangular harbor is often quoted as a "one-quarter wave length resonator", because the resonant condition for a harbor of infinitely small width is given by:

$$k\ell = \frac{2m + 1}{2}\pi \tag{1.1}$$

where: m = number of transverse nodal lines in harbor = 0,1,2,...
k = wave number = $2\pi/\lambda$
ℓ = harbor length
λ = wave length

On the other hand, a completely enclosed basin must satisfy the following condition in order to develop a resonant oscillation in it (see Lamb [1932], art. 190):

$$(k\ell)^2 = \pi^2 \left[m^2 + \frac{n^2}{(2b/\ell)^2}\right] \tag{1.2}$$

where: n = number of longitudinal nodal lines = 0,1,2,...
b = half-width of harbor

Thus, the resonant harbor length must be a multiple of one-half wave length for an enclosed basin. Then, what resonant harbor length is to be expected for a rectangular harbor with a partial opening? In addition, equation (1.1) does not hold for a harbor of finite width in a strict sense. What correction in equation (1.1) should be made for a harbor of finite width?

Recently, Miles and Munk [1961] have answered these questions to some extent. For a narrow rectangular harbor with a small opening, they have shown that a resonant harbor length of a fully open harbor becomes smaller than the length given by equation (1.1) as a harbor width increases. A resonant harbor length of a partially open harbor also decreases from the length of a fully open harbor toward the length of equation (1.2) as the harbor entrance is narrowed down. Although the resonant amplification factor of a fully open harbor decreases as a harbor becomes wide, that of a partially open harbor increases as the entrance becomes narrow. Since this is contrary to an engineer's concept on the function of breakwaters, they called this increase of amplification factor the "harbor paradox". Although their theory was a major step to the solution of the problem, the analysis is limited only to the vicinity of the fundamental resonant point of a narrow harbor with a small opening (see Chapter V). The study also lacks experimental evidence. Although Iribarren, et al. [1957], Hensen [1959], and LeMéhauté [1954, 1961] have conducted fundamental experiments on generalized models of rectangular harbors, the boundary conditions at the ocean side are different from those assumed in Miles and Munk's theory and from the actual open-sea conditions; for this reason, these experimental data are not available for the comparison with the above theory. Hence, the present study has two major objectives: (1) to develop a more rigorous theory of wave induced oscillations in harbors and (2) to verify it with adequate experimental data.

Theoretically, the problem is one of the boundary-value problems for the velocity potential ϕ; that is, to solve the Helmholtz equation

$$\nabla^2 f + k^2 f = 0 \qquad (1.3)$$

for the wave pattern function $f(x,y)$ at the appropriate boundary conditions. Difficulties have been met in dealing with the boundary condition at the harbor entrance and in evaluating the outgoing waves radiated from the harbor entrance. McNown [1950] assumed the entrance to remain as a node of standing waves in his analysis of a circular harbor. As in his later work with Kravtchenko [1955] for a rectangular harbor, he paid little attention to the radiated waves. For this reason, they could not predict the change of the resonant condition for varying width of a harbor entrance. Miles and Munk [1961] employed a measure of an artificial boundary at the entrance to separate the two regions inside and outside the harbor: continuity of water surface elevation and normal velocity through the entrance. As for the outgoing waves, they applied the method of point sources and expressed them in the integral forms of Hankel functions. But they imposed the restrictions

of $2kb \ll 1$ and $2b < \ell$ in order to obtain analytical expressions for the resonant condition and maximum amplification factors.

Differing from the point-source method, Howard [1959] applied the method of Fourier transformation to evaluate the outgoing waves, and expressed these waves in integral forms. Although he only showed the solutions of two special harbors (a fully open narrow rectangular harbor and a circular harbor with a small opening), his method can be easily extended to a harbor of any shape with the aid of a digital computer. This is the approach taken in the present study.

1.3 Simulation of the Open-Sea Conditions for Model Experiments

Since the problems of long period oscillations in specific harbors are very serious and the theoretical solutions have yet been limited to harbor of very simple geometry, many scale model tests have been conducted in various countries. A number of model studies may be cited: Knapp and Vanoni [1945], and Hudson [1947] for the Naval Operating Base, Terminal Island, California: Knapp [1949] for the Apra Harbor, Guam, M. I.: Wilson [1960] for the Table Bay Harbor, Cape Town, South Africa: Abecasis, et al. [1957] for the port of Funchal on the Island of Madeira: Barrillon [1938] for the port of Tamatave, Madagascar (reported by Larras [1957]). This is only a partial list of such studies.

As in any scale model, the prototype conditions must be simulated in the model for a study of long period oscillation. One of the difficulties in the modelling for long period oscillations is how to eliminate the limitation of the finite area of a wave basin; reflected waves from coast lines and harbor die away in the infinite region of the "open-sea" in the prototype, whereas reflected waves in the model may be reflected again from the periphery of a basin and wave generator and interfere with the original wave system. This is especially important in the modelling for long period oscillations, because the steepness of long period waves in question is extremely small and such waves are reflected totally even from gently sloping beaches. For the purpose of overcoming this difficulty, it is a current technique of modelling to place wave absorbers in the periphery of a wave basin and to locate wave filters in front of a wave generator, so that the reflected waves from the model may be dissipated there. The wave filters and absorbers must be effective enough so as to keep the wave basin free from undesirable multi-reflections between basin walls, the wave generator and model harbor. In order to obtain a good effectiveness for waves of very low steepness, wave filters and absorbers may become so large that they may occupy the largest portion of a test basin (Biesel [1954]).

A question arises at this point: namely, how high must be the effectiveness of the wave filters and absorbers? To answer this question, Ippen and Raichlen [1962] started their study on a model

system with the most unfavorable modelling situation of no wave filter and absorber. They have shown that such a system is characterized by the presence of a number of resonant spikes on a frequency response curve, and concluded that effective wave filters and absorbers will be necessary to significantly reduce the coupling effect of a highly reflective main basin and a model harbor. Then, Ippen, Raichlen, and Sullivan [1962] have observed how the relative effectiveness of such wave energy dissipators affects the resonant characteristics of a model harbor of rectangular shape, using several energy dissipators of different effectiveness but with the same dimension. They concluded that wave filters and wave absorbers are indispensable and the transmission coefficient of the wave filters should be much smaller than 0.5 (which was true of the best filter applied) to approach an open-sea condition. The question of minimum effectiveness of wave energy dissipators for the simulation of the open-sea condition remains still unsolved. Hence, it is also the purpose of the present study to find out the minimum requirement for the wave energy dissipators for the modelling of long period oscillations in harbors.

The above three objectives, to establish a rigorous theory, to verify the theory with experimental data, and to find out the minimum requirements for wave energy dissipators, will be dealt with in the subsequent chapters.

II. THEORY OF WAVE INDUCED OSCILLATION IN A RECTANGULAR HARBOR

2.1 Solution of Wave Induced Oscillation in the Ideal Fluid

2.1.1 Method of Analysis - Separation of Two Regions Outside and Inside the Harbor

Although the actual harbors which suffer from resonant oscillations are usually of complicated configuration and the adjoining coast lines are not straight, a rectangular harbor connected to the open-sea with a straight coast line seems to be the most practical model for analysis. A harbor of rectangular shape is often constructed because it provides a port with many berths. The assumption of a straight coast line extending infinitely is less applicable to the actual case; some harbor may be located in the depth of a narrow bay. However, the shore line adjoining to the harbor entrance does end at the coast line of the open-sea which can be defined mathematically as the semi-infinite region. In this sense, the analysis of a rectangular harbor connected to the open-sea has sufficient value for practical application.

The following conditions are assumed in the analysis;

1. The oscillations in a harbor are induced by the incident waves of regular wave train moving normal to the coast line.

2. All boundaries reflect waves totally.

3. The water depth is constant over the whole region in consideration.

4. The harbor entrance is small enough to guarantee the uniform wave motion through it.

5. All wave motions are of small amplitude in the ideal fluid.

The system in the analysis is sketched in Figure 1. The origin of the coordinates is taken at the center of the harbor

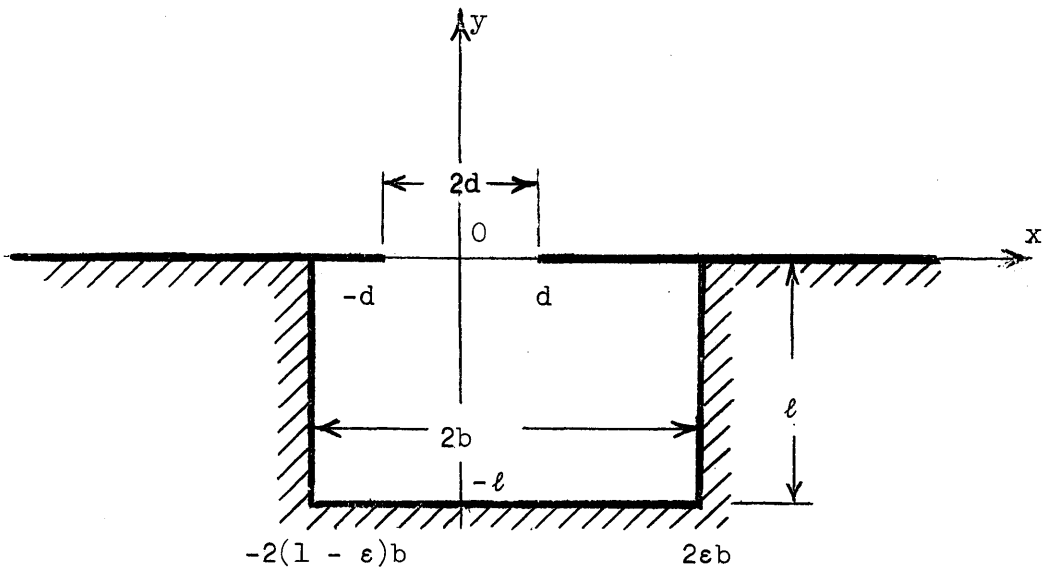

Figure 1. Definition Sketch of the Model Harbor

entrance. The vertical coordinate, z, is measured upward from the mean water level. Since the fluid is assumed ideal and the motion is induced by a regular train of incident waves under the effect of gravity, there exists a velocity potential which satisfies the Laplace equation:

$$\nabla^2 \phi = 0 \tag{2.1}$$

If we assume the velocity potential as a product of functions of x and y, z, and t, such as,

$$\phi(x,y,z,t) = \frac{1}{i\sigma} f(x,y)\, Z(z) e^{i\sigma t} \tag{2.2}$$

where: σ = angular frequency = $2\pi/T$

T = wave period

then the functions of $f(x,y)$ and $Z(z)$ must satisfy the equation

$$\frac{1}{f}\left(\frac{\partial^2 f}{\partial x^2} + \frac{\partial^2 f}{\partial y^2}\right) + \frac{1}{Z}\frac{d^2 Z}{dz^2} = 0 \qquad (2.3)$$

After separating the first and second terms of equation (2.3) and equating them to a constant, say k^2, the function $Z(z)$ is solved and determined from the boundary conditions at the bottom as:

$$Z(z) = ag\,\frac{\cosh k(z + h)}{\cosh k\,h} \qquad (2.4)$$

where: k = constant (which is proved to be the wave number = $2\pi/\lambda$)

h = water depth

a = wave amplitude

The water surface elevation is derived from the surface condition as:

$$\eta(x,y,t) = \frac{1}{g}\left(\frac{\partial \phi}{\partial t}\right)_{z=0} = a\ f(x,y)e^{i\sigma t} \qquad (2.5)$$

The constant k in equations (2.4) and (2.5) is determined from the continuity condition at the water surface:

$$\frac{\partial \eta}{\partial t} = -\left(\frac{\partial \phi}{\partial z}\right)_{z=0}$$

hence,

$$\sigma^2 = gk \tanh kh \qquad (2.6)$$

The function $f(x,y)$ which determines the wave pattern in the system must satisfy the equation:

$$\frac{\partial^2 f}{\partial x^2} + \frac{\partial^2 f}{\partial y^2} + k^2 f = 0 \qquad (2.7)$$

The boundary conditions for $f(x,y)$ are:

$$\begin{cases} \dfrac{\partial f}{\partial x} = 0 \qquad \text{at } x = 2\varepsilon b \text{ and } -2(1-\varepsilon)b \\ \qquad\qquad -\ell \le y \le 0 \end{cases} \tag{2.8.1}$$

$$\frac{\partial f}{\partial y} = 0 \qquad \text{at } |x| > d,\ y = 0 \tag{2.8.2}$$

$$\frac{\partial f}{\partial y} = 0 \qquad \text{at } -2(1-\varepsilon)b \le x \le 2\varepsilon b, \quad y = -\ell \tag{2.8.3}$$

$$f(x,y) = \cos ky \quad \text{as } x^2 + y^2 \to \infty \tag{2.8.4}$$

The last condition represents a plain standing wave system, this is so required because any disturbance from the harbor does die away as it travels outward.

In addition to the boundary conditions of equations (2.8.1) through (2.8.4), it is convenient and useful for the analysis to separate the system into two regions: one outside and one inside the harbor. This procedure of separating the system is justified if the continuity conditions for water surface elevation and normal velocity at the harbor entrance are satisfied. These conditions are expressed as:

$$\eta_1(x,0) = \eta_2(x,0) \quad \text{at } |x| \le d \tag{2.9}$$

$$\left(\frac{\partial f_1}{\partial y}\right)_{y=0} = \left(\frac{\partial f_2}{\partial y}\right)_{y=0} \quad \text{at } |x| \le d \tag{2.10}$$

where: subscripts 1 denote the outside of the harbor
subscripts 2 denote the inside of the harbor

Since the harbor entrance is assumed as relatively small compared to the wave length ($kd \lesssim 1$, see Section 4.2.1 for experimental data), an approximation of a uniform oscillating flow may be applied on the harbor entrance. Then, the both sides of equation (2.10) are set equal to some constant with respect to x as:

$$\left(\frac{\partial f_1}{\partial y}\right)_{y=0} = \left(\frac{\partial f_2}{\partial y}\right)_{y=0} \equiv kc\, e^{i\omega} \quad \text{at } |x| \le d \tag{2.11}$$

The constant c represents some magnitude of a uniform flow through the entrance. A phase angle ω is introduced here, because the wave motion through the entrance in general has a different phase with the outside standing wave at the region far from the entrance. Both c and ω are to be determined later from the condition of the same water surface elevation at both sides of the entrance, equation (2.9).

2.1.2 Wave Pattern Outside the Harbor

As stated in equation (2.8.4), the wave pattern becomes a plain standing wave in the region far from the harbor entrance. Since this standing wave satisfies equation (2.7) and has a zero water surface slope at y = 0, the wave pattern function $f_1(x,y)$ may be expressed as a sum of the standing wave and some unknown function $f_3(x,y)$:

$$f_1(x,y) = \cos ky + kc\, e^{i\omega} f_3(x,y) \tag{2.12}$$

The water surface elevation outside the harbor, η_1, is written with $f_3(x,y)$ as:

$$\eta_1(x,y,t) = a \cos ky\, e^{i\sigma t} + akc\, f_3(x,y) e^{i(\sigma t + \omega)}$$

The boundary conditions for $f_3(x,y)$ are obtained from equations (2.8.2), (2.8.4) and (2.11) as

$$\left(\frac{\partial f_3}{\partial y}\right)_{y=0} = \begin{cases} 1 & \text{at } |x| \le d \\ 0 & \text{at } |x| \ge d \end{cases} \tag{2.13.1}$$

$$f_3(x,y) = 0 \quad \text{as } x^2 + y^2 \to \infty \tag{2.13.2}$$

Now let F(u,y) be the Fourier transform of $f_3(x,y)$ on x, then the differential equation for F(u,y) is derived from equation (2.7) as:

$$\frac{\partial^2 F}{\partial y^2} + (k^2 - u^2) F = 0 \tag{2.14}$$

where:

$$F(u,y) = \int_{-\infty}^{\infty} e^{-ius} f_3(s,y)\, ds$$

$$f_3(x,y) = \frac{1}{2\pi} \int_{-\infty}^{\infty} e^{iux} F(u,y)\, du$$

The boundary conditions of equation (2.13) are transformed for $F(u,y)$ as:

$$\left[\frac{\partial F(u,y)}{\partial y}\right]_{y=0} = \int_{-\infty}^{\infty} e^{-ius}\left[\frac{\partial f_3(s,y)}{\partial y}\right]_{y=0} ds$$

$$= \frac{2 \sin ud}{u} \qquad (2.15.1)$$

$$F(u,y) = 0 \qquad \text{as } y \to \infty \qquad (2.15.2)$$

The general solution of equation (2.14) is given by:

$$F(u,y) = C_1(u)\, e^{\sqrt{u^2 - k^2}\, y} + C_2(u)\, e^{-\sqrt{u^2 - k^2}\, y} \qquad (2.16)$$

In order to determine the coefficients $C_1(u)$ and $C_2(u)$ in the right-hand side of equation (2.16), two ranges of u must be considered separately; i.e., $|u| > k$ and $|u| < k$.

i) $|u| > k$

In this case, $C_1(u)$ must be zero because of equation (2.15.2). Hence, $C_2(u)$ is obtained from equation (2.15.1), and $F(u,y)$ is determined as:

$$F(u,y) = -\frac{2 \sin ud}{u\sqrt{u^2 - k^2}}\, e^{-\sqrt{u^2 - k^2}\, y} \qquad (2.17)$$

ii) $|u| < k$

In this case, both terms of equation (2.16) become oscillating functions because of the imaginary power factor, i.e.,

$$F(u,y) = C_1(u) e^{i\sqrt{k^2 - u^2}\, y} + C_2(u) e^{-i\sqrt{k^2 - u^2}\, y}$$

Since the term of $e^{i\sigma t}$ is employed for the time function of the velocity potential as well as of the water surface elevation, the first term of $F(u,y)$ represents incoming waves and the second term represents outgoing waves. (The resultant $f_3(x,y)$ from the first term of $F(u,y)$ has a term of $\exp[i(\sqrt{k^2 - u^2}\, y + \sigma t)]$; hence, incoming waves.) Since outgoing

waves are of present interest, $C_1(u)$ is set to zero. The Fourier transformation $F(u,y)$ is then determined from equation (2.15.1) as:

$$F(u,y) = i \frac{2 \sin ud}{u\sqrt{k^2 - u^2}} e^{-i\sqrt{k^2 - u^2}\, y} \tag{2.18}$$

Although $F(u,y)$ obtained in the above does not go to zero as y goes to infinity, it can be proved that the resultant $f_3(x,y)$ does converge to zero as $(x^2 + y^2)$ goes to infinity.

Now the wave pattern function $f_3(x,y)$ is recovered from equations (2.17) and (2.18) as:

$$f_3(x,y) = i\, I_1 - I_2 \tag{2.19}$$

where:

$$I_1 = \frac{2}{\pi} \int_0^k \frac{\sin ud}{u\sqrt{k^2 - u^2}} \cos ux\, e^{-i\sqrt{k^2 - u^2}\, y}\, du \tag{2.19.1}$$

$$I_2 = \frac{2}{\pi} \int_k^\infty \frac{\sin ud}{u\sqrt{u^2 - k^2}} \cos ux\, e^{-\sqrt{u^2 - k^2}\, y}\, du \tag{2.19.2}$$

The water surface elevation outside the harbor is thus obtained as:

$$\eta_1 = a \cos ky\, e^{i\sigma t} + akc(i\, I_1 - I_2)\, e^{i(\sigma t + \omega)} \tag{2.20}$$

2.1.3 Wave Pattern Inside the Harbor

As for the wave pattern inside the harbor, a solution of separated type is sought:

$$f_2(x,y) = X(x) \cdot Y(y) \tag{2.21}$$

Then, equation (2.7) becomes:

$$\frac{1}{Y} \frac{d^2Y}{dy^2} + k^2 = -\frac{1}{X} \frac{d^2X}{dx^2} \tag{2.22}$$

Since the left-hand side of equation (2.22) is a function of y only and the right-hand side is a function of x only, they must be equal to a common constant, say α^2. Then, the function X(x) and Y(y) have the general solutions of

$$X(x) = Ae^{i\alpha x} + Be^{-i\alpha x} \tag{2.23}$$

$$Y(y) = Ce^{\sqrt{\alpha^2 - k^2}\, y} + De^{-\sqrt{\alpha^2 - k^2}\, y} \tag{2.24}$$

From the boundary condition of equation (2.8.1) which describes the condition of no velocity across the walls of the harbor, the equations for the constants A and B are:

$$\left[\frac{dX}{dx}\right]_{x = 2\varepsilon b} = i\alpha\left[Ae^{2i\alpha\varepsilon b} - Be^{-2i\alpha\varepsilon b}\right] = 0$$

$$\left[\frac{dX}{dx}\right]_{x = 2(\varepsilon - 1)b} = i\alpha\left[Ae^{2i\alpha(\varepsilon - 1)b} - Be^{-2i\alpha(\varepsilon - 1)b}\right] = 0$$

Since these are homogeneous, simultaneous equations for A and B, the following relation must hold so that there exist the solutions for A and B:

$$e^{2i\alpha b} - e^{-2i\alpha b} = 0$$

or

$$\sin 2\alpha b = 0$$

Therefore, the constant α must be a real number of

$$\alpha = \frac{n\pi}{2b} \qquad n = 0, 1, 2, \ldots. \tag{2.25}$$

With α determined by equation (2.25), the constants A and B are derived as:

$$A = \frac{B_n}{2} e^{-i\varepsilon n\pi}$$

$$B = \frac{B_n}{2} e^{i\varepsilon n\pi}$$

Thus, the function X(x) becomes:

$$X(x) = B_n \cos \frac{n\pi}{2b} (x - 2\varepsilon b) \tag{2.26}$$

The constants C and D for Y(y) in equation (2.24) are obtained from the boundary condition of equation (2.8.3) at the back wall of the harbor:

$$\left[\frac{dY}{dy}\right]_{y = -\ell} = \sqrt{\alpha^2 - k^2} \left[Ce^{-\ell\sqrt{\alpha^2 - k^2}} - De^{\ell\sqrt{\alpha^2 - k^2}} \right] = 0$$

hence,

$$C = \frac{C_n}{2} e^{\ell\sqrt{\alpha^2 - k^2}}$$

$$D = \frac{C_n}{2} e^{-\ell\sqrt{\alpha^2 - k^2}}$$

Thus, the function Y(y) is determined as:

$$Y(y) = C_n \cosh [\beta_n k (y + \ell)] \tag{2.27}$$

where: $\beta_n = \sqrt{\left(\frac{n\pi}{2kb}\right)^2 - 1}$ (either real or imaginary) (2.28)

If the product of B_n and C_n is denoted by A_n, the function $f_2(x,y)$ is expressed as:

$$f_2(x,y) = \sum_{n=0}^{\infty} A_n \cos[\frac{n\pi}{2b}(x - 2\varepsilon b)] \cosh [\beta_n k(y + \ell)] \tag{2.29}$$

The differentiation of $f_2(x,y)$ with respect to y at y = 0 yields the following Fourier cosine series with a period of 4b:

$$\left[\frac{\partial f_2}{\partial y}\right]_{y = 0} = - A_o k \sin k\ell + \sum_{n=1}^{\infty} A_n \beta_n k \sinh(\beta_n k\ell) \cos[\frac{n\pi}{2b}(x - 2\varepsilon b)]$$

Being given the boundary conditions of equations (2.8.2) and (2.11), the coefficients A_o and A_n are determined with the formulae of Fourier cosine series as:

$$A_o = -\frac{\int_{2\varepsilon b - d}^{2\varepsilon b + d} kc\, e^{i\omega}\, dx}{2bd \sin k\ell} = -\frac{cd\, e^{i\omega}}{b \sin k\ell}$$

$$A_n = \frac{\int_{2\varepsilon b - d}^{2\varepsilon b + d} kc\, e^{i\omega} \cos \frac{n\pi x}{2b}\, dx}{b\, \beta_n k \sinh \beta_n k\ell} = \frac{4ce^{i\omega} \sin \frac{n\pi d}{2b} \cos \varepsilon n\pi}{n\pi \beta_n \sinh \beta_n k\ell}$$

Thus the wave pattern function $f_2(x,y)$ is uniquely determined as:

$$f_2(x,y) = -\frac{cd\, e^{i\omega}}{b \sin k\ell} [\cos k(y + \ell) - S(x,y)] \tag{2.30}$$

where:
$$S(x,y) = \frac{4b \sin k\ell}{\pi d} \sum_{n=1}^{\infty} \left\{ \frac{\sin \frac{n\pi d}{2b} \cos \varepsilon n\pi}{n\, \beta_n \sinh \beta_n k\ell} \right.$$

$$\left. x \cos \frac{n\pi}{2b}(x - 2\varepsilon b) \cosh \beta_n k(y + \ell) \right\}^{*} \tag{2.31}$$

The water surface elevation inside the harbor is obtained as:

$$\eta_2(x,y,t) = -\frac{acd}{b \sin k\ell} e^{i(\sigma t + \omega)} [\cos k(y + \ell) - S(x,y)] \tag{2.32}$$

---

*Note: In this expression, the following changes should be recalled where $n\pi < 2kb$.

$$\beta_n = i\beta_n' = i\sqrt{1 - \left(\frac{n\pi}{2kb}\right)^2} \tag{2.28.1}$$

$$\frac{\cosh \beta_n k(y + \ell)}{\beta_n \sinh \beta_n k\ell} = -\frac{\cos \beta_n' k(y + \ell)}{\beta_n' \sin \beta_n' k\ell}$$

2.1.4 Evaluation of the Amplification Factor

The next task is to determine the unknown constant c and phase angle ω through equation (2.9) which specifies the continuity of water surface elevation at the harbor entrance. As indicated in equations (2.20) and (2.32), the water surface elevations have some variation along the harbor entrance. Instead of matching the surface elevations outside and inside the harbor at every point along the entrance, the average values of water surface elevations over the entrance are employed here for equation (2.9) as an approximation.

First, the average value of the wave pattern function outside the harbor is calculated from equation (2.19):

$$\overline{f_3(x,0)} = \frac{1}{2d}\int_{-d}^{d} f_3(x,0)\,dx$$

$$= \frac{1}{\pi d}\left[i\int_{-d}^{d} dx \int_{0}^{k} \frac{\sin ud}{u\sqrt{k^2 - u^2}} \cos ux\,du \right.$$

$$\left. -\int_{-d}^{d} dx \int_{k}^{\infty} \frac{\sin ud}{u\sqrt{u^2 - k^2}} \cos ux\,du \right]$$

By changing the order of integration and evaluating the integral with respect to x, the average value of $f_3(x,0)$ is obtained as:

$$\overline{f_3(x,0)} = \frac{2}{\pi d}\left[i\int_{0}^{k} \frac{\sin^2 ud}{u^2\sqrt{k^2 - u^2}}\,du - \int_{k}^{\infty} \frac{\sin^2 ud}{u^2\sqrt{u^2 - k^2}}\,du \right]$$

Now by the change of the integral variable from u to $\alpha = ud$, the above expression is rewritten as:

$$\overline{f_3(x,0)} = \frac{1}{k}\left[i\psi_1 - \psi_2 \right] \tag{2.33}$$

where:

$$\psi_1 = \psi_1(kd) = \frac{2}{\pi} kd \int_{0}^{kd} \frac{\sin^2 \alpha}{\alpha^2\sqrt{(kd)^2 - \alpha^2}}\,d\alpha \tag{2.34.1}$$

$$\psi_2 = \psi_2(kd) = \frac{2}{\pi} kd \int_{kd}^{\infty} \frac{\sin^2 \alpha}{\alpha^2\sqrt{\alpha^2 - (kd)^2}}\,d\alpha \tag{2.34.2}$$

With these functions ψ_1 and ψ_2, the average water surface elevation outside the harbor at the entrance is expressed as:

$$\overline{\eta_1(x,0)} = ae^{i\sigma t} + ace^{i(\sigma t + \omega)}[i\psi_1 - \psi_2] \tag{2.35}$$

Since the functions ψ_1 and ψ_2 defined in equations (2.34.1) and (2.34.2) represent the contribution of outgoing waves to the average water surface elevation, they might be called the radiation functions. These radiation functions, ψ_1 and ψ_2, are functions of a single parameter, kd. The evaluations of ψ_1 and ψ_2 have been carried out with the aid of an IBM 7090 digital computer. The results of the computations are shown in Figure 2 for the value of kd up to 1.6 although the assumption of uniform velocity distribution may not be valid for such large values of kd. Details of the computation method are described in Appendix A.

Second, the average water surface elevation inside the harbor at the entrance is calculated from equation (2.32) as:

$$\overline{\eta_2(x,0)} = \frac{1}{2d}\int_{-d}^{d} \frac{-acd}{b \sin k\ell}\, e^{i(\sigma t + \omega)}\, [\cos k\ell - S(x,0)]\, dx$$

$$= -\frac{acd}{b}\, e^{i(\sigma t + \omega)}[\cot k\ell - S_1] \tag{2.36}$$

where: $$S_1 = 8\left(\frac{b}{\pi d}\right)^2 \sum_{n=1}^{\infty} \frac{(\sin \frac{n\pi d}{2b} \cos \varepsilon n\pi)^2}{n^2 \beta_n \tanh \beta_n k\ell} \tag{2.37}$$

Now the substitution of equations (2.35) and (2.36) into equation (2.9) yields the following equation for c and ω:

$$a + ac\, e^{i\omega}\, [i\psi_1 - \psi_2] = -\frac{acd}{b}\, e^{i\omega}\, [\cot k\ell - S_1]$$

Divided by a $e^{i\omega}$, the above equation becomes:

$$e^{-i\omega} + c[i\psi_1 - \psi_2] = -\frac{cd}{b}\, [\cot k\ell - S_1] \tag{2.38}$$

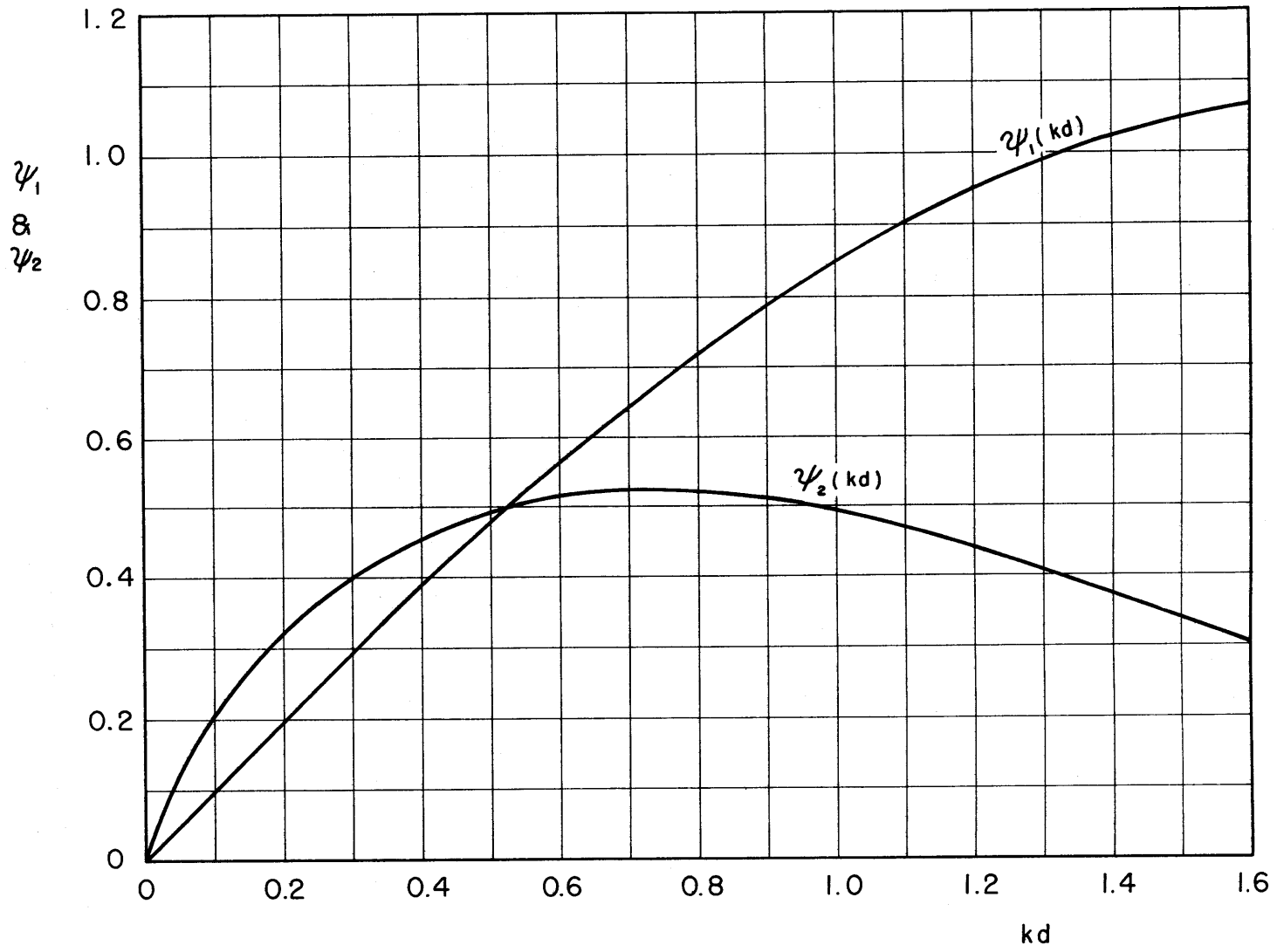

Fig. 2. Radiation Functions, ψ_1 & ψ_2, vs. Relative Half-Opening, kd

From the real and imaginary parts of equation (2.38), two simultaneous equations for c and ω are obtained:

$$\cos \omega + c \left[\frac{d}{b} (\cot k\ell - S_1) - \psi_2\right] = 0$$

$$- \sin \omega + c \psi_1 = 0$$

From the above equations, the constant c and the phase angle ω are determined as:

$$c = \frac{1}{\sqrt{\left[\frac{d}{b} (\cot k\ell - S_1) - \psi_2\right]^2 + \psi_1^2}} \tag{2.39}$$

$$\omega = - \tan^{-1} \frac{\psi_1}{\frac{d}{b}(\cot k\ell - S_1) - \psi_2} \tag{2.40}$$

Thus, the entire wave motion inside and outside the harbor has been solved completely.

The next step is to define the amplification factor. The most reasonable one would be the ratio of a standing wave amplitude inside the harbor to the outside standing wave amplitude. Since such an amplification factor may be defined at any point in the harbor, the amplification factor is derived from equations (2.32) and (2.39) in the general form as:

$$R_{x,y} = \frac{|\eta_2(x,y)|}{a}$$

$$= \frac{\left| \cos k (y + \ell) - S(x,y) \right|}{\sqrt{\left[\cos k\ell - (S_1 + \frac{b}{d}\psi_2) \sin k\ell\right]^2 + (\frac{b}{d}\psi_1 \sin k\ell)^2}} \tag{2.41}$$

This equation gives the amplification factor at any point (x,y) inside the harbor. In order to define the largest amplification factor in the harbor, one needs to know the maximum amplitude in the harbor

for a given relative harbor length. The location of the maximum amplitude in the harbor is not fixed, but varies depending upon the wave pattern inside the harbor. However, it is found that the amplitude at the corner of the back wall ($x = 2\varepsilon b$ and $y = -\ell$) is the largest or close to the largest one in the harbor when it is in resonance. In this sense, the amplification factor is defined here as the one at the corner of the back wall, unless otherwise stated. Then,

$$R = \frac{\left|\eta_2(2\varepsilon b, -\ell)\right|}{a}$$

$$= \frac{\left|1 - S_2\right|}{\sqrt{[\cos k\ell - (S_1 + \frac{b}{d}\psi_2)\sin k\ell]^2 + (\frac{b}{d}\psi_1 \sin k\ell)^2}} \qquad (2.42)$$

where:

$$S_2 = \frac{4b}{\pi d} \sin k\ell \sum_{n=1}^{\infty} \frac{\sin \frac{n\pi d}{2b} \cos \varepsilon n\pi}{n\beta_n \sinh \beta_n k\ell} \quad . \qquad (2.43)$$

The computation of the amplification factor in equation (2.42) is very tedious because of two infinite series and two irrational integrals involved. The resonant condition, or the condition which gives maximum amplification factors for a given harbor, cannot be obtained in explicit form in general, but has to be sought by successive computations of the amplification factor for a varying relative harbor length, $k\ell$. Such computations have been carried out with the aid of the IBM 7090 digital computer at the Computation Center in M.I.T. for a number of harbor geometries. The results of these computations are discussed in Chapter IV.

2.1.5 Some Characteristics of the Amplification Factor

Before going into numerical analyses of equation (2.42), an examination of the equation reveals some characteristics of the amplification factor of a rectangular harbor. They are:

i) The amplification factor has a finite value at resonance even without energy dissipation.

Since $\cos k\ell$ and $\sin k\ell$ cannot be zero at the same time, the denominator in equation (2.42) does not go to zero. Hence, the

amplitude of resonant oscillation in a rectangular harbor remains finite, even if there is no energy dissipation. (Any energy dissipation in a harbor will decrease the amplitude of resonant oscillation.) The amplitude of the oscillation in a harbor is established on the balance of incident wave energy and radiating wave energy carried by the outgoing waves from the harbor entrance. These outgoing waves are an essential feature of resonant oscillation; any study without proper consideration of these outgoing waves would not yield fruitful results.

As for the possible transversal resonances ($2b = n\lambda/2$), it should be first noted that a symmetrical harbor does not respond to the waves with the period of odd resonance mode ($n = 2p + 1$). (The terms of odd number in the series, S_1 and S_2, vanish because of $\cos \varepsilon(2p + 1)\pi = 0$ for $\varepsilon = 1/2$.) When one of β_n approaches to zero, the series S_2 in the numerator of equation (2.43) increases rapidly except for the odd number of n for a symmetrical harbor. At the same time, however, the series S_1 in the denominator also increases with the same speed as S_2, thus keeping the amplification factor at a finite value.

ii) The amplification factor is unity for $k\ell = m\pi$.

For $k\ell = m\pi$,

$$\cos k\ell = 1 \quad \text{and} \quad \sin k\ell = 0$$

hence,

$$\mathbb{R} = \frac{1}{\cos k\ell} = 1$$

unless S_1 and S_2 go to infinity at $k\ell = m\pi$. This implies that breakwaters will not reduce the wave action in a rectangular harbor if the length of incoming waves is such that $\lambda = 2\ell/m$ ($m = 0,1,2,\ldots$). This paradoxical result is due to the assumption of no energy dissipation in the harbor, but on the other hand it indicates the importance of a suitable energy dissipation mechanism in the harbor. An engineer should provide a harbor basin with some effective mechanisms of energy dissipation in order to protect the harbor from the action of incoming waves.

iii) The amplification factor may be smaller than unity.

This is easily demonstrated for the case of a nearly closed harbor. If one increases the width of a harbor while keeping the size of the entrance the same, the terms of $(b/d)\psi_1$ and $(b/d)\psi_2$ increase linearly with the increase of the width. At a certain point, the denominator of equation (2.42) will exceed unity, thus reducing the amplification factor to less than 1. This may also be proved with the fact that $\mathbb{R} = 1$ at $k\ell = m\pi$ and the

derivative ($d\mathbb{R}/dk$) is positive at $k\ell = m\pi$. Such amplification factors smaller than unity simply mean that the water mass in the harbor basin cannot oscillate as fast as the outside waves, as in the case of a single-degree-of-freedom oscillator subject to an exciting force of high frequency.

iv) The response of an asymmetric harbor with an opening at one side is not the same as that of a symmetrical harbor with twice the width.

Although two harbors shown in Figure 3 may seem to have the same resonant characteristics because of similar wave patterns (both series, S_1 and S_2, coincide for the two harbors), the resonant periods and amplification factors will not be the same.

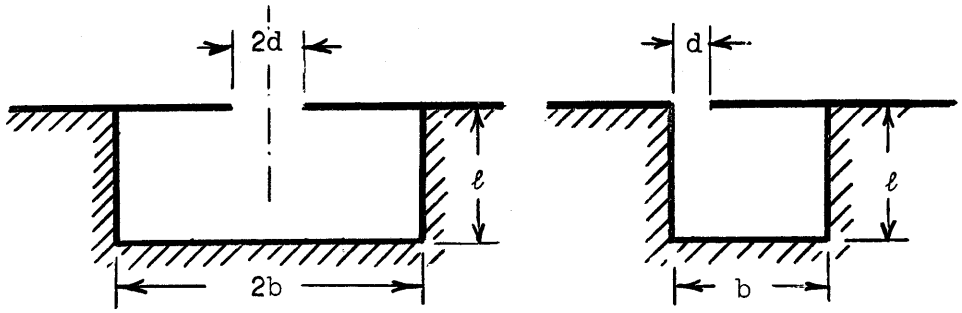

Figure 3. Sketches of a Symmetrical and an Asymmetric Harbor

The reason is that the magnitudes of the radiation functions $\mathcal{Y}_1$ and $\mathcal{Y}_2$ are different for the different absolute sizes of the two harbor entrances, thus differentiating resonant conditions of the two harbors.

2.1.6 Resonant Characteristics of a Fully Open Harbor

If the harbor is a fully open one, or d = b and $\varepsilon = 1/2$, then both S_1 and S_2 become zero, leaving the amplification factor in the following simple form:

$$\mathbb{R} = \frac{1}{\sqrt{(\cos k\ell - \mathcal{Y}_2 \sin k\ell)^2 + \mathcal{Y}_1^2 \sin^2 k\ell}} \qquad (2.44)$$

This equation may be rewritten into the following form after a few trigonometric manipulations:

$$\mathbb{R} = \left[\frac{1}{2}(1 + \mathcal{Y}_1^2 + \mathcal{Y}_2^2) + \frac{1}{2}\sqrt{(1 - \mathcal{Y}_1^2 - \mathcal{Y}_2^2)^2 + 4\mathcal{Y}_2^2}\ \cos(2k\ell + \theta)\right]^{-\frac{1}{2}} \qquad (2.45)$$

where: $\theta = \tan^{-1} \dfrac{2\psi_2}{1 - (\psi_1^2 + \psi_2^2)}$ (2.46)

The resonant condition of a harbor with a varying length is immediately obtained as $[\cos(2k\ell + \theta) = -1]$ from equation (2.45), since ψ_1 and ψ_2 are constant for a fixed value of kd. Hence,

$$(k\ell)_{Res} = \frac{2m + 1}{2}\pi - \frac{1}{2}\tan^{-1}\frac{2\psi_2}{1 - (\psi_1^2 + \psi_2^2)} \tag{2.47}$$

where: m = integer = 0,1,2,...

$(k\ell)_{Res}$ = value of relative harbor length at resonance.

The resonant amplification factor is determined from the above condition as:

$$R_{Res} = \frac{1}{\psi_1}\sqrt{\frac{1}{2}(1 + \psi_1^2 + \psi_2^2) + \frac{1}{2}\sqrt{(1 - \psi_1^2 - \psi_2^2)^2 + 4\psi_2^2}} \tag{2.48}$$

where: R_{Res} = value of amplification factor at resonance.

Equation (2.48) indicates that the resonant amplification factor is governed by one parameter of relative half-opening width, kd, and independent of the mode of resonance. This is only true for a harbor with a varying length, however. In the more practical case of "frequency response" (response of a harbor with fixed geometry to the waves of varying periods), the resonant condition cannot be given by $[\cos(2k\ell + \theta) = -1]$ because the parameter of kd does vary as a wave period varies, thus changing the values of ψ_1 and ψ_2.

If the analysis is restricted to a very narrow harbor ($kb \ll 1$), equations (2.47) and (2.48) can be used to evaluate the resonant characteristics of such a harbor because the variations of the values of ψ_1 and ψ_2 are small compared to 1. Moreover, the radiation functions ψ_1 and ψ_2 are approximated with the following expressions for such a harbor according to Howard [1959] (see Appendix A):

$$\psi_1 = kd + O(k^3d^3) \tag{2.49.1}$$

$$\psi_2 = \frac{2}{\pi}kd\left(\frac{3}{2} - \gamma - \ln kd\right) + O(k^2d^2) \tag{2.49.2}$$

where: γ = Euler's constant = 0.5772.....

The substitution of equation (2.49) into equation (2.47) with d = b yields the relative harbor length at resonance of

$$(k\ell)_{Res} \simeq \frac{2m+1}{2}\pi - \frac{2}{\pi} kb \left(\frac{3}{2} - \gamma - \ln kb\right) \qquad (2.50)$$

The first term of equation (2.50) is the same as equation (1.1) and the second term represents a "mouth correction factor". The expression is in agreement with the results of Honda, Terada, and Ishitani [1908], but not with that of Miles and Munk [1961].

The amplification factor at resonance for a very narrow harbor is also obtained from equations (2.48) and (2.49) as:

$$\mathbb{R}_{Res} \simeq \frac{1}{kb} \simeq \frac{4}{(2m+1)\pi} \cdot \frac{\ell}{2b} \qquad (2.51)$$

This result gives a higher amplification factor by the amount of 28 per cent for the fundamental mode than Miles and Munk's calculation, since they give the amplification factor as $\ell/2b$.

Equation (2.51) also indicates that the value of the amplification factor at resonance becomes smaller as the value of m increases. The amplification factors at the second and third modes are about one-third and one-fifth of the amplification factor at the fundamental mode, respectively. Such decreases of amplification factors at resonance are very reasonable. For a fully open rectangular harbor at the second mode of resonance, a vertical wall may be erected at a location of one-half wave length away from the back wall without changing the wave motions. The new short harbor thus formed has a length of approximately one-third of the original one. Hence the new wideness ratio $2b/\ell$, or effective wideness ratio, is about three times the original one; the amplification factor is to be one-third of that of the fundamental one, accordingly. Therefore, higher modes of resonance will not present serious problems for a fully open rectangular harbor.

2.2 Effect of Energy Dissipation in Harbors on Resonant Characteristics

The theory developed in the preceding sections is based on the assumption of the ideal fluid; no energy dissipation is taken into account. In the actual harbors, however, there exists always some energy dissipation mechanisms: turbulence around the entrance, frictional loss on the bottom, wave breaking on beaches (for wind waves), and so on. These mechanisms cause some energy dissipation, even though the dissipation may be less than 5 per cent

of the total energy. In ordinary wave problems, this amount of energy dissipation is negligible; but not in the problem of resonant oscillation. A resonant oscillation gains its high amplitude only through the accumulation of energy differences between incoming waves and outgoing waves. Any amount of energy dissipation interferes with this accumulation process, thus decreasing the resonant amplification factor. In this section, an attempt is presented to estimate the effect of wave energy dissipation upon the resonant characteristics of a fully open rectangular harbor, since the harbor allows the assumption of one-dimensional wave motion inside it and makes it possible to apply the method of a partial standing wave system.

If the amount of wave energy dissipation inside the harbor is small, its effect may be represented by an adjustment of the reflection coefficient. In other words, whatever the mechanism of energy dissipation is, the wave profile may be approximately expressed as the sum of an undamped incident wave and a reflected wave attenuated at the back wall by a factor of $\mathbb{K}_R$ less than unity. Then, the incident and reflected waves are:

$$\eta_I = A_o\, e^{i[(\sigma t + \omega) + k(y + \ell)]}$$

$$\eta_R = \mathbb{K}_R\, A_o\, e^{i[(\sigma t + \omega) - k(y + \ell)]}$$

Hence, the resultant wave profile in the harbor, η_2, is expressed as:

$$\eta_2 = \eta_I + \eta_R = A_o e^{i(\sigma t + \omega)}\left[e^{ik(y + \ell)} + \mathbb{K}_R\, e^{-ik(y + \ell)}\right]$$

The amplitude of the standing wave at the back wall is

$$A = A_o(1 + \mathbb{K}_R)$$

Using this amplitude, the wave profile is written as:

$$\eta_2 = \frac{A}{1 + \mathbb{K}_R}\, e^{i(\sigma t + \omega)}\left[e^{ik(y + \ell)} + \mathbb{K}_R e^{-ik(y + \ell)}\right] \qquad (2.52)$$

Although the wave pattern inside the harbor has been expressed in terms of an unknown constant, c, in the Section 2.1.3, it is convenient to replace the constant, c, with the amplitude, A, through equation (2.11) for this case; thus,

$$\left[\frac{\partial \eta_2}{\partial y}\right]_{y=0} = ik \frac{A}{1 + \mathbb{K}_R} e^{i(\sigma t + \omega)} [e^{ik\ell} - \mathbb{K}_R e^{-ik\ell}]$$

$$= kac\, e^{i(\sigma t + \omega)}$$

hence,

$$c = i \frac{A}{a(1 + \mathbb{K}_R)} [e^{ik\ell} - \mathbb{K}_R e^{ik\ell}] = \frac{A}{a} [i \frac{1 - \mathbb{K}_R}{1 + \mathbb{K}_R} \cos k\ell - \sin k\ell] \tag{2.53}$$

Then, the amplitude, A, and the phase angle, ω, are derived from the continuity condition at the entrance, equation (2.9). The average amplitudes outside and inside the harbor at the entrance are obtained from equations (2.37) and (2.52) with equation (2.53) as:

$$\overline{\eta_1(x,0)} = a\, e^{i\sigma t} + A\, e^{i(\sigma t + \omega)} [i \psi_1 - \psi_2] [i \frac{1 - \mathbb{K}_R}{1 + \mathbb{K}_R} \cos k\ell - \sin k\ell]$$

$$\eta_2(0) = A [\cos k\ell + i \frac{1 - \mathbb{K}_R}{1 + \mathbb{K}_R} \sin k\ell]\, e^{i(\sigma t + \omega)}$$

With these average amplitudes, the condition of equation (2.9) is rewritten as:

$$ae^{-i\omega} - A[i\psi_1 - \psi_2] [\sin k\ell - i \frac{1 - \mathbb{K}_R}{1 + \mathbb{K}_R} \cos k\ell]$$

$$= A[\cos k\ell + i \frac{1 - \mathbb{K}_R}{1 + \mathbb{K}_R} \sin k\ell] \tag{2.54}$$

In a similar way as in the derivation of equations (2.39) and (2.40), the amplitude, A, and the phase angle, ω, are determined as:

$$A = a\left\{\left[(\cos k\ell - \gamma_2 \sin k\ell) + r\gamma_1 \cos k\ell\right]^2 + \left[\gamma_1 \sin k\ell + r\,(\gamma_2 \cos k\ell + \sin k\ell)\right]^2\right\}^{-\frac{1}{2}} \tag{2.55}$$

$$\omega = -\tan^{-1} \frac{\gamma_1 \sin k\ell + r\,(\gamma_2 \cos k\ell + \sin k\ell)}{(\cos k\ell - \gamma_2 \sin k\ell) + r\gamma_1 \cos k\ell} \tag{2.56}$$

where: $r = \dfrac{1 - \mathbb{K}_R}{1 + \mathbb{K}_R}$

The amplification factor is immediately derived from equation (2.55). After some trigonometric manipulations, the amplification factor is expressed as:

$$\mathbb{R} = \frac{A}{a} = \left[\frac{1}{2}(1 + r^2)\,(1 + \gamma_1^2 + \gamma_2^2) + 2r\gamma_1 + \frac{1}{2}\,(1 - r^2)\sqrt{(1 - \gamma_1^2 - \gamma_2^2)^2 + 4\gamma_2^2}\,\cos(2k\ell + \theta)\right]^{-\frac{1}{2}} \tag{2.57}$$

where:

$$\theta = \tan^{-1} \frac{2\gamma_2}{1-(\gamma_1^2 + \gamma_2^2)} \tag{2.58}$$

The angle θ is the factor which primarily governs the resonant condition. Note that equation (2.58) does not involve the quantity of $\mathbb{K}_R$ (which represents the amount of energy dissipation) and the equation is exactly the same as that of ideal fluid [equation (2.46)].

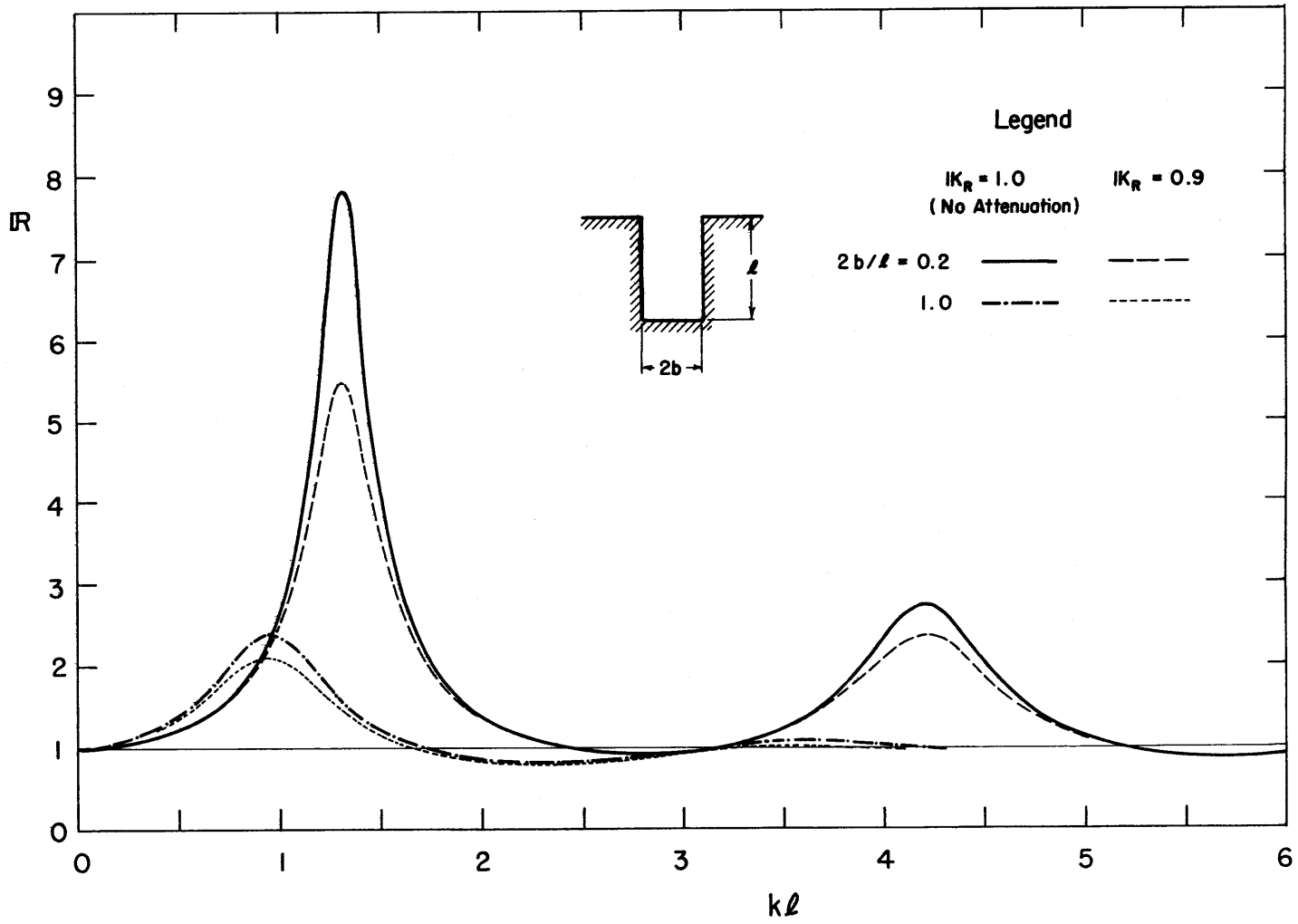

Fig. 4. Frequency Response Curves of Fully Open Harbors with & without Energy Dissipation

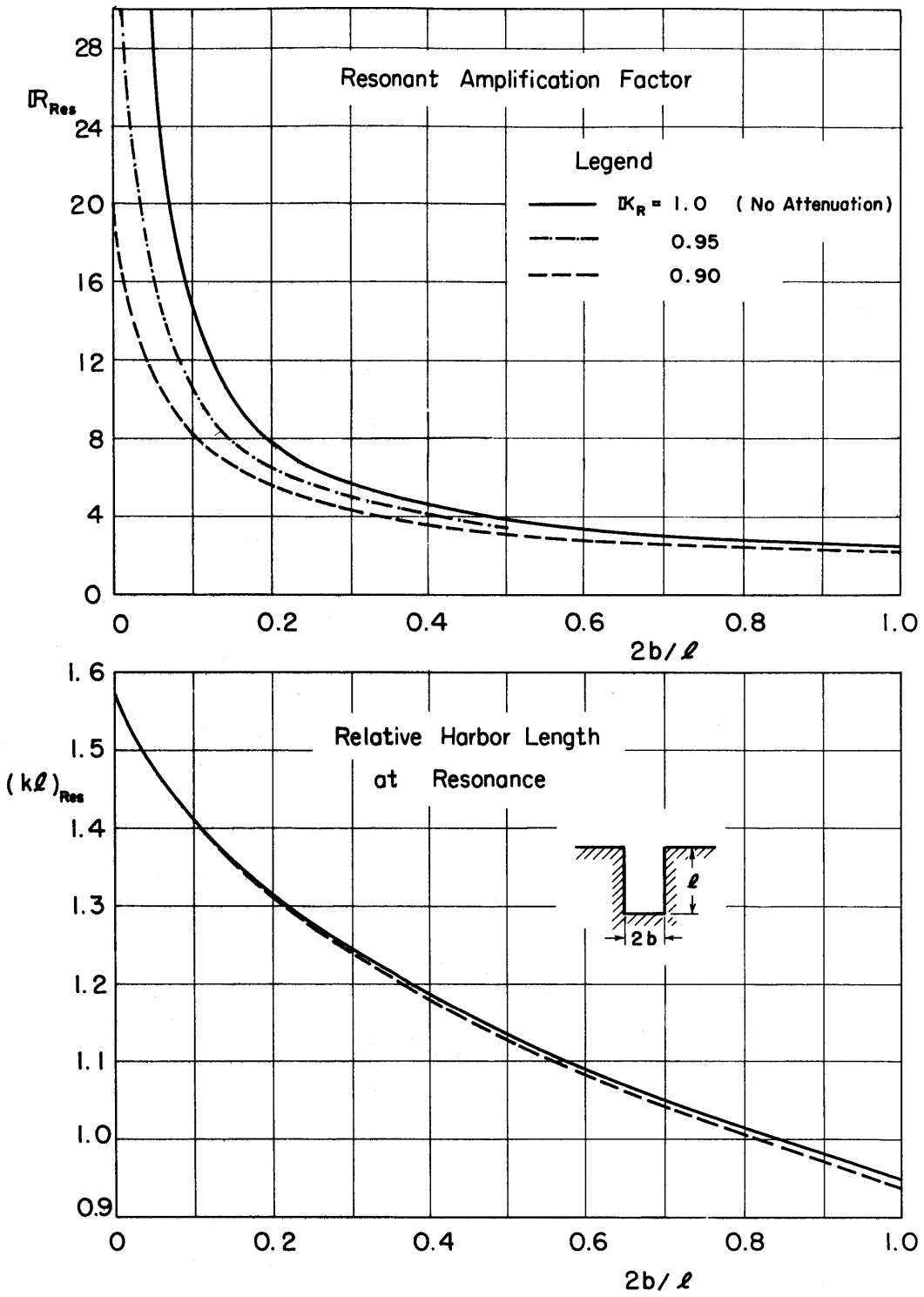

Fig. 5. Effect of Energy Dissipation on Resonant Characteristics of Fully Open Harbor (Fundamental Mode)

However, the resonant amplification factor $\mathbb{R}_{Res}$ is greatly reduced by the presence of energy dissipation. For a very narrow harbor, the magnitudes of the radiation functions ψ_1 and ψ_2 become small as indicated in equations (2.49.1) and (2.49.2). The resonant amplification factor for this case is evaluated from equation (2.57) by setting $[\cos(2k\ell + \theta) = -1]$ and by neglecting higher order terms of r and kd as:

$$\mathbb{R}_{Res} \simeq \frac{1}{kd + r} \simeq \frac{2\,\mathbb{R}_o}{2 + \mathbb{R}_o\,(1 - \mathbb{K}_R)} \leq \frac{2}{1 - \mathbb{K}_R} \qquad (2.59)$$

where: $\mathbb{R}_o$ = resonant amplification factor of the ideal fluid = $1/kd$

Thus the maximum amplification factor has a limiting value determined by the magnitude of the energy dissipation inside the harbor. Equation (2.59) also shows that the effect of energy dissipation on the amplification factor is larger for a large value of $\mathbb{R}_o$ than for a small one.

Although the above analysis is restricted to a very narrow harbor, the conclusions of little change in the resonant condition and of large reduction of the resonant amplification factor have been confirmed for a wide range of harbor geometry by the numerical analysis of equation (2.57). Figure 4 shows frequency responses of two harbors, with and without energy dissipation. A reflection coefficient of 0.9 is employed for both harbors to illustrate the effect of energy dissipation. As it is seen in Figure 4, the effect of energy dissipation is more apparent at high values of the amplification factor than at low values. The resonant amplification factor of a narrow harbor ($2b/\ell = 0.2$) drops from 7.8 to 5.5 for the fundamental mode, while a square harbor ($2b/\ell = 1.0$) shows a slight decrease of amplification factor from 2.4 to 2.1. It is also noted that the effect of energy dissipation is concentrated around the resonant points; there is little change of the amplification factor at the region of anti-resonance.

The resonant characteristics of a fully open rectangular harbor with and without energy dissipation are compiled in Figure 5. The relative harbor length and amplification factor at the fundamental mode of resonance are plotted against the aspect ratio of harbor, $2b/\ell$. The resonant amplification factor of a harbor with no energy dissipation increases rapidly as the harbor becomes narrow, but the resonant amplification factor of a harbor with a reflection coefficient of 0.9 increases slowly toward the limiting value of 20. The lower part of Figure 5 also shows that the resonant harbor length, $(k\ell)_{Res}$, decreases slightly with the presence of energy dissipation. But the change is so small that it is negligible for practical purposes.

III. EXPERIMENTAL EQUIPMENT AND PROCEDURES

3.1 Adoption of Deep Water Waves for the Experimental Study

In the present study, the deep water waves were employed for most of the experiments. Such an approach may seem to contradict the nature of long period oscillations because they apparently belong to shallow water waves. However, the theory of wave induced oscillation indicates that the characteristics of the oscillation are governed by the wave length, not by the water depth nor by the wave period in a direct manner. The wave length is, of course, determined by the water depth and the wave period, but its relative magnitude to the dimensions of a harbor (length, width, and opening) is the factor which defines the characteristics of the oscillation. Although the velocity potential has a term of a depth function, $Z(z)$, defined in equation (2.4), its effect is limited only to the variations in the vertical direction; the velocity pattern on a plane at any depth has the same pattern as that at the water surface. Furthermore, the water surface elevation is not affected by the water depth as shown in equation (2.5). Hence, the theory can be applied to a harbor of any water depth as long as local variations of wave amplitude due to the change of water depth are not of major importance. The choice of wave characteristics, therefore, can be made from the viewpoint of experimental feasibility.

The deep water waves have several advantages over the shallow water waves for the basic experiments of resonant oscillation. They are:

i) "The wave length of deep water waves is not affected by the wave amplitude and variation of water depth."

The shallow water wave changes its length according to the change of water depth. In order to maintain the same wave length, the water level must be kept constant. The bottom of a wave basin must be also horizontal without any appreciable irregularity so that the wave length does not vary locally. On the other hand, the wave length of the deep water wave is determined by the wave period only. Hence, it is not difficult to measure and control the wave length of the deep water waves, compared to the case of the shallow water waves.

The wave length of a shallow water wave is also subject to the magnitude of its amplitude. If the celerity of the solitary wave is employed to estimate the celerity of a shallow water wave with a finite amplitude, the wave length may be expressed as (see Lamb [1932], art. 252):

$$\lambda_f = \lambda_s \sqrt{1 + \frac{2a}{h}} \simeq \lambda_s \left(1 + \frac{a}{h}\right) \qquad (3.1)$$

where: λ_s = wave length of shallow water wave with small amplitude
$= T\sqrt{gh}$

λ_f = wave length of shallow water wave with finite amplitude

a = wave amplitude

h = water depth

The wave amplitude being 5 per cent of the water depth, for example, will increase the actual wave length by 5 per cent from the length of small amplitude wave. An error of such magnitude may be crucial for the study of resonant oscillations because a slight change of wave length often produces very different responses for the same harbor. Hence, the wave amplitude must be sufficiently small compared to the water depth; this usually requires the accurate measurements of very small amplitudes which are not easy to record.

The effect of wave amplitude on the wave length of a deep water wave is shown by the theory of Stokes' wave as (see Lamb [1932], art. 250):

$$\lambda_a = \lambda_o \sqrt{1 + 4(\frac{\pi a}{\lambda})^2} \simeq \lambda_o \left[1 + 2(\frac{\pi a}{\lambda_o})^2\right] \qquad (3.2)$$

where: λ_o = wave length of deep water wave with small amplitude
$= gT^2/2\pi$

λ_a = wave length of deep water wave with finite amplitude

Equation(3.2) shows that the increase of wave length will be only 1.2 per cent even if the wave steepness has a value of 0.05; waves with such magnitude of steepness are easily measured with sufficient accuracy.

ii) "Wave filters and absorbers are more effective for the deep water waves than for the shallow water waves."

The effectiveness of wave filters and absorbers is usually governed by the steepness of incident waves. The steepness of the shallow water waves for a resonant oscillation model is required to be very small (0.001 or less) so that the wave length does not increase from that of small amplitude waves. Wave filters and absorbers of ordinary sizes cannot dissipate such low amplitude waves effectively. In order to obtain good effectiveness, wave filters and absorbers will need to be very large in sizes. On the other hand, the deep water waves can have

a large steepness as discussed in the paragraph i). Hence, wave filters and absorbers of small sizes may dissipate these deep water waves effectively, thus simulating the open-sea conditions in a wave basin.

iii) "The wave basin can be a small one for the model using the deep water waves."

The size of a wave basin for resonance study must be at least three or four times the wave length in test. If the deep water waves are employed, the wave length can be small, as well as the basin size. For the shallow water waves, however, the water depth should be at least a few inches so that the accurate measurements of the water depth and the wave amplitudes can be made. This leads to the minimum wave length of several feet; hence a wave basin needs to be fairly large. The wave filters and absorbers must also be of large dimensions for the shallow water waves. On the other hand, the employment of the deep water waves makes it possible to use a small wave basin, which is much more efficient to operate compared to a big one, without sacrificing accuracy of measurements.

As discussed in the above, the use of deep water waves is more suitable than the use of shallow water waves for the basic experiments of resonant oscillations in a region of constant water depth. For this reason, the experiments were conducted mainly with the deep water waves.

3.2 Wave Basin and Model Harbor

The experiments were carried out in a wave basin shown in Figure 6. The basin is 11.33 ft. long, 9.0 ft. wide and 14 in. deep. Waves are originated with a flap-type wave paddle, 6.0 ft. wide, which is driven by a variable speed motor. The stroke of the paddle can be varied continuously so as to produce waves of desirable heights. The water depth was maintained at $h = 0.844$ ft. throughout the experiments.

To regulate the wave period with a great accuracy, two measures are employed. First, the power voltage supplied to the motor is controlled from 60 to 120 Volt with a Variac voltage regulator. The decrease of power voltage from 120 to 60 Volt corresponds to about 4 per cent increase of wave period. Second, the wave period thus adjusted is monitored with a Hewlett Packard 521C Industrial Counter which counts the number of holes (spaced on the periphery of a rotating disk connected to the paddle-driving wheel) crossing the light beam of a photo-cell-light-source combination over a fixed period of time (1 sec. or 10 sec.). With these instruments, the wave period is measured and controlled within 0.06 per cent in the period range from 0.5 to 2 sec.

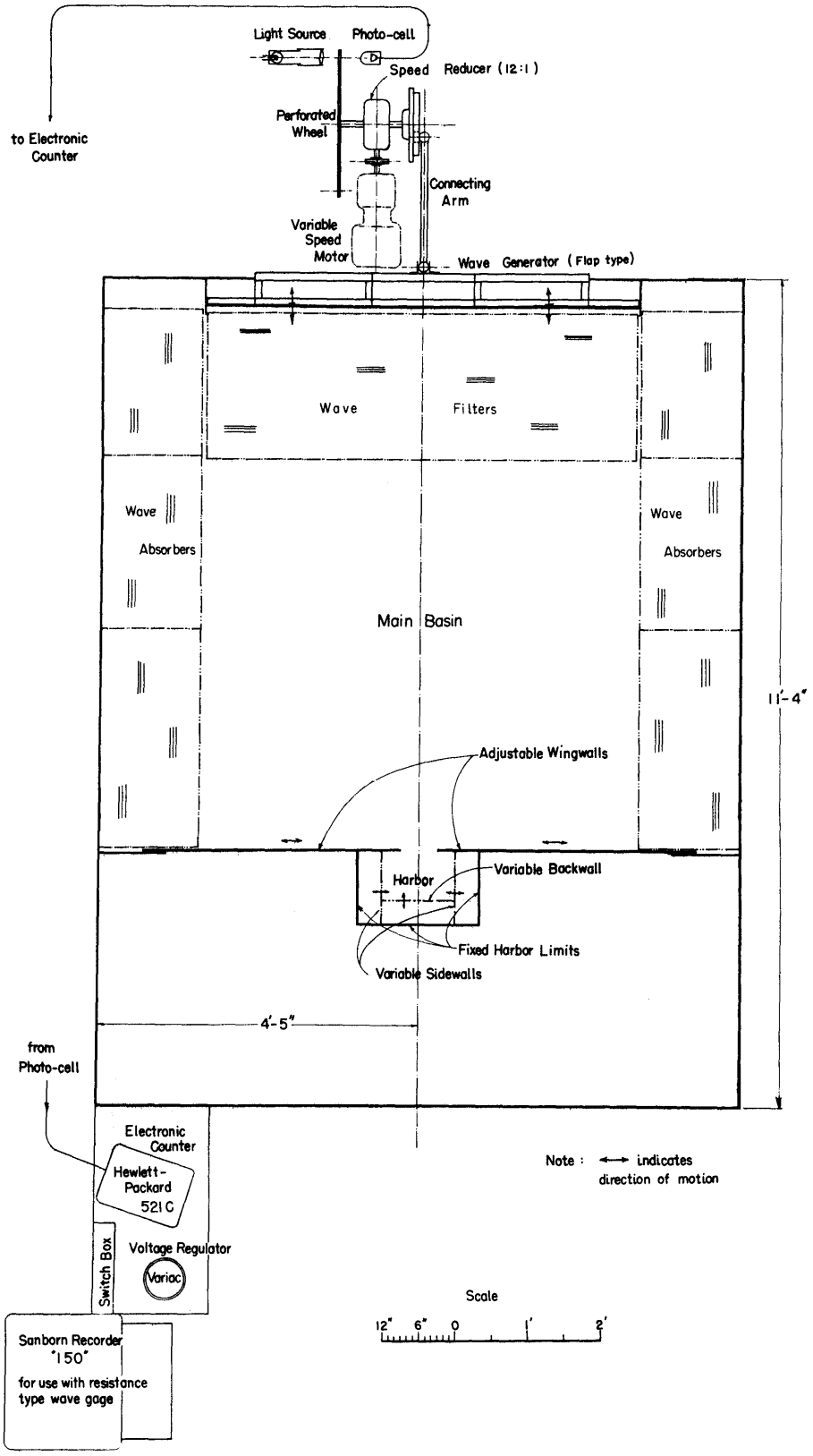

Fig. 6. Experimental Apparatus

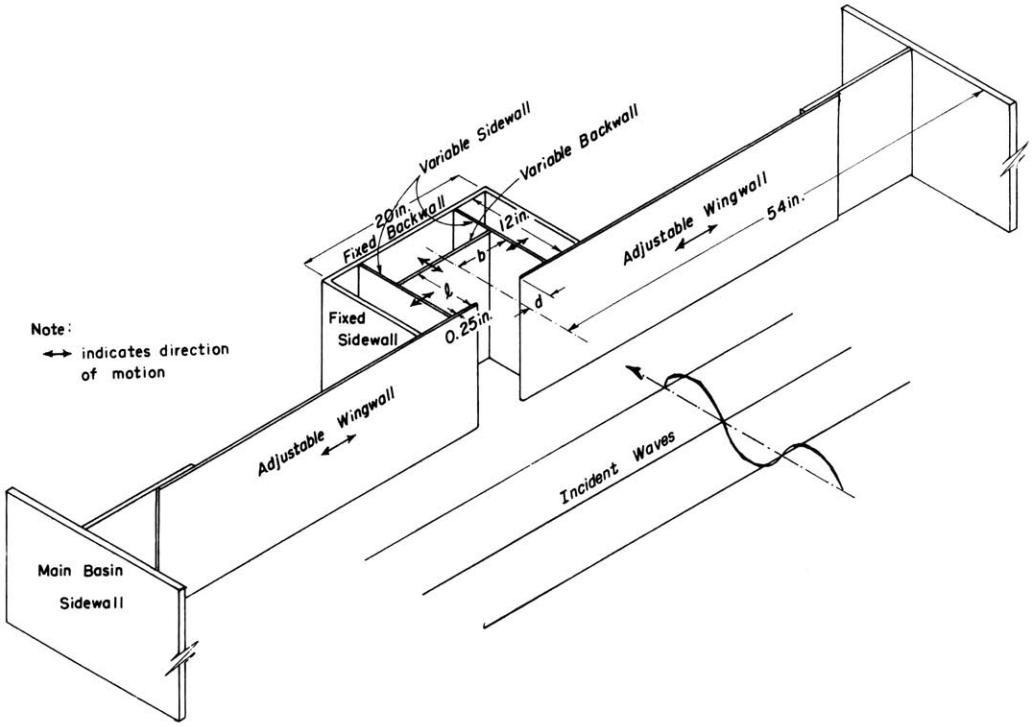

Fig. 7. Detail of Model Harbor Arrangement

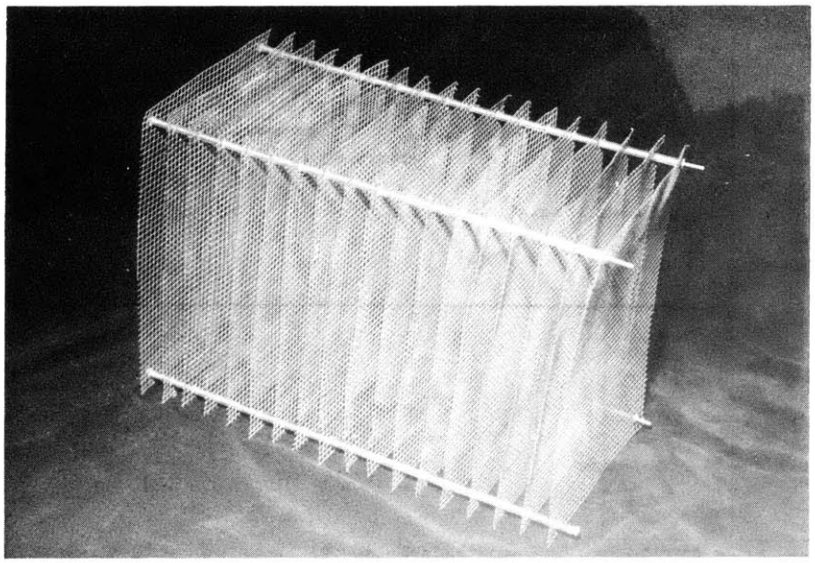

Fig. 8. Test Section of Wave Energy Dissipator (No. 4)

The model harbor is located at a distance of 7.44 ft. from the wave paddle. Two vertical wing walls, representing the straight coast lines, are extended from the harbor entrance to the side walls of the wave basin. These wing walls (made of lucite) are 0.25 in. thick and their ends at the harbor side are rounded in semi-circles. The size and plan form of a model rectangular harbor are flexible. With two variable side walls, one movable back wall and the adjustable wing walls, a model harbor can be constructed with any width, length and opening within the maximum size of 20 in. wide and 12 in. long (see Figure 7 for the arrangements of variable walls). Such flexibility of harbor geometry facilitated greatly the experiments. For a more detailed description of the wave basin and model harbor, the reader is referred to the report by Ippen and Raichlen [1962].

3.3 Wave Energy Dissipators

The wave energy dissipators employed in the present study are composed of vertical wire mesh screens normal to the direction of incident waves. A test section of these dissipators is shown in Figure 8. The screens are fastened with 1/8 in. aluminum rods, and the spacing is maintained with segments of lucite tubing (1/8 in. I.D.). The wave filters, dissipators placed in front of the wave paddle, are 2 ft. wide, 6 ft. long (divided into two pieces each 3 ft. long), and 1 ft. high. The wave absorbers, dissipators placed along the side walls of the basin, are 17 in. wide, 7.4 ft. long (divided into 3 pieces for the absorber No. 6), and 1 ft. high. The sizes of screens and the spacing between them for the four dissipators employed are listed in Table 1. (The dissipators are so numbered after Ippen, Raichlen, and Sullivan [1962].) The dissipators Nos. 5, 4, and 1 are constructed with galvanized iron wire, whereas the dissipator No. 6 is made with bronze wire.

Table 1

Dissipator Spacing Arrangement

Dissipator No.	Mesh (in.)	Wire Diameter (in.)	Spacing (in.)	Number of Screens for Filter	Number of Screens for Absorber
5	0.25	0.028	2.1	13	9
4	0.25	0.028	1.0	25	18
1	0.25	0.028	0.5	49	35
6	0.0625	0.012	0.5	49	35

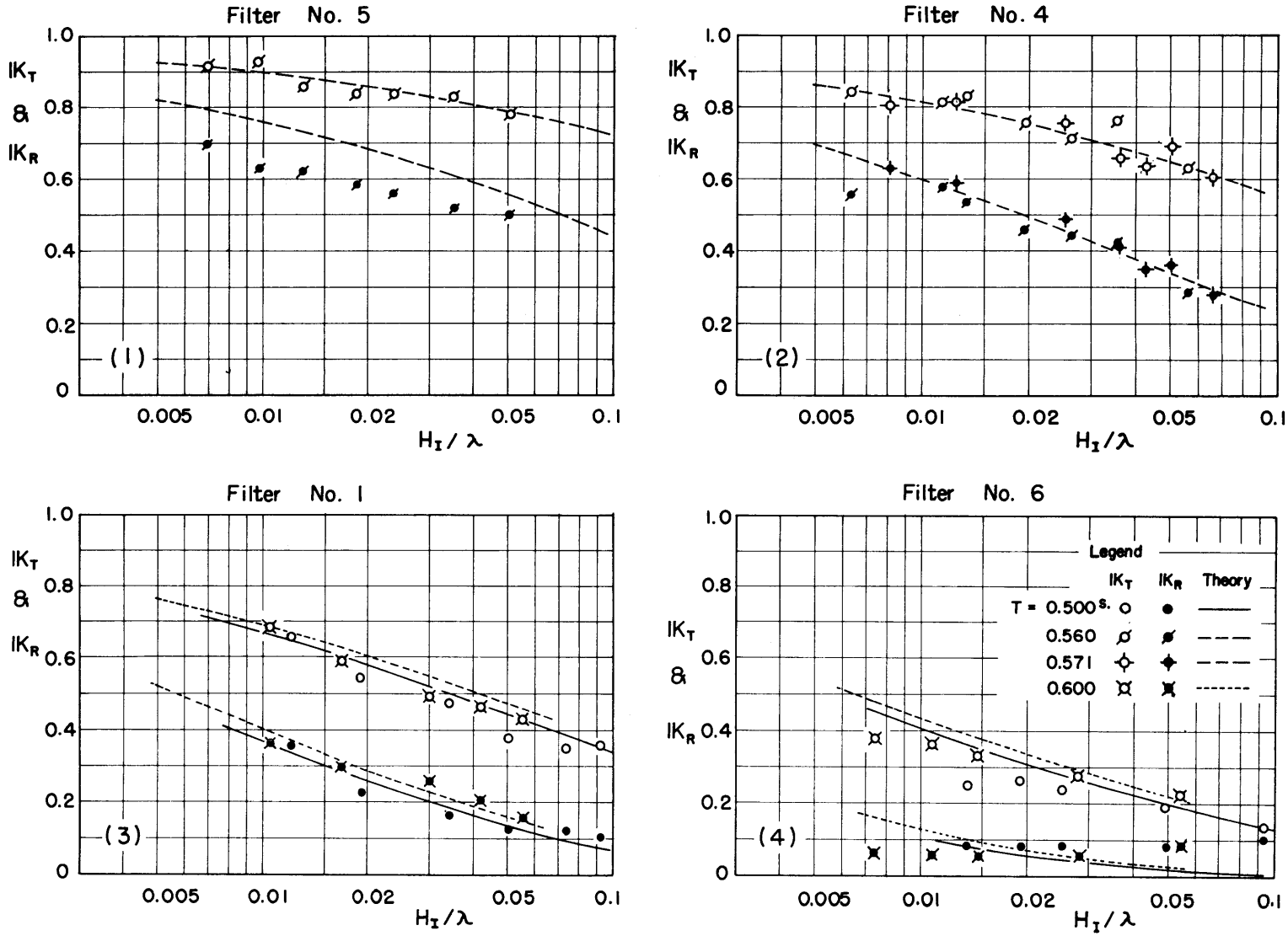

Fig. 9. Transmission and Reflection Coefficients of Wave Filters vs. Incident Wave Steepness

This type of wave energy dissipator was primarily chosen because the coefficients of transmission and reflection can be adjusted by changing the size and number of screens without changing the dimensions of dissipators. The transmission and reflection coefficients of the dissipators employed are expressed with the following semi-empirical equations (see Ippen and Goda [1963]):

$$\mathbb{K}_T = \left[1 + 13.4\, N \frac{D}{L} \left(\frac{\sigma D \lambda}{\nu}\right)^{-0.5} \left(\frac{H_I}{\lambda}\right)^{0.5} G(h/\lambda)\right]^{-2} \qquad (3.3)$$

$$\mathbb{K}_R \simeq \mathbb{K}_T{}^{2.5} \qquad (3.4)$$

where: $\mathbb{K}_T$ = transmission coefficient = H_T/H_I

$\mathbb{K}_R$ = reflection coefficient = H_R/H_I

N = number of screens

D = diameter of wire

L = center-to-center distance between wires

H_I = incident wave height

$G(h/\lambda)$ = depth effect factor (1.81 for the deep water waves)

The expression for the reflection coefficient is applicable for both wave filters and absorbers when they are placed in a standing wave system (i.e., between a wave paddle and a vertical back wall). Hence, it represents a coefficient of total reflection from a back wall and dissipating screens.

The transmission and reflection coefficients are mainly governed by three factors: number of screens, ratio of wire diameter to center-to-center distance, and incident wave steepness. The effects of these factors are illustrated in Figure 9 which shows the variations of $\mathbb{K}_T$ and $\mathbb{K}_R$ against the incident wave steepness for the four filters employed. These data have been obtained in the tests in a small wave channel constructed in the present wave basin. The reader is referred to the report by Ippen and Goda [1963] for the details of the tests and results.

Out of the four dissipators, three dissipators, Nos. 5, 4 and 1 were used only to investigate how the resonant characteristics of a fully open harbor are affected by the effectiveness of wave energy dissipators. The dissipator No. 6, the most effective one, was worked to simulate the open-sea condition after its ability for the simulation had been proved.

3.4 Measurements of Wave Heights and Determination of Amplification Factor

The wave heights were measured with resistance-type wave gages and recorded with a Sanborn 152-100B two-channel recorder. The gage consists of two parallel platinum wires, 0.028 in. diameter and 3/16 in. apart (see Ippen and Raichlen [1962] for the detail of the wave gage). Since the test waves were of small heights, 0.05 to 1.0 in., a dynamic calibration test was conducted before the experiment of wave energy dissipators (see Ippen and Goda [1963]). A wave gage was attached to a vertically oscillating arm and forced to oscillate in the undisturbed water of a pail. From the records of such oscillations and statical calibration curves, the amplitudes of the oscillations were calculated and compared with the stroke of the oscillating arm which was measured mechanically. The comparison showed that the error involved in the measurement of wave height with the wave gage was less than ±5 per cent for the wave height of 0.15 to 1.5 in.

The determination of amplification factors requires two measurements of wave heights, outside and inside the harbor. As for the outside wave height, the standing wave height at the harbor entrance when the harbor was closed was employed as an approximate value. (It was almost impossible to obtain the incident wave height when the harbor was open, because the wave system outside the harbor was that of standing waves superimposed with the outgoing waves radiated from the harbor entrance.) Thus, the experimental amplification factor was calculated by:

$$\mathbb{R} = \frac{H_{inside}}{2a} \simeq \frac{H_{inside}}{H_{closed}} \qquad (3.5)$$

where: a = amplitude of outside standing wave (twice the incident wave amplitude)

H_{inside} = wave height inside the harbor (at a corner of back wall, unless otherwise specified)

H_{closed} = wave height at the harbor entrance when the harbor is closed

The error involved in the approximation may be said to be dependent on the relative size of a main wave basin compared to the model harbor. In the present case, the main basin was considered to be large enough to justify the approximation.

IV. RESULTS OF EXPERIMENTS AND NUMERICAL ANALYSES

4.1 Approach to the Open-Sea Conditions

4.1.1 Criteria for the Open-Sea Conditions

One of the objectives of the present study is to determine the minimum effectiveness of wave energy dissipators to simulate the open-sea conditions in a wave basin. This requires the evaluation of whether the open-sea conditions are satisfied in a wave basin. For the measures of of the evaluation, the following criteria were set up in the course of the experiments:

I. The response of a harbor to the incident wave excitation should be independent of incident wave heights.

II. The frequency response of a harbor should be a smooth curve, free from multi-resonance-spikes such as those demonstrated by Ippen and Raichlen [1962].

III. The outside standing waves should have uniform wave heights.

As seen in equation (2.41), the amplification factor of a harbor connected to the open-sea has no term of wave amplitudes. Hence, it is independent of incident wave heights. If the wave filters and absorbers are effective enough, the criterion I will be satisfied. However, if the dissipators are not effective enough, a part of outgoing wave energy radiated from the harbor will remain in the main basin and distort the amplification factor. The remaining wave energy is a function of effectiveness of energy dissipators. Since the effectiveness of energy dissipators is governed by incident wave steepness, a change in incident wave heights will produce different amplification factor for a given harbor and a given wave period if the dissipators are not effective. This is the purpose of the criterion I.

The effectiveness of the wave energy dissipators is also checked by the criterion II for the frequency response. The term of "frequency response" is used here to denote the response of a harbor basin with a fixed geometry to the waves of varying periods. Another term of "geometry response" will be used later to denote the response of a harbor basin with a varying harbor length to a wave of fixed period. As demonstrated by Ippen and Raichlen [1962], a frequency response of a rectangular harbor in a wave basin without any energy dissipator is characterized by numerous resonant spikes and zero responses. Ippen, Raichlen, and Sullivan [1962] then showed how these spikes on a frequency response were diminished with the increasing effectiveness of wave energy dissipators.

The last criterion, III, concerns the condition of the outside standing wave system. An accumulation of wave energy (represented by high standing wave heights) towards the center of the back wall of the main basin was observed by Ippen, Raichlen, and Sullivan [1962] with effective dissipators. Although the cause of such energy accumulation has not been well explained, it is certainly not the situation in the open-sea and may affect the response curve of a model harbor. Hence, it is desirable to have the outside standing waves as uniform as possible.

4.1.2 Effect of Wave-Energy-Dissipator Efficiency on the Simulation of the Open-Sea Conditions

The first task of the experiment was to choose the correct wave energy dissipator to simulate the open-sea conditions. A simple geometry of a model harbor, a fully open rectangular basin, was chosen to study the effect of the efficiency of wave energy dissipators. The width of the harbor was fixed at 4.5 in. The length of the harbor was varied from 0 to 6.5 in. to produce the "geometry responses" for the wave periods of 0.5 and 0.6 sec. The width of the wave basin was reduced to 6.0 ft. with two temporary side walls so that the analysis of Ippen and Raichlen [1962] and a part of experimental data obtained by Ippen, Raichlen, and Sullivan [1962] could be utilized. After the installation of wave absorbers, a width of 3.2 ft. was left for outside standing waves in the narrow basin.

Four energy dissipators, combinations of wave filters and absorbers listed in Table I, were tested for the "geometry response" of the

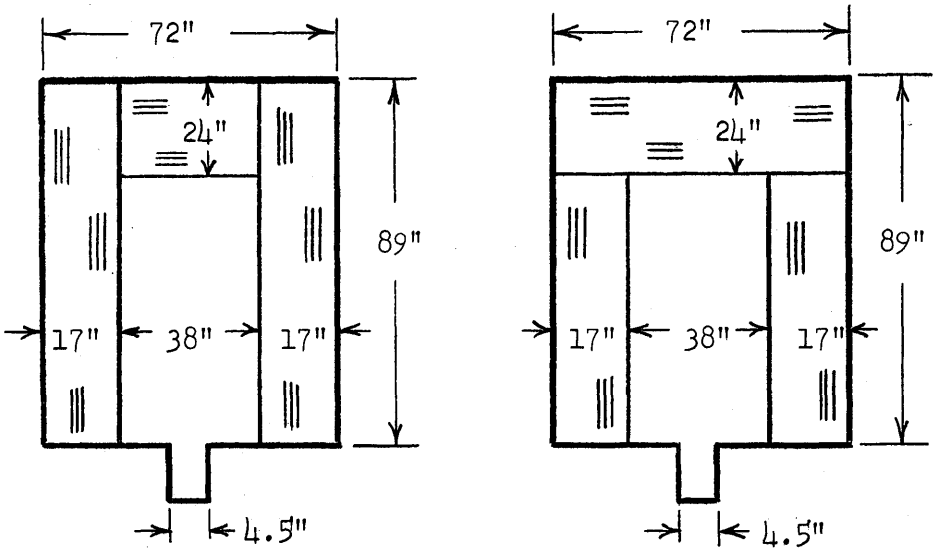

Arrangement A Arrangement B

Figure 10. Arrangements of Wave Energy Dissipators

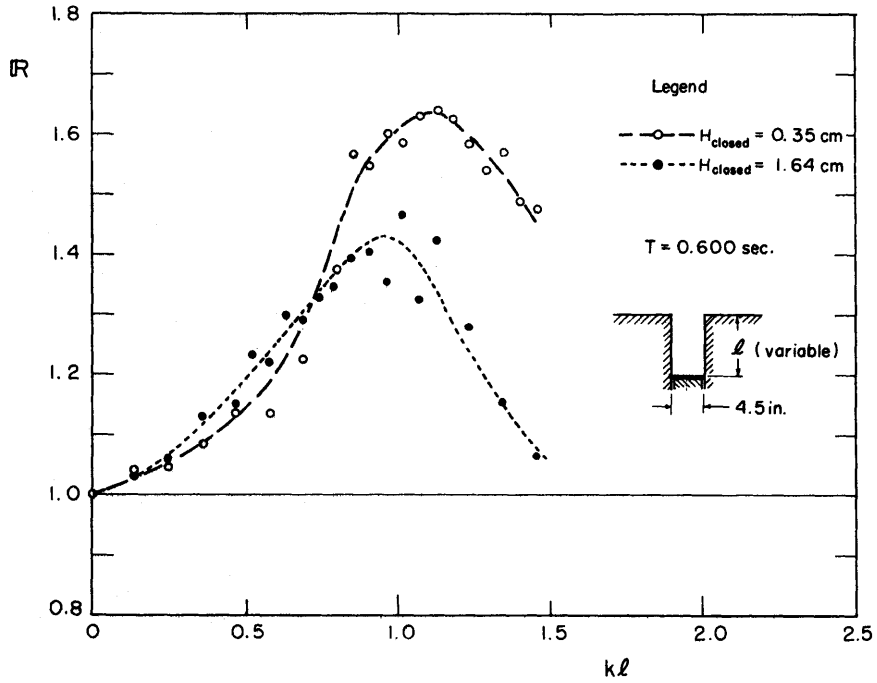

Fig. 11-a. Geometry Response of Test Harbor, Dissipators No. 5

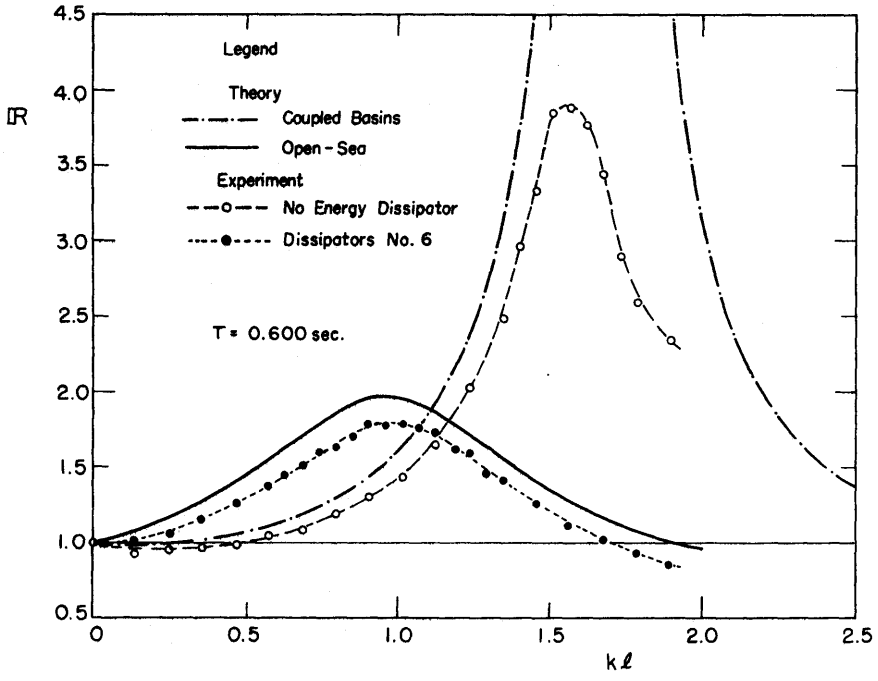

Fig. 11-b. Geometry Response of Test Harbor, No Dissipator & Dissipators No.6

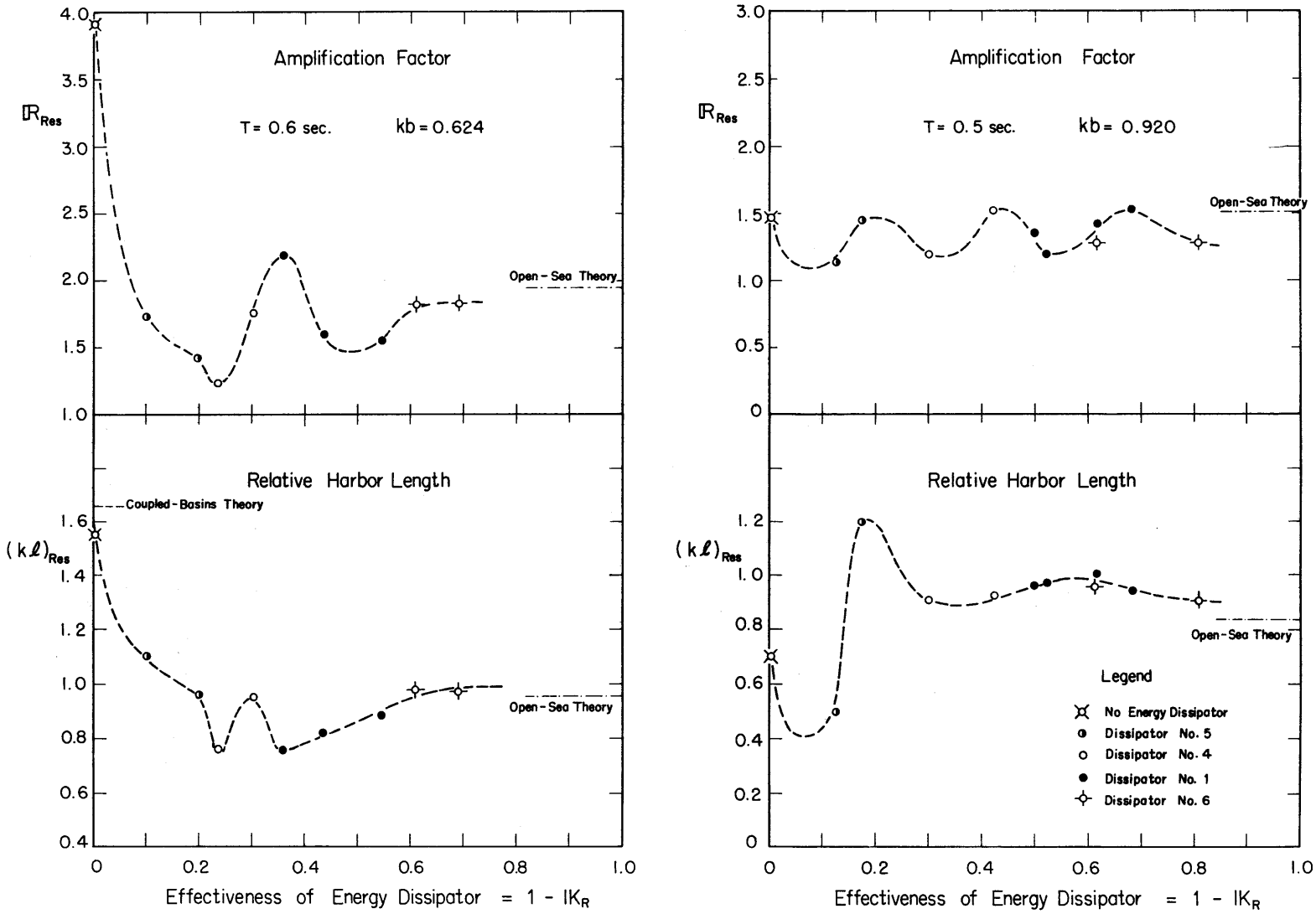

Fig. 12. Variation of Resonant Characteristics due to Changes in Effectiveness of Energy Dissipator

model harbor with two incident wave heights for each period. The arrangements of wave energy dissipators are shown in Figure 10. Arrangement A was used for the dissipators, Nos. 5, 4, and 1. For the dissipator No. 6. however, the different arrangement B (longer wave filters and shorter absorbers) was employed because the arrangement A produced highly distorted outside standing waves. The case of no energy dissipator was also investigated.

A "geometry response" of a fully open rectangular harbor was obtained in the experiments as follows. The back wall of the harbor was moved to the harbor entrance (the harbor closed) and the outside standing wave height was measured. Then, the back wall and the wave gage were carried back by 0.38 in. each time, and a wave height at each point was measured. This process was repeated until the harbor length became 6.5 in. ($k\ell$ = 2.7 for T = 0.5 sec. and $k\ell$ = 1.9 for T = 0.6 sec). After this backward movement, the back wall and the wave gage were moved forward. The same kind of measurements were taken during the forward movement in the neighborhood of maximum amplification factor so as to eliminate any possible bias associated with the direction of the back wall movement. The outside wave height was measured again at the end of each run. The difference between the first and the last readings of outside standing wave height, if any, was distributed linearly across the measurements made during the run to yield the appropriate value of outside wave height for each inside wave height. The amplification factor for each harbor length was then calculated with equation (3.5) and plotted against the corresponding relative harbor length, $k\ell$. Typical geometry response curves are shown in Figure 11.

Figure 11 clearly demonstrates how geometry response curves are affected by the effectiveness of wave energy dissipators. In Figure 11-a, two geometry response curves with the dissipators No. 5 are presented. The only difference in experimental conditions is the outside standing wave height, 0.35 versus 1.64 cm. The wave period is 0.6 sec. for both response curves. The difference in the two response curves is only explained as the difference in the effectiveness of the energy dissipators due to different incident wave steepness. A comparison of the case of no energy dissipators and the case for the most effective dissipators (No. 6) is shown in Figure 11-b. The resonant harbor length and amplification factors for the two cases are so different that it is hard to recognize the two response curves as those for the same harbor. The theoretical curve for the first case is reproduced from Ippen, Raichlen, and Sullivan [1962], and the one for the second case is computed from equation (2.44)

The effect of energy dissipating efficiency is more closely examined in Figure 12 where the maximum amplification factors and corresponding relative harbor lengths are plotted against the effectiveness of the wave energy dissipator. The effectiveness of wave energy dissipator is defined here as unity minus the reflection coefficient of the wave absorber, or $(1 - K_R)$. The reflection coefficient is that calculated by equation (3.4) with the steepness of waves incident to the harbor ($H_{closed}/2\lambda$), because the actual steepness of waves incident to the absorber could not be

measured. However, the definition is justified when used to express the relative efficiency of wave energy dissipators for a given size of main wave basin, since the magnitude of outgoing waves is primarily proportional to the height of waves incident to the harbor.

Although the variation of the effectiveness was obtained by the changes of both outside wave heights and the wave energy dissipators themselves, the variations of resonant characteristics are well described by the effectiveness of energy dissipators, thus defined, as shown in Figure 12. As for the case of T = 0.6 sec. (kb = 0.642), both the resonant harbor length and maximum amplification factor start from the values of the coupled-basin theory by Ippen and Raichlen [1962] and move toward the values of the present open-sea theory while showing a kind of damped oscillation, as the effectiveness of the energy dissipators increases. As for the case of T = 0.5 sec. (kb = 0.920), the starting points do not agree with those of the coupled-basin theory. But the resonant harbor length and the maximum amplification factor approach toward the solutions of the open-sea theory, as the effectiveness of energy dissipator increases.

From Figure 12, it may be concluded that the reflection coefficient of the wave absorbers should be 0.2 or less in order to eliminate the variations of resonant characteristics due to the change of incident wave heights, although it is difficult to draw a definite line. The wave filters are also recommended to be more effective than the wave absorbers if the above value is applied to the absorbers, since the wave filters were more effective than the absorbers in the present study.

4.1.3 Effect of Wave Basin Size on the Simulation of the Open-Sea Conditions

Although the wave energy dissipators No. 6 produced a close simulation of the open-sea conditions in the main basin, the extent of the simulation was not satisfactory for two reasons. First, the test harbor showed different geometry responses for two outside wave heights with a period of 0.5 sec. as shown in the upper half of Figure 13. The difference of the two response curves becomes noticeable at the large value of relative harbor length. Second, the outside standing wave was not uniform, but showed a marked increase of the wave height near the harbor entrance.

The left half of Figure 14 shows the transversal wave envelopes along the anti-nodal lines in the narrow basin with the temporary walls when the harbor was closed. The wave period of 0.6 sec. was chosen for the test. If the situation were an exact simulation of the open-sea, these envelopes should have been horizontal lines having the same height. The actual wave envelopes showed increasing wave heights toward the center of the back wall, however. The slopes of the wave envelopes also became steeper near the back wall than near the wave paddle. The cause of such distortion of the wave envelopes is not clear, but it is considered as a phenomenon similar to the diffraction of waves through the gap of a breakwater.

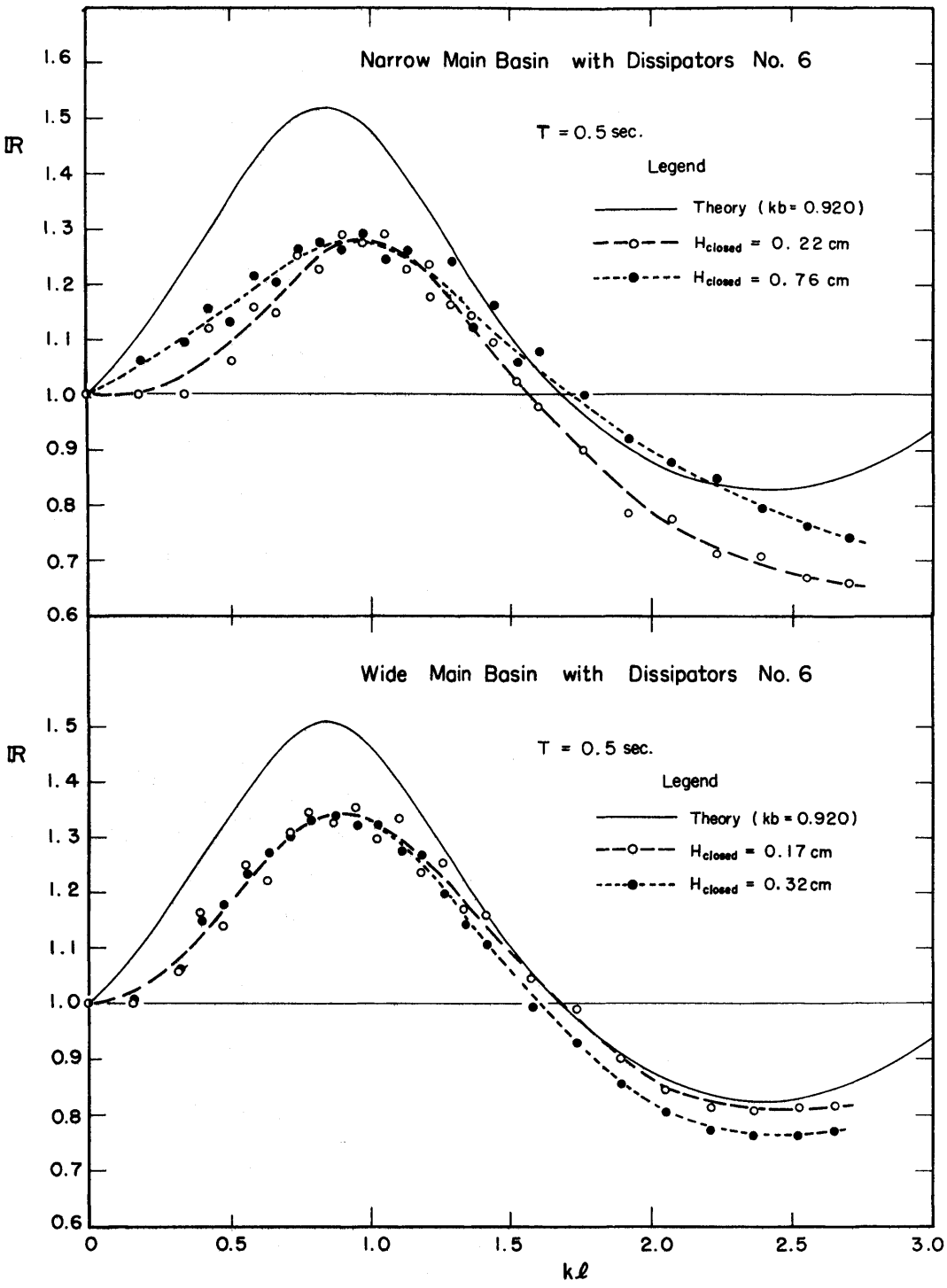

Fig. 13. Geometry Responses of Test Harbor: Effect of Main Basin Size on Simulation of the Open-Sea Conditions

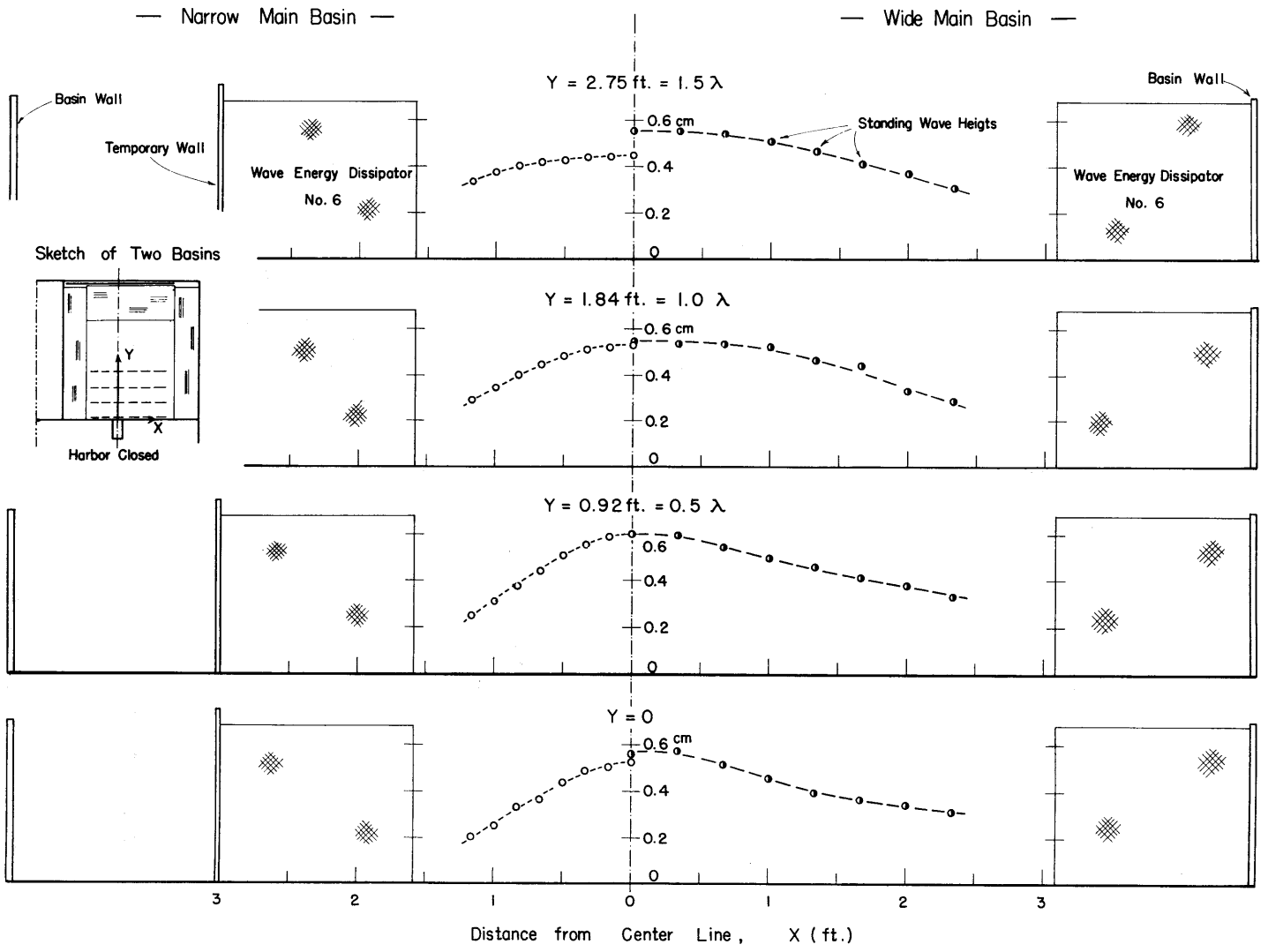

Fig. 14. Transversal Wave Envelopes in Narrow & Wide Main Basins (T = 0.6 sec.)

In order to improve such non-uniformity of outside standing waves, the temporary walls were removed and wave envelopes were measured again in the original basin (9.0 ft. wide) with the wave energy dissipators No. 6 installed as shown in Figure 6. The wave envelopes for T = 0.6 sec. are shown in the right half of Figure 14. Although the transversal wave envelopes are still inclined, the slopes of the envelopes are much flatter than in the narrow basin and the wave heights on the center line are almost the same. Hence, the criterion III for the open-sea conditions is considered to be satisfied practically.

As in the narrow basin, the geometry response of the fully open harbor was then investigated for two wave periods, each with two wave heights. The lower part of Figure 13 shows the geometry response to the waves of T = 0.5 sec. The effect of incident wave height on the response curves which is visible in the upper half of Figure 13 has almost disappeared in the lower half for the case of the original main basin. The geometry response curve to the waves of T = 0.6 sec. was also not affected by the magnitude of incident wave height. Thus, the criterion I for the open-sea conditions is satisfied with the dissipators No. 6 in the wave basin shown in Figure 6. The remaining criterion, II, is also shown to be satisfied; this is discussed in Section 4.2.2. Therefore, the conditions of the "open-sea" can be said to be well simulated in the wave basin with the wave energy dissipators No. 6.

4.2 Resonant Characteristics of Fully Open Rectangular Harbor

4.2.1 Geometry Response of Fully Open Harbor

After the correct basin size and wave energy dissipators had been established, systematic tests of geometry responses of fully open rectangular harbors were conducted to verify the validity of the theory. The choice of the geometry response for the systematic test, as opposed to the frequency response test, was made from the viewpoint of experimental time. However, it should be mentioned again that the resonant conditions obtained through a geometry response test are not the same as those obtained by a frequency response test except for a very narrow harbor as discussed in Section 2.1.6.

The geometry response tests were conducted for four harbor widths, 1.0, 1.678, 2.875, and 4.5 in., each for three wave periods of 0.5, 0.545, and 0.6 sec. With these harbor widths and wave periods, twelve values of the relative harbor half-width, kb, were obtained, ranging from 0.14 to 0.92 (the ratio of the harbor width to the wave length was from 1/22 to 1/3.4). The test procedure was the same as that described in Section 4.1.2. Each experimental response curve was compared with the theoretical one computed from equation 2.44. Figure 15 shows typical experimental and theoretical geometry responses of fully open harbors. Although the change of response curve from one harbor to the other is well predicted with the theory, the experimental amplification factors are smaller than the theoretical ones and all the experimental curves are shifted a little to the right (large value of $k\ell$).

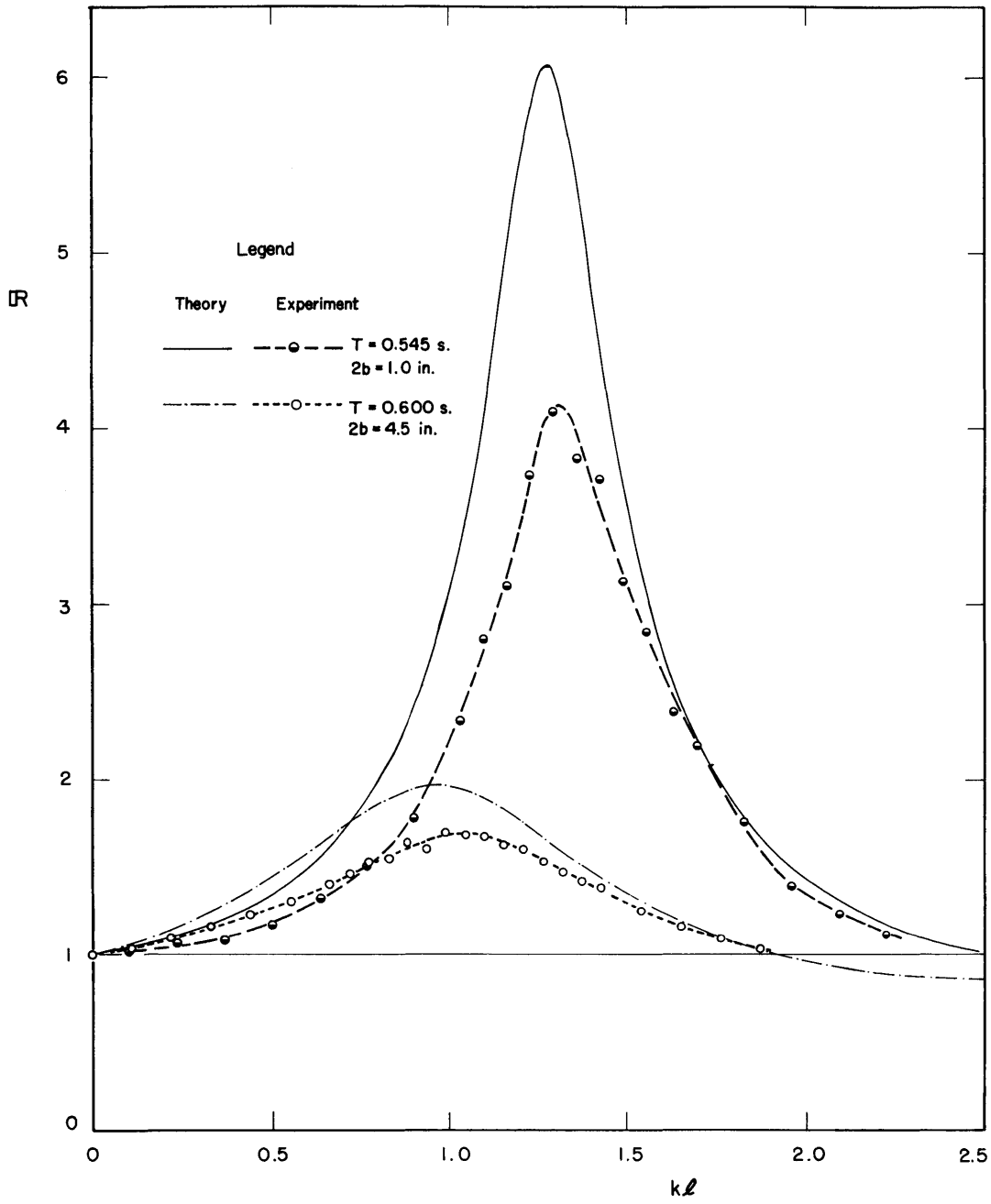

Fig. 15. Typical Geometry Responses of Fully Open Harbors

From such an experimental curve, a resonant point is determined as the point of maximum amplification factor. The relative harbor lengths at resonance and the maximum amplification factors thus obtained are compared to theoretical values by equations (2.47) and (2.48), as shown in Figure 16. The relative harbor half-width, kb, is chosen as the abscissa because it is the parameter which governs the geometry response. Figure 16 clearly shows the increases of resonant harbor length and the maximum amplification factor with the decrease of kb.

It is seen in Figure 16 that the experimental harbor length at resonance is longer than the theoretical one as indicated in Figure 15. The difference is approximately proportional to the value of kb, or roughly to the harbor width. This suggests a kind of contraction factor at the entrance. Figure 17 shows the path-line patterns of surface particles under the wave motions at resonance and anti-resonance. It is clear in Figure 17 that there is a contraction of path-lines at the harbor entrance at resonance. The wave motion inside the harbor shows a tendency toward a two-dimensional motion, though the theory predicts a one-dimensional motion. This contraction of path-lines is considered responsible for the decrease in the effective harbor width and thus the increase in the resonant length of a harbor.

The maximum amplification factors shown in the right half of Figure 16 are smaller than those predicted by the theory for the ideal fluid. However, the discrepancy is well explained as the effect of a small amount of energy dissipation inside the harbors. The experimental maximum amplification factors are located between two theoretical curves with reflection coefficients of 0.9 and 0.8 computed from equation (2.57).

In the harbors tested, there were three causes of energy dissipation: eddies around the entrance, friction along the side walls, and leakage through the gaps between the side walls and the moving back wall. Of the three causes, only the amount of the side-wall friction may be estimated reasonably. For the progressive waves, Hunt [1952] has derived the rate of wave amplitude attenuation due to the friction along the side walls and on the bottom of a rectangular channel as:

$$H = H_o e^{-Kx} \tag{4.1}$$

where: K = attenuation factor $= \frac{2k}{B}\sqrt{\frac{\nu}{2\sigma}}\ \frac{kB + \sinh 2kh}{2kh + \sinh 2kh}$

B = channel width

ν = viscosity

Since the waves are deep water waves and the amount of energy dissipation is small, the reflection coefficient due to the side wall friction is approximated from equation (4.1) as:

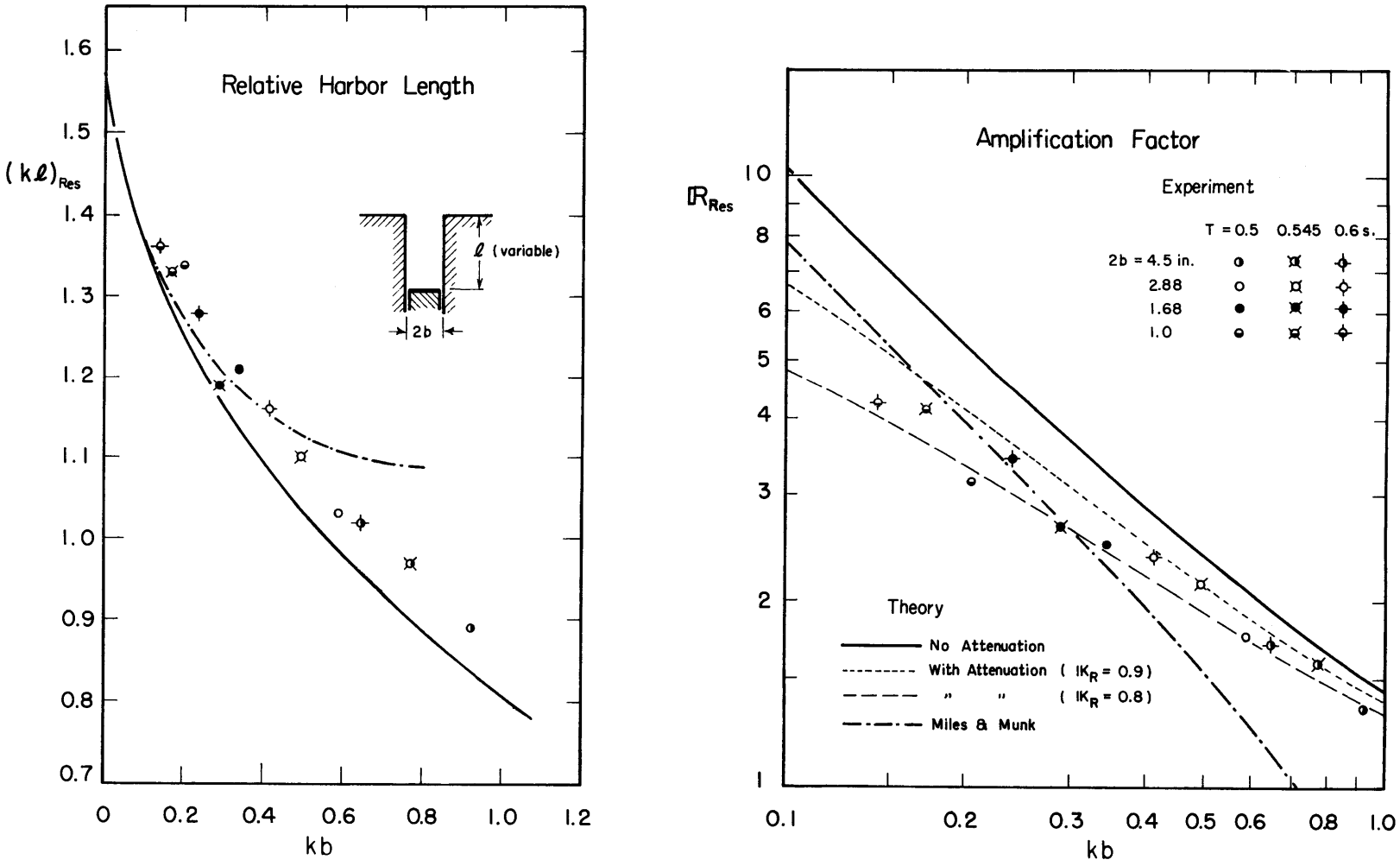

Fig. 16. Resonant Characteristics of Fully Open Harbor with Varying Length

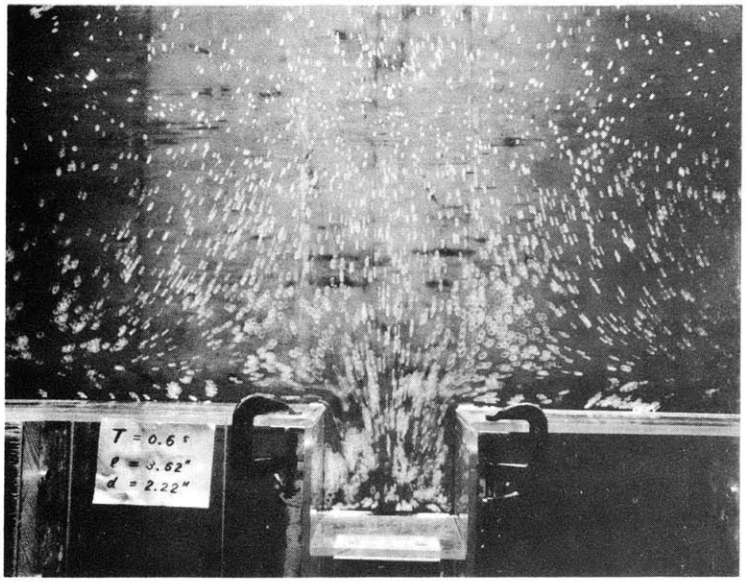

Resonance (T = 0.6 sec.)

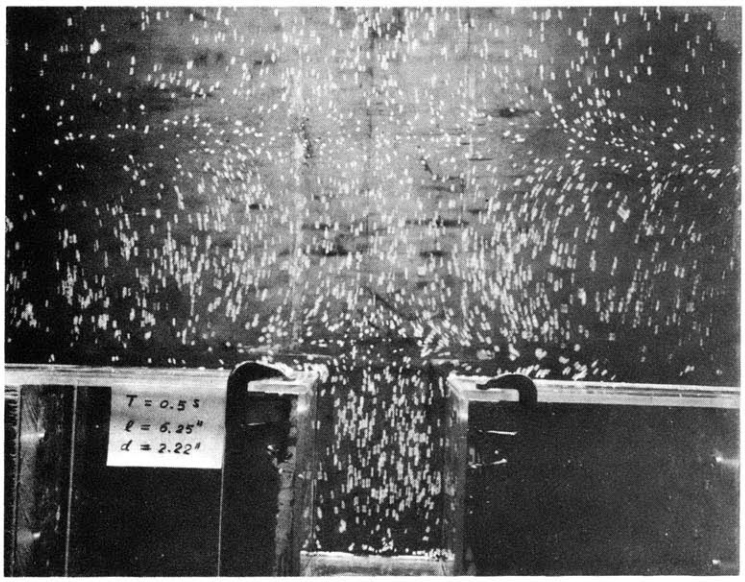

Anti-Resonance (T = 0.5 sec.)

Fig. 17. Path-line Patterns, Fully Open Harbor

$$1 - K_R = 1 - e^{-2K\ell} \simeq \frac{2k\ell}{(2b)}\sqrt{\frac{\nu T}{\pi}} \qquad (4.2)$$

This equation gives the attenuation rate of 4.1 per cent for the harbor width of 1.0 in. and 0.6 per cent for 4.5 in. If another 10 per cent of amplitude attenuation is presumed for the other two energy dissipations and added to the above frictional damping, the resultant attenuation rate of 11 ~14 per cent presents a well fitting theoretical curve for the experimental amplification factor.

Figure 16 also shows the theoretical values of Miles and Munk [1961]. Their resonant harbor length and amplification factor are rewritten with the present notations as:

$$(k\ell)_{Res} = \cot^{-1}\left\{2kb\,[0.478 - \frac{1}{\pi}\,\ell n(2kb)]\right\} \qquad (4.3)$$

$$K_{Res} = \frac{1}{2kb}\,\frac{2k\ell + \sin 2k\ell}{1 - \cos 2k\ell} - \frac{1}{\pi} \qquad (4.4)$$

Although these equations show some agreements with the experimental data for the region of $kb < 0.3$, the overall tendencies of these equations are different from the experimental data and the present theory.

4.2.2 Frequency Response of Fully Open Harbor

Since the geometry response of fully open rectangular harbors was proved to be well predicted with the present theory, a frequency response test was then conducted. A model harbor (12.25 in. long and 2.375 in. wide) was set in the basin and the periods of incident waves were varied from 0.5 sec. to 1.38 sec. with an increment of about 1.5 per cent each time. The relative harbor length was decreased from 5.0 to 0.98 as the period increased. The stroke of the wave paddle at the water surface was adjusted from 0.16 to 0.63 in. so that the incident wave heights would be of the same order of magnitude. For each wave period, the outside wave height at the entrance when the harbor was closed and the inside wave height at the back wall when the harbor was opened were measured, and the corresponding amplification factor was calculated from equation (3.5). The plotting of amplification factor versus relative harbor length gave the experimental frequency response curve which is shown in Figure 18. The theoretical curve is that computed from equation (2.44) for $2b/\ell = 0.194$ for this case. Although there are some fluctuations of experimental data around the fundamental mode of resonance, good agreement between experimental data and theory is observed for the wide range of $k\ell$.

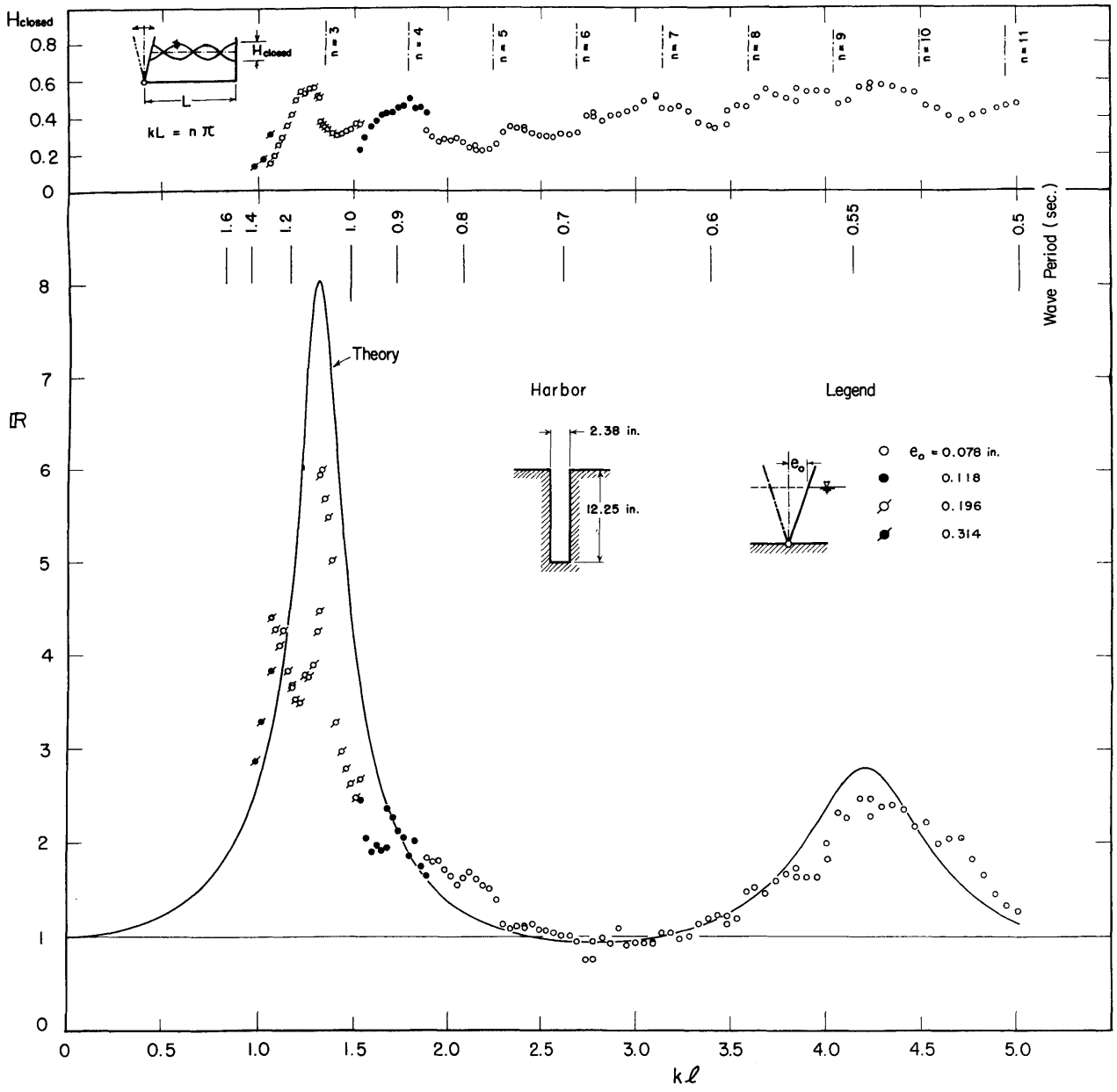

Fig. 18. Frequency Response of a Fully Open Harbor and Variation of Outside Standing Wave Height with Wave Period

Since there is no spike of amplification factor for the range of $k\ell$ greater than 2.0, it can be said that the open-sea conditions are well simulated in the main basin according to the criterion III of Section 4.1.1. The general agreement between the experimental frequency response and the theoretical one proves the applicability of the present theory.

The fluctuations of the experimental amplification factors around the fundamental mode of resonance are mainly due to the inefficiency of wave energy dissipators for the very low steepness of the incident waves. The wave length in this range was three to five times longer than the length near the second resonant mode and the wave height was about one half; hence, very low wave steepness. As shown in the upper part of Figure 18, the magnitude of outside wave height fluctuation does increase as the wave period becomes long, indicating the increasing transmission coefficient of wave filters. The maximum points of this wave height fluctuation roughly correspond to the resonant points of the main wave basin. The positions and numbers of modes of resonance with the effective basin length of 7.0 ft. are indicated in the figure. Such fluctuations of standing wave heights are inevitable in the experiments of resonant oscillations in harbors. An increase in the effectiveness of wave filters will diminish the amplitude of fluctuations, but the fluctuation itself cannot be eliminated unless the wave filters dissipate all incident wave energy. (Some analysis of the action of wave filters in the standing wave system is presented in Ippen and Goda [1963].)

4.3 Resonant Characteristics of Partially Open Symmetrical Harbors

4.3.1 Numerical Analysis

The partially open harbor with the entrance at the center has a second parameter of the opening ratio, d/b, which governs the resonant characteristics with the first parameter of the aspect ratio, $2b/\ell$; the response of a fully open harbor is readily determined with the parameter, $2b/\ell$, and the variable, $k\ell$. Since the combination of the two parameters produces a number of harbor geometries to be analyzed, the approach by a numerical analysis was taken first, and then some of them were compared with the experimental results.

The numerical analysis was based on equation (2.42) with equations (2.34.1), (2.34.2), (2.37), and (2.43) for the case of $\varepsilon = 1/2$. For a given harbor geometry, or given values of d/b and $2b/\ell$, successive computations of the amplification factor were ordered from the IBM 7090 digital computer at the Computation Center in M.I.T. with a small increment of the relative harbor length, $k\ell$ (see Appendix B for the computer program). The frequency response of the specific harbor was then constructed by plotting the amplification factor versus the relative harbor length. Figure 19 shows some of these frequency responses. A narrow harbor ($2b/\ell = 0.2$) and a wide harbor ($2b/\ell = 2$) with varying opening ratios (d/b = 0.01, 0.1, and 1.0) are chosen as the examples.

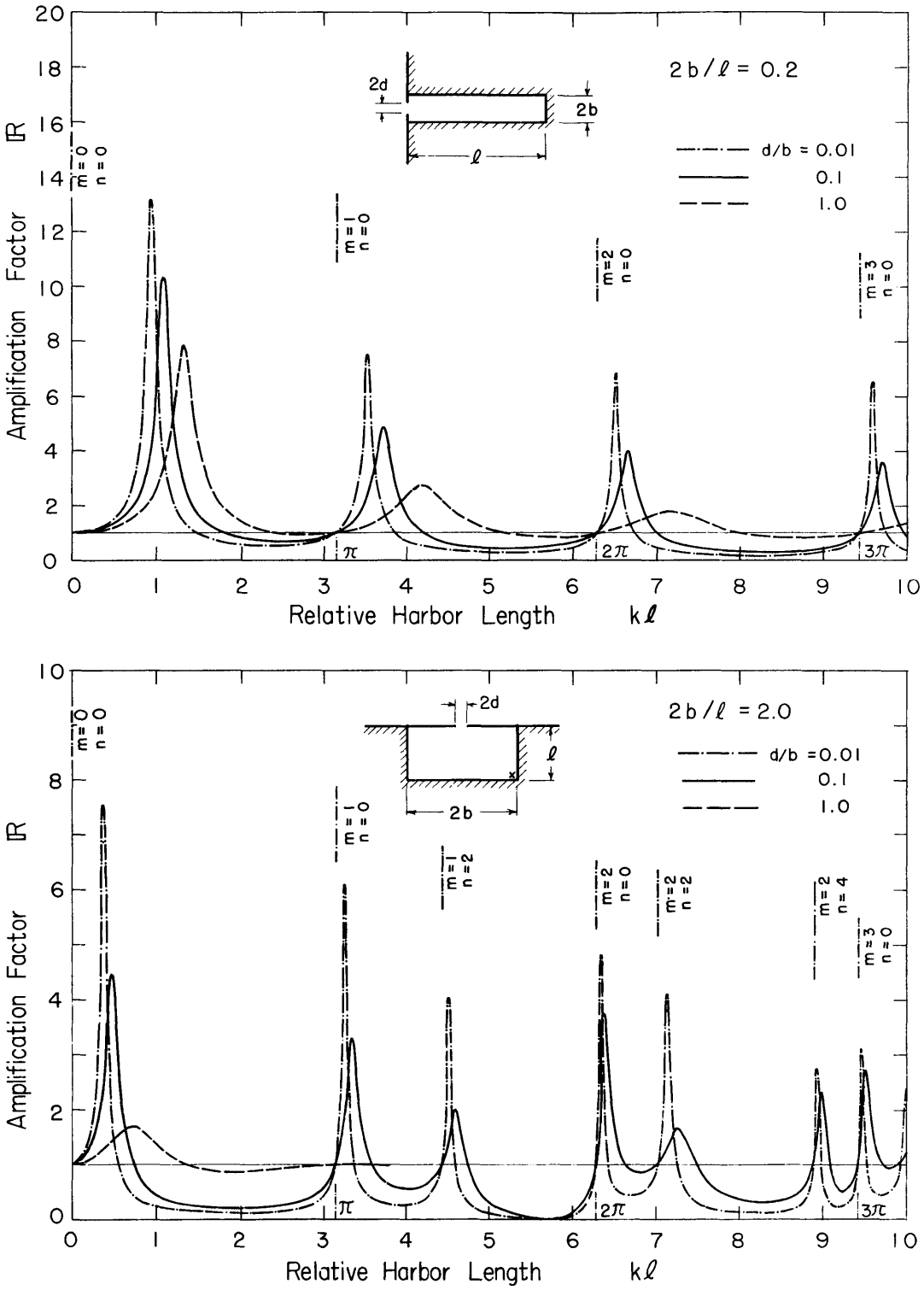

Fig. 19. Theoretical Frequency Response Curves of Symmetrical Harbors

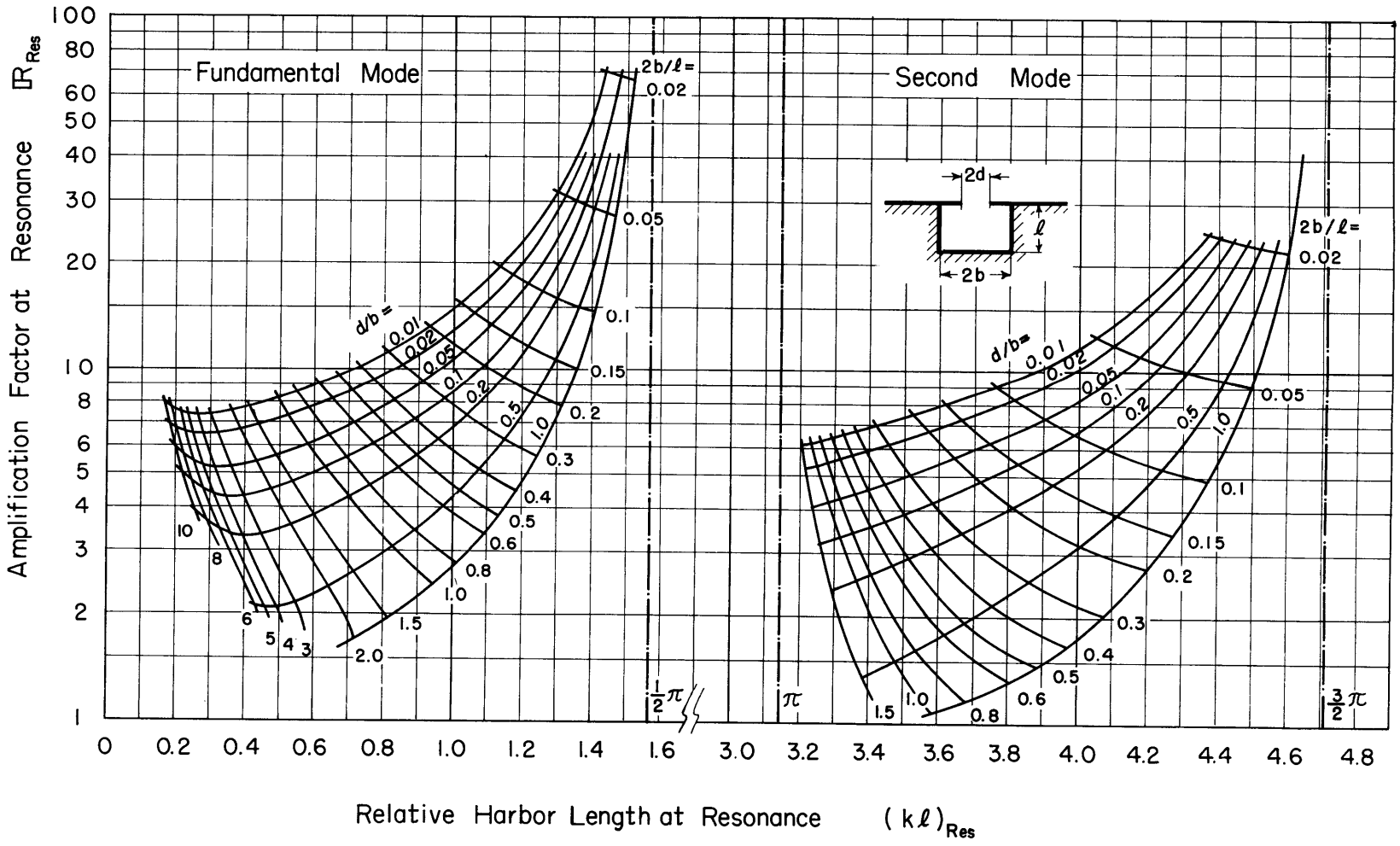

Fig. 20. Resonant Length & Amplification Factor of Symmetrical Rectangular Harbor

From this figure, several characteristics of a symmetrical rectangular harbor are evident. First of all, the narrowing of the harbor entrance leads to higher amplification factors at resonance and to longer resonant periods. This seems to confirm what was called the "Harbor Paradox" by Miles and Munk [1961] and criticized by engineers as contradictory to experimental data and field observation (Wilson [1962]). However, the increasing sharpness of the response curve reduces the realization of the harbor paradox in actual harbors (see Chapter V for more discussions). Second, the relative harbor length at resonance approaches toward that of the enclosed basin, equation (1.2), as the harbor entrance is narrowed down. Since this is what is expected, this may serve as another proof for the validity of the present theory. The difference between the resonant conditions of a partially open harbor and an enclosed basin becomes smaller as the harbor becomes wider. Hence, equation (1.2) may be used as an approximation to the exact solution of resonant periods for a wide rectangular harbor basin with small corrections toward shorter periods. Third, a partially open harbor has large amplification factors at higher modes of resonance; hence every possible resonant period should be taken into account in the design of a rectangular harbor basin with a partial opening.

In order to examine these characteristics more closely, the variations of amplification factors around the fundamental and second modes of resonance were computed for nearly 140 geometries of rectangular harbors. The results of these computations are compiled in Figure 20 which shows the relative harbor length at resonance as the abscissa and the corresponding amplification factor as the ordinate. The case of a fully open harbor is represented here with the most right-hand curve of a family of curves with positive slopes. The curve shows that both the relative harbor length and amplification factor at resonance decrease as the harbor becomes wide. The effect of the opening ratio on the resonant characteristics is evaluated with a family of curves with negative slopes. A narrowing of the entrance is thus shown to result in the shortening of relative harbor length and in the increase of amplification factor. At the same time, Figure 20 serves a good design chart on the resonant oscillations of rectangular harbors, showing the locations and magnitudes of resonant oscillations. As an example, take a rectangular harbor of a length of 3,000 ft. and of a width of 2,000 ft. with an opening of 500 ft. at the center. Then, the relative harbor lengths at the first and second resonant modes are read from Figure 20 as 0.83 and 3.47 for the corresponding aspect ratio of 0.67 and the opening ratio of 0.25. The resonant wave lengths are therefore 22,700 and 5,430 ft., respectively. If the water depth of the harbor is 40 ft., this gives the resonant periods of 10.5 and 2.52 minutes, respectively. At these resonant periods, the amplification factors may be as high as 4.8 and 2.4.

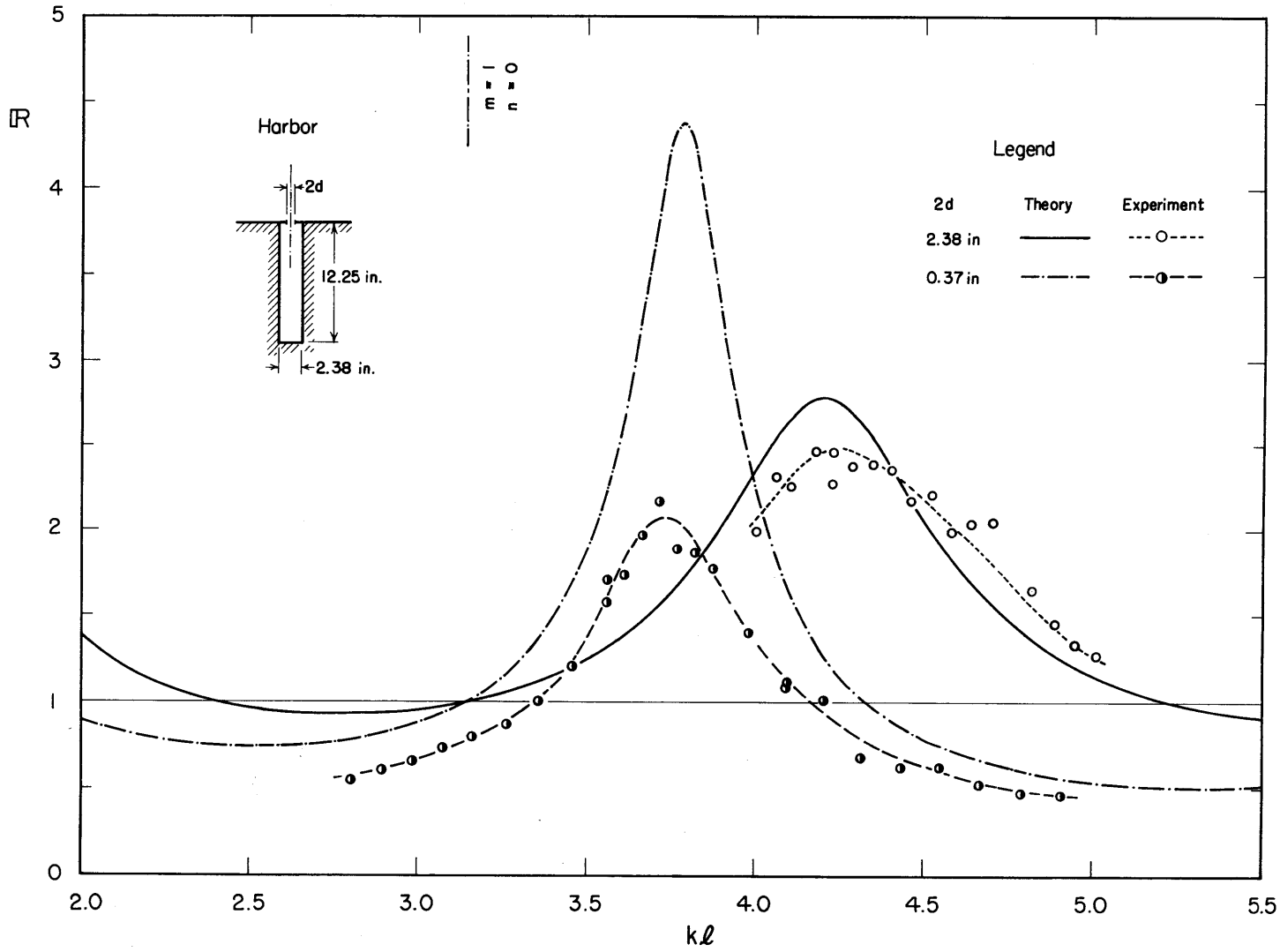

Fig. 21. Frequency Response of a Narrow Harbor, Fully Open & Partially Open

4.3.2 Comparison of the Theory with the Experiments

The experiments on the frequency response were carried out for three shapes of partially open rectangular harbors: narrow, square, and wide. The theoretical and experimental frequency response curves of these harbors are shown in Figures 21, 22, and 23.

The comparison of the response curves of the fully and partially open narrow harbors is given in Figure 21. The harbor is 12.25 in. long and 2.375 in. wide, which is the same as that of Figure 18, and a part of frequency response curve of the fully open harbor is reproduced here for the comparison. When the harbor entrance is narrowed to 0.37 in. ($d/b = 0.156$), the location of the second resonant mode is shifted to the left-hand side (or in reference to Figure 18 to the longer wave period). The distance of the shift obtained experimentally is in good agreement with the theoretical one. However, the experimental amplification factor at resonance does not rise higher than that of the fully open harbor, although the theoretical amplification factor of the partially open harbor is nearly twice that of the fully open harbor. This is regarded as the effect of energy dissipation around the entrance caused by strong oscillating flow through the narrow opening.

The effect of the harbor opening on the frequency response curve is more fully examined in Figure 22 which shows the frequency response curves of a square harbor (12 in. in length and width) for three different openings (6.0, 1.67, and 0.37 in.). As found above, a narrowing of the harbor entrance reduces the relative harbor length at resonance, but it also increases the resonant amplification factor. These effects of the narrowing of the entrance are confirmed in part by the experiment. First, the shift of the relative harbor length at resonance observed in the experiment agrees very well with the shift of the theoretical relative harbor length at resonance; the difference between the theoretical and experimental resonant points is less than 2 per cent. On the other hand, the experimental amplification factor near resonance shows a marked decrease from the theoretical one. When the harbor entrance is wide ($d/b = 0.5$), the difference is negligible so that the agreement between the theory and the experiment is excellent over the range of $k\ell$ from 2.8 to 4.9. When the entrance is reduced to 1.67 in. ($d/b = 0.139$), the experimental amplification factor at resonance rises to 1.8 from 1.4 which is for the case of wider opening (thus confirming the harbor paradox), but it is far less than the theorectical one of 2.9. Nevertheless, the experimental data other than in the vicinity of the resonant point shows good agreement with the theoretical frequency response curve. When the entrance is further reduced to 0.37 in. ($d/b = 0.031$), the experimental amplification factor at resonance does not rise but falls from 1.8 to 1.5 while the theoretical one shows the high value of 4.8. The agreement between the theoretical and experimental response is not as good as for the cases of wider openings. The decrease in the experimental amplification factor around the resonant points is due to the energy dissipation around the narrow harbor entrance. It should be

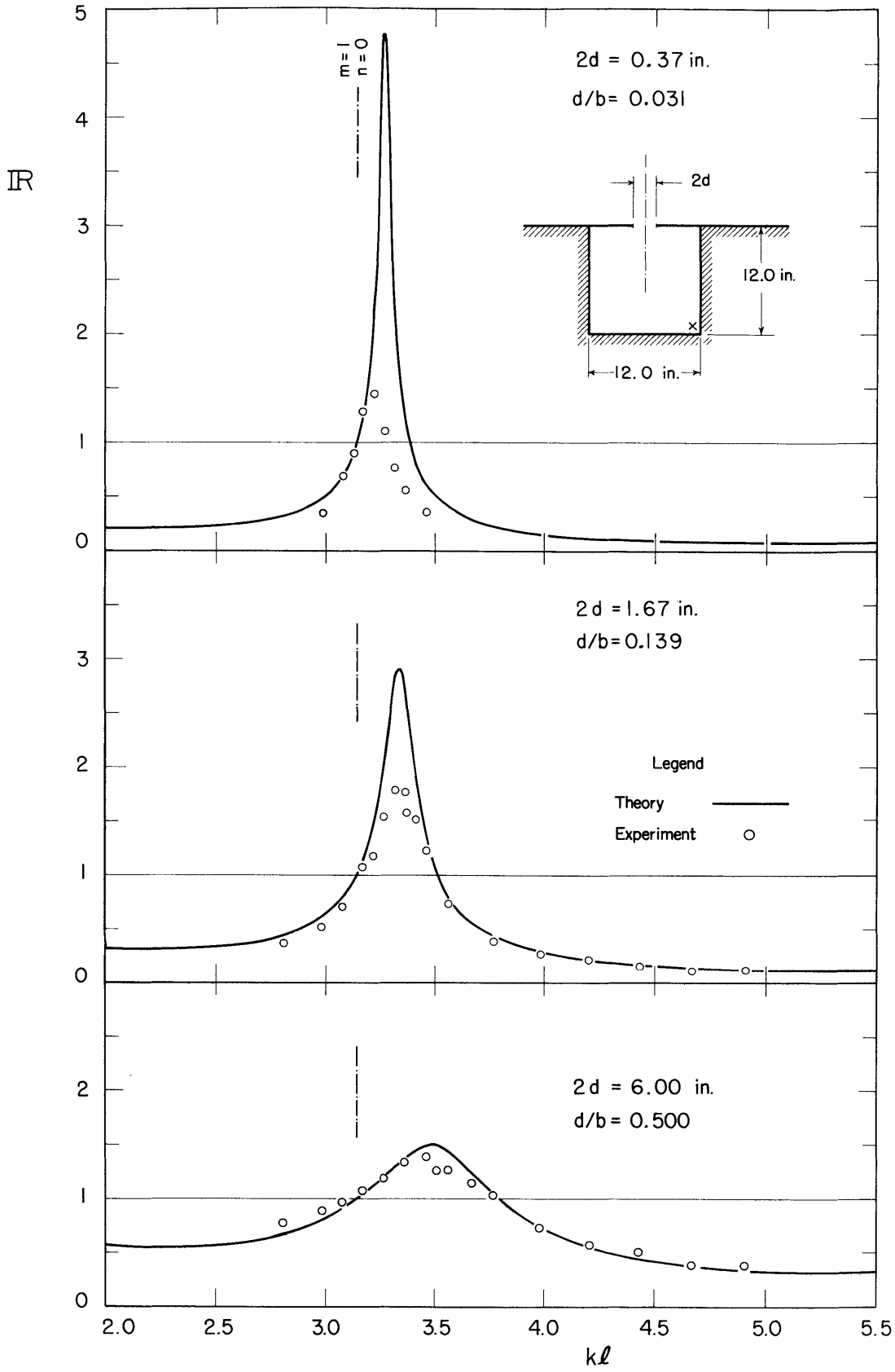

Fig. 22. Frequency Responses of Square Harbors with Partial Openings

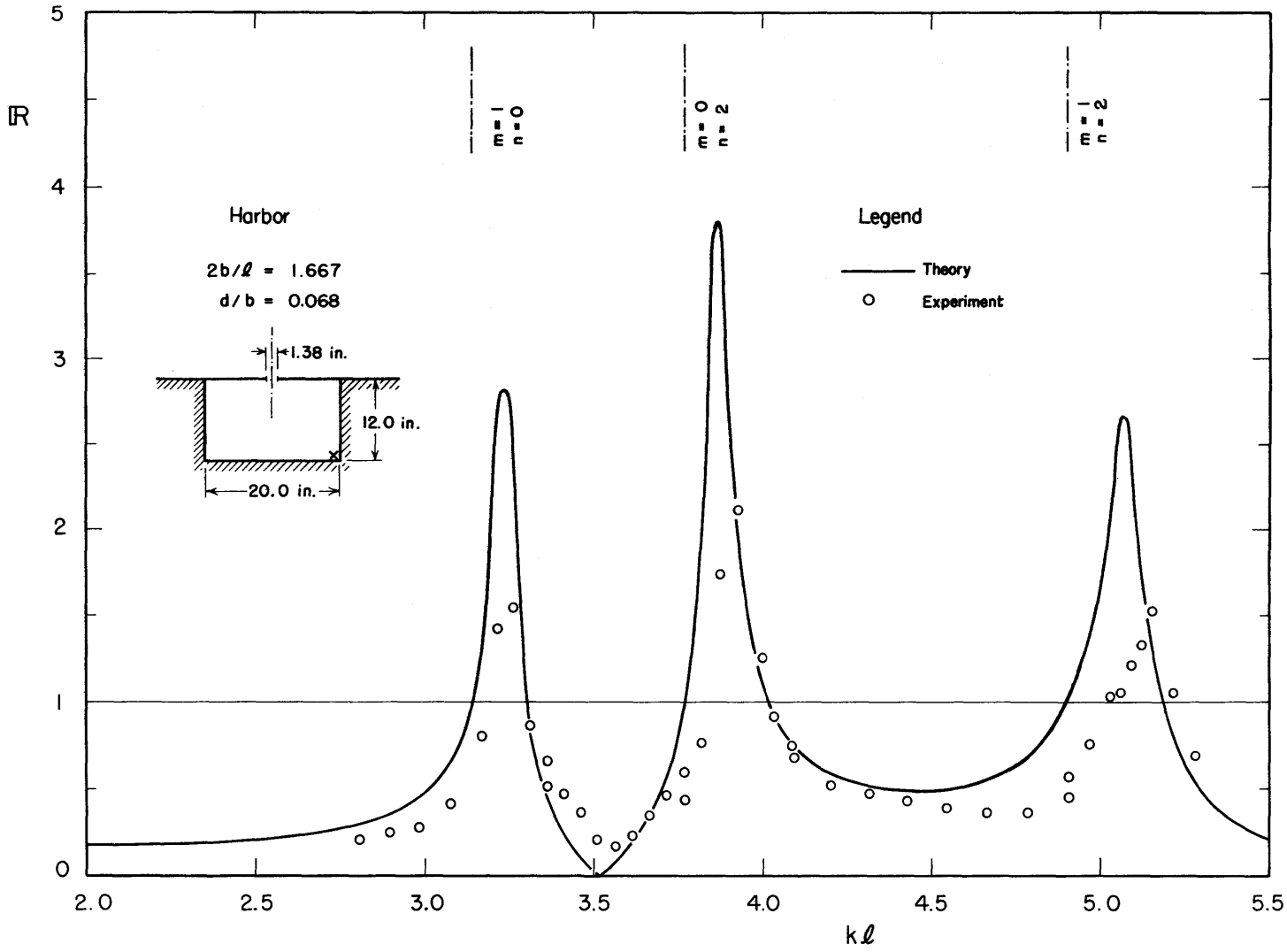

Fig. 23. Frequency Response of a Wide Harbor with a Partial Opening

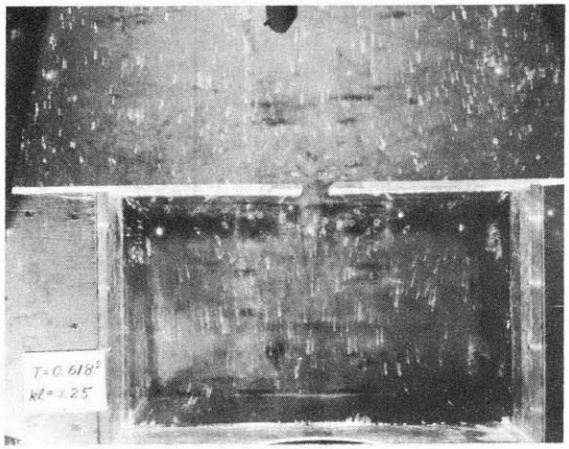

Resonance [m = 1, n = 0]
T = 0.618 sec.

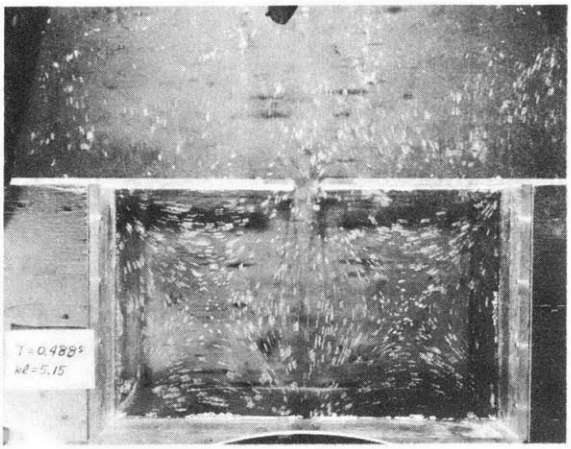

Resonance [m = 1, n = 2]
T = 0.488 sec.

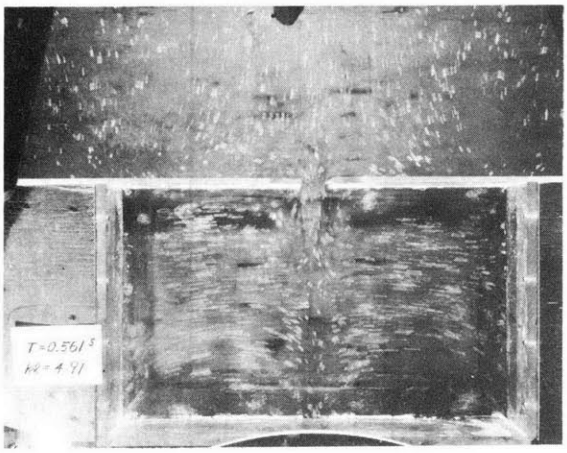

Resonance [m = 0, n = 2]
T = 0.561 sec.

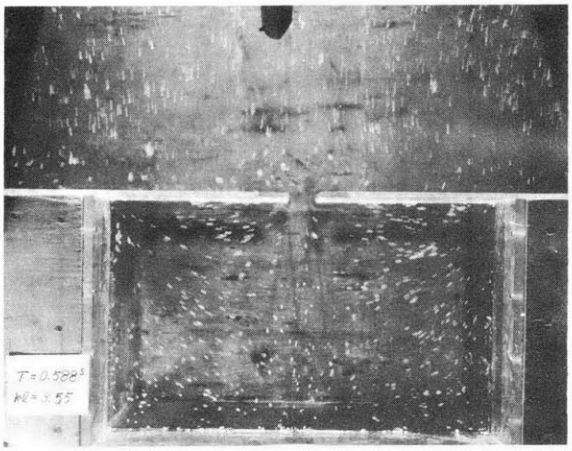

Zero-Response at the Back Corners
T = 0.588 sec.

Fig. 24. Path-line Pattern, Partially Open Harbor

noted however that the resonant peak of the theoretical frequency response curve of this harbor ($d/b = 0.031$) is so sharp that the range of $k\ell$ where $\mathbb{R} \geq 1$ is only 0.25 or ± 4 per cent of $(k\ell)_{Res.}$

The case of multi-resonant modes is presented in Figure 23 which shows the frequency response curve of a wide harbor with length of 12 in., width of 20 in., and opening of 1.35 in. ($2b/\ell = 1.667$ and $d/b = 0.068$). This harbor has three resonant periods for the range of $k\ell$ from 2.0 to 5.5, corresponding to the resonant modes of [m = 1, n = 0], [m = 0, n = 2], and [m = 1, n = 2]. The locations of these resonant points for an enclosed basin are indicated in Figure 23 with the numbers of mode. The wave patterns at these resonant modes are shown in Figure 24 with path-line patterns of surface particles. The nodal lines are represented with long path-lines. It will be noted that the numbers of transversal and longitudinal nodal lines are exactly the same as m and n. The experimental resonant periods at these modes show some differences with the theoretical ones; however, the differences are less than 2 per cent. The experimental amplification factors at resonance are again smaller than the theoretical ones. Since the frictional energy dissipation along the side and back walls is considered negligible for this wide harbor, the energy dissipation is mainly due to eddies around the entrance. But its magnitude could not be as large as in the narrow harbor. This may imply that the effect of energy dissipation inside the harbor on the amplification factor is enlarged when the sharpness of a frequency response curve increases.

One comment should be made on the point of zero response ($\mathbb{R} = 0$ at $k\ell = 3.52$). Since the amplification factor $\mathbb{R}$ is computed by equation (2.42) and measured at a corner of the back wall, a zero response simply means that the amplitude at a corner of the back wall is null; other locations have some amplitudes. The picture at the lower right of Figure 24 shows the wave pattern inside the harbor when the back corner has a zero response.

4.4 Resonant Characteristics of Asymmetric Harbor

The frequency response of an asymmetric harbor is governed by three parameters: they are the aspect ratio, $2b/\ell$, the opening ratio, d/b, and the relative location of the entrance, ε. The last parameter ε characterizes an asymmetric harbor opening. The most characteristic feature of an asymmetric harbor is the occurrence of transverse resonant oscillations of odd modes which are not experienced in a symmetrical harbor as already discussed in Section 2.1.5. This feature is clearly seen in the frequency response curves of two asymmetric harbors ($2b/\ell = 1.0$ and 2.0) computed numerically and shown in Figure 25. The computation was carried out in a manner similar to that of a symmetrical harbor, except for the addition of odd terms of the series S_1 and S_2. The reader is referred to Appendix B for the computer programming.

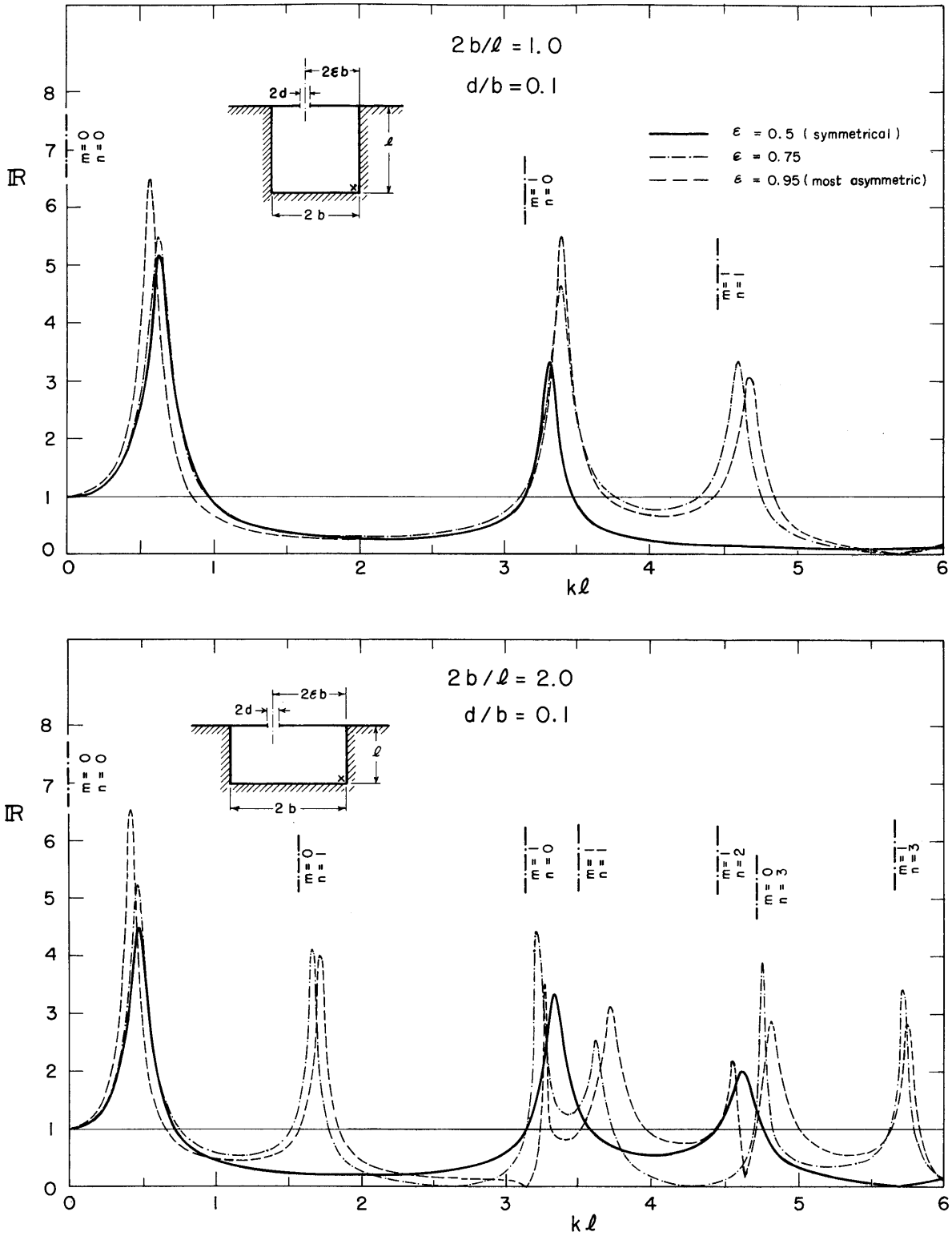

Fig. 25. Theoretical Frequency Response Curves of Asymmetric Harbors

The case of the square harbor is shown in the upper half of the figure and the case of the wide harbor in the lower half. The entrance width which is one tenth of the harbor width is located either at one side ($\varepsilon = 0.95$), at an intermediate position ($\varepsilon = 0.75$), or at the center ($\varepsilon = 0.5$, i.e., symmetrical harbor). Compared to the symmetrical harbors, there appears one additional transverse resonant mode for the square harbor and four for the wide harbor over the range of $k\ell$ from 0 to 6.0. These new resonant peaks are comparable in height with the peaks for symmetrical harbors and cannot be neglected. The locations of the new peaks are closely approximated by those computed for enclosed basins (equation (1.2)) which are indicated with short segments of dash-dot lines in Figure 25.

Another feature of asymmetric harbors is the possible increase of amplification factors due to superposition of longitudinal and transverse oscillations in comparison to those of symmetrical harbors, indicating more severe action of resonant oscillations. For example, the resonant amplification factor of the square harbor at the second mode of $m = 1$ and $n = 0$ increases from the value of 3.3 for the symmetrical case to 5.5 for the case of the entrance at one side. Thus, with the relocation of the entrance from the center to the side, a partially open rectangular harbor seems to be more severely affected by resonant oscillations. In other words, the entrance at the center of a harbor seems to provide less trouble with respect to resonant oscillations.

These two features of resonant characteristics of asymmetric harbors - occurrence of transverse resonant oscillations of odd modes and possible increase of resonant amplification factor - were confirmed in the experiment. Figure 26 shows the experimental frequency response curve as well as the theoretical one of a square harbor with an entrance at one side. The length, width, and opening are the same as those of the symmetrical harbor shown in the middle of Figure 22. While the symmetrical harbor in Figure 22 shows only one resonant peak of $R_{Res} = 1.8$ at $k\ell = 3.34$, the asymmetric harbor with the same dimension shows two resonant peaks of $R_{Res} = 3.0$ at $k\ell = 3.39$ and of $R_{Res} = 1.5$ at $k\ell = 4.70$. The first peak of the asymmetric harbor is higher than that of the symmetrical harbor and the second peak appears where no peak is observed in the case of the symmetrical harbor. Comparing the theoretical and experimental amplification factors, it is seen that the agreement is good near $k\ell = \pi$, but in other zones the experimental values appear below the theoretical ones. This is expected in view of the effect of energy dissipation, because there is little oscillating flow through the entrance near $k\ell = \pi$ (hence little energy dissipation), but the oscillating flow increases in intensity as $k\ell$ exceeds the value of π.

At this point, the question arises as to what will happen to the transverse oscillations of odd resonant modes when the location of the entrance is moved from one side toward the center. The question was studied both numerically and experimentally. Figure 27 shows the results of the investigation. The dimension of the model harbor is the same as that

analyzed in Figures 22 and 26, but the location of the entrance varies by a small increment of distance from the side wall. For each harbor, the location of resonant oscillation of odd mode of m = 1 and n = 1, $(k\ell)_{Res.}$, and the resonant amplification factor, $\mathbb{R}_{Res.}$, were sought by numerical analysis and by the experiment. The lower part of Figure 27 shows the theoretical and experimental resonant amplification factors and the upper part shows the relative harbor length at resonance.

Theoretically, the resonant amplification factor at the odd transverse mode increases very rapidly as the entrance is moved toward the center, and there seems no upper limit on the increase of the resonant amplification factor (see sketch to the left-hand side of Figure 27). Nevertheless, if the entrance is exactly at the center, there can be no resonant oscillation. Thus the value of $\varepsilon = 1/2$ presents a singularity* with respect to transverse resonant oscillation. This kind of singularity has also been observed in the case of the wide harbor shown in

---

*Note: This kind of singularity can be observed in equation (2.42) for the amplification factor. If one value of β_n, say β_m, is very near to zero, let it be denoted by δ ($\delta \ll 1$); then,

$$\frac{m\pi}{2kb} = 1 + \delta \quad \text{and} \quad \beta_m = \delta \quad (\delta \ll 1)$$

also

$$\sinh \beta_m k\ell \cong \tanh \beta_m k\ell \cong \delta k\ell$$

The two infinite series S_1 and S_2 are then approximated with the m-th terms which include β_m, as δ approaches zero; thus

$$S_1 \cong 8\left(\frac{b}{\pi d}\right)^2 \frac{\left(\sin \frac{m\pi d}{2b} \cos \varepsilon m\pi\right)^2}{m^2 \delta k\ell}$$

$$S_2 \cong \frac{4b}{\pi d} \sin k\ell \; \frac{\sin \frac{m\pi d}{2b} \cos \varepsilon m\pi}{m \delta k\ell}$$

Since these terms become very large as δ approaches zero, the other terms of ψ_1, ψ_2, and cos $k\ell$ in equation (2.42) can be neglected compared to S_1 and S_2. Hence, the amplification factor at $kb = m\pi$ is obtained as the limiting value of $\mathbb{R}$ at $\delta \to 0$:

$$\lim_{\delta \to 0} \mathbb{R} = \lim_{\delta \to 0} \left| \frac{S_2}{S_1 \sin k\ell} \right| = \frac{\pi d}{2bm \left| \sin \frac{m\pi d}{2b} \cos \varepsilon m\pi \right|}$$

Although this is not the resonant amplification factor but one at $kb = m\pi$, this amplification factor increases very rapidly as ε approaches 1/2; hence, the singularity is inherent in equation (2.42).

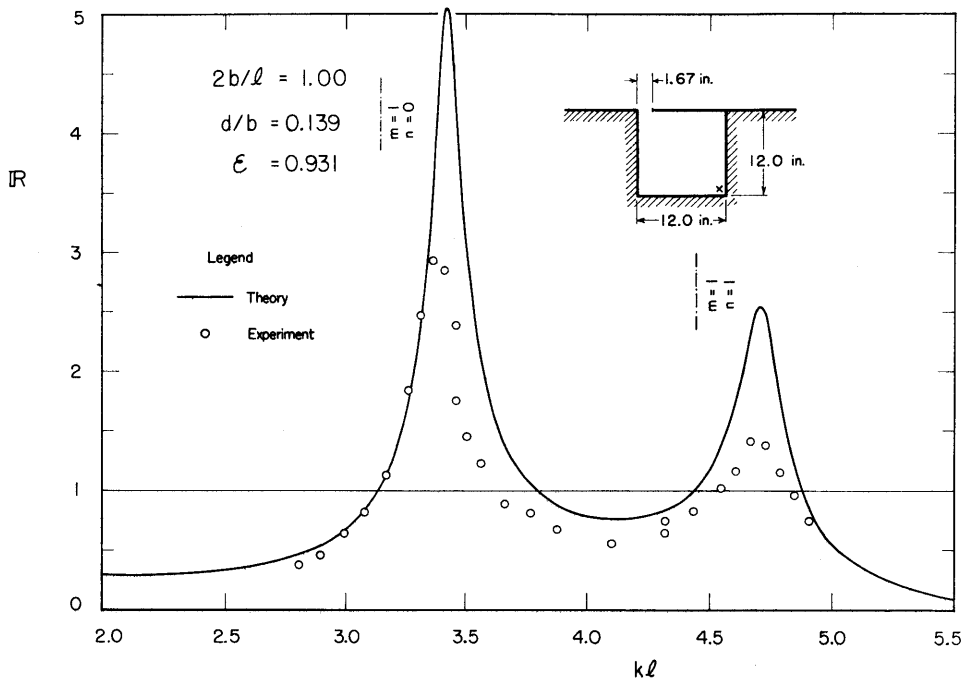

Fig. 26. Frequency Response of an Asymmetric Harbor

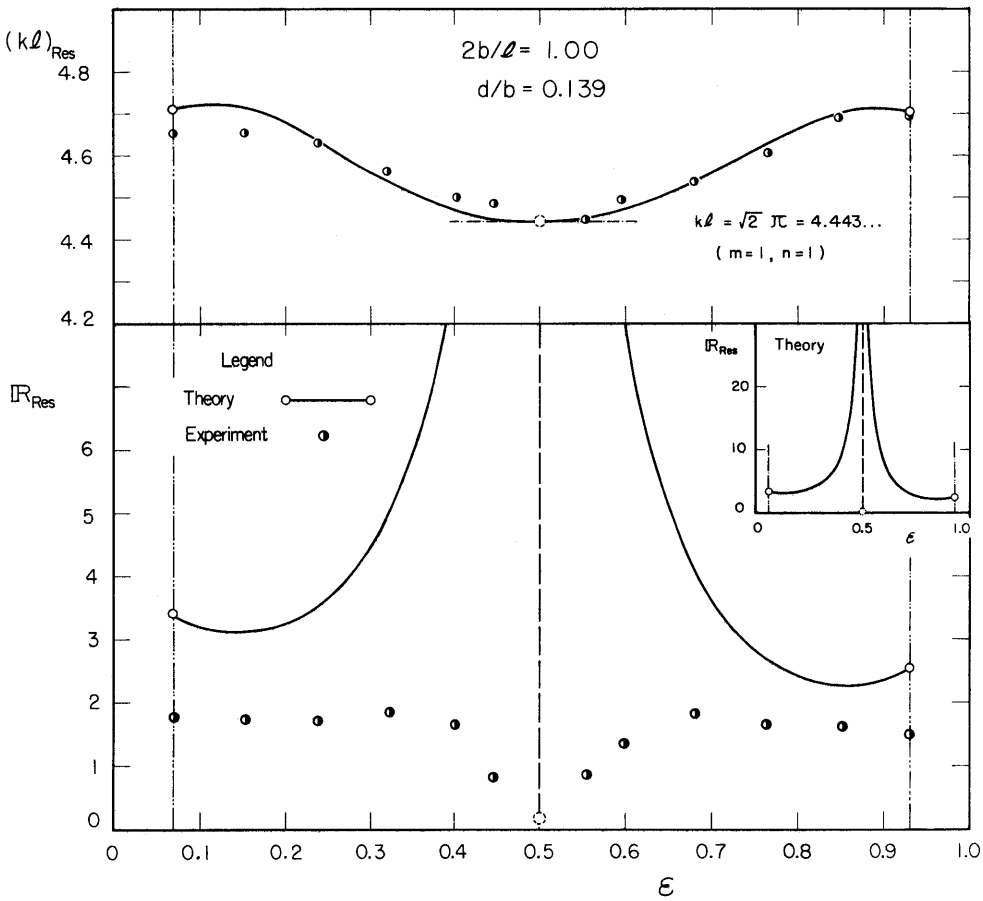

Fig. 27. Effect of Entrance Location on Transversal Resonant Oscillation of Odd Mode

Figure 25 at a resonant mode of m = 0 and n = 1. However, this kind of singularity may not be of true nature of the resonant oscillation, because the assumption of uniform flow through the entrance may be deficient for the transverse oscillation of odd mode when the entrance is near the center. Since the direction of the water surface movement in the harbor is reversed at the center line for the transverse oscillation of odd mode, the oscillating flow through the entrance may be non-uniform if the entrance is located across the center line. As seen in Figure 27, the experimental amplification factor at resonance shows a wide difference with the theoretical one. The experimental amplification factor is about one-half to two-thirds of the theoretical one when the entrance is near one side and shows a slight increase from 1.5 to 1.8 and from 1.7 to 1.9 as the entrance is shifted from one side toward the center. The difference between the theoretical and experimental amplification factors at this stage seems to be due to the energy dissipation around the entrance as in the previous tests of square and wide harbors. However, when the entrance is further moved near the center, the experimental resonant amplification factor decreases rather than increases as the theory predicts. Therefore, the validity of the assumption of uniform flow for the odd transverse mode needs to be examined further.

The relative harbor length at resonance varies slowly toward the resonant point of the enclosed basin as the entrance is moved toward the center. In the case shown in Figure 27, the limiting value of the resonant relative harbor length is $2\pi = 4.443$. The variation of resonant relative harbor length is well confirmed by the experiment; the difference between the theory and experiment is about 1 per cent for the largest one.

V. DISCUSSION OF HARBOR PARADOX

The harbor paradox, "a narrowing of the entrance leads not to a reduction in harbor surging, but to enhancement" as stated by Miles and Munk [1961], might be a grave problem for a design and construction of a harbor basin if the paradox really existed in actual harbors. Although the results of the present analysis also show increases of amplification factors at resonance with a narrowing of the entrance, several factors must be taken into account for the possibility of the harbor paradox.

5.1 Sharpness of Response Curve near Resonant Points

The first factor to be considered is the sharpness of response curve near resonant points. As noted in Figure 19, a frequency response curve near resonant points becomes sharper as well as higher as the entrance is narrowed down. The period range for the waves which can excite an oscillation of high amplitude becomes narrower. If the analogy of a single-degree-of-freedom oscillator can be applied to the oscillation in a harbor, the sharpness may be defined with a quantity Q as:

$$\frac{(k\ell)_{1/2}}{(k\ell)_{Res}} = 1 \pm \frac{1}{2Q} \qquad (5.1)$$

where: $(k\ell)_{1/2}$ = value of $k\ell$ at the half-power points where $R = \frac{1}{\sqrt{2}} R_{Res}$

$(k\ell)_{Res}$ = value of $k\ell$ at resonance

In the case of a single-degree-of-freedom oscillator, the quantity $1/Q$ is a linear measure of the damping and the quantity Q is identical to the amplification factor at resonance. However, this analogy is only applicable to the fundamental resonance mode of wave induced oscillations in a harbor.

Table 2 shows a comparison of the quantity Q obtained from the frequency response curve by equation (5.1) with the resonant amplification factor for a narrow harbor (aspect ratio of 0.2). The table also shows the quantity Q given by Miles and Munk [1961].

TABLE 2

Comparison of Q with R_{Res} $(2b/\ell = 0.2)$

	Fundamental Mode			Second Mode		
Opening ratio, d/b	0.01	0.1	1.0	0.01	0.1	1.0
R_{Res}	13.2	10.3	7.8	7.5	4.9	2.7
Q (equation (5.1))	11.2	8.4	5.7	38.3	17.7	6.0
Q (Miles and Munk)	11.5	8.4	5.8	39.7	15.3	6.2

For the fundamental mode of resonance, the quantity Q is about 80 per cent of the resonant amplification factor R_{Res}. But, for the second mode of resonance, the quantity Q is much larger and increases more rapidly than R_{Res} as the opening ratio d/b decreases. In other words, a harbor at the second mode of resonance does not respond as high as it is expected from the sharpness of response curve. This suggests a re-examination of the harbor paradox, since it is based on the presumption that the frequency response near resonance is well described with the quantity Q.

Another interesting point in Table 2 is an excellent agreement between two Q's, one measured from the frequency response curve with equation (5.1) and the other given by Miles and Munk [1961]. (The values for a fully open case are calculated according to equation (4.3).) This suggests that Miles and Munk may have calculated the quantity Q excellently, but not the amplification factor at resonance. They have also stated that the second mode is more highly amplified than the fundamental mode, based on their calculation of the quantity Q. Since the resonant amplification factor at the second mode is smaller than at the fundamental mode as seen in Table 2, the statement is incorrect.

5.2 Response to Waves with Continuous Power Spectrum

The second factor to be considered is the continuous power spectrum of incoming waves. Except the tidal motion, the waves which induce resonant oscillation in actual harbors are not waves of regular train with discrete periods as assumed in the analysis. The incoming waves are rather regarded as random waves with different periods and amplitudes. The characteristics of these waves are described with a power spectrum $P_1(\sigma)$; the energy in a frequency interval $\sigma - \frac{1}{2}d\sigma$ to $\sigma + \frac{1}{2}d\sigma$ is represented by $P_1(\sigma)\, d\sigma$; the mean wave amplitude is proportional to E where E is the integral of $P_1(\sigma)$ from $\sigma = 0$ to ∞.

When the waves with a continuous power spectrum induce resonant oscillations in a harbor, the induced oscillations also have a power spectrum $P_2(\sigma)$ which is given by

$$P_2(\sigma) = R^2(\sigma)\, P_1(\sigma) \tag{5.2}$$

The amplitude of the oscillations which may be observed visually is calculated by integrating the above power spectrum for some predominant frequency range and by taking its square root.

$$\bar{A}^2 = \int_{\sigma_1}^{\sigma_2} P_2(\sigma)\, d\sigma = \int_{\sigma_1}^{\sigma_2} R^2(\sigma) P_1(\sigma) d\sigma \tag{5.3}$$

where: $\bar{A}$ = root-mean-square amplitude of the oscillations in the harbor

As a measure to examine the response to actual waves, incident waves of constant power spectrum within a frequency range of ±10 per cent from a resonant frequency are considered here: i.e.,

$$P_1(\sigma) = \frac{a^2}{0.2\sigma_o} \qquad \text{for} \quad |\sigma/\sigma_o - 1| \leq 0.1$$

$$= 0 \qquad \text{for} \quad |\sigma/\sigma_o - 1| > 0.1 \qquad (5.4)$$

where: σ_o = resonant angular frequency

Substitution of equation (5.4) into equation (5.3) yields the root-mean-square response factor of $\overline{R}_P$ as:

$$\overline{R}_P^2 = \left(\frac{\overline{A}}{a}\right)^2 = \frac{1}{0.2\sigma_o} \int_{0.9\sigma_o}^{1.1\sigma_o} R^2(\sigma) d\sigma \qquad (5.5)$$

Since the angular frequency is proportional to the wave number for the shallow water waves, the above expression is rewritten as:

$$\overline{R}_P^2 = \frac{1}{0.2\ k_o \ell} \int_{0.9k_o\ell}^{1.1k_o\ell} R^2(k\ell)\ d(k\ell) \qquad (5.6)$$

where: k_o = resonant wave number

Although the power spectrum of actual incident waves may not be the same as that employed here, this kind of response factor is what actually determines the amplitude of resonant oscillations. To re-examine the problem of the harbor paradox, the root-mean-square response factor has been computed with equation (5.6) for three symmetrical harbors, each having three opening ratios. The results of computations, listed in Table 3, show only a slight increase of root-mean-square response factors for the second mode of resonance with a narrowing of the entrance.

TABLE 3

Root-Mean Square Response Factors of Symmetrical Harbors

Narrow Harbor ($2b/\ell = 0.2$)

	Fundamental Mode			Second Mode		
Opening ratio, d/b	0.01	0.1	1.0	0.01	0.1	1.0
$\mathbb{R}_{Res}$	13.2	10.3	7.8	7.5	4.9	2.7
$\overline{\mathbb{R}}_P$	9.4	8.1	6.6	3.3	2.9	2.3

Square Harbor ($2b/\ell = 1.0$)

	Fundamental Mode			Second Mode		
Opening ratio, d/b	0.01	0.1	1.0	0.01	0.1	1.0
$\mathbb{R}_{Res}$	8.2	5.2	2.4	6.2	3.3	1.2
$\overline{\mathbb{R}}_P$	6.6	4.7	2.2	1.7	1.6	1.0

Wide Harbor ($2b/\ell = 2.0$)

	Fundamental Mode			Second Mode		
Opening ratio, d/b	0.01	0.1	1.0	0.01	0.1	1.0
$\mathbb{R}_{Res}$	7.5	4.5	1.7	6.1	3.3	1.0
$\overline{\mathbb{R}}_P$	6.2	4.1	1.6	1.8	1.8	0.9

Hence, the narrowing of the entrance does not make the situation worse appreciably even if no energy dissipation takes place in harbors.

Although the root-mean-square response factor for the fundamental mode increases with almost the same rate as the resonant amplification factor as the opening ratio decreases, the oscillation is rather uniform without any longitudinal or transversal nodal lines. The water mass in a harbor basin moves up and down in unison and there is only minor horizontal movement. Hence, the resonant oscillations at the fundamental mode do not cause much troubles to moored ships. A possible hazard of oscillating

currents at the entrance is also restrained with energy dissipation due to friction and turbulence in the vicinity of the entrance, since the magnitudes of friction and turbulence increase with the increase of velocity at the entrance.

5.3 Scale Effect in Model Experiments

The analysis in previous sections has not taken into account the effect of energy dissipation in harbors. As discussed in Section 2.2 and Chapter IV, a small amount of energy dissipation can reduce the amplification factor near resonance appreciably. This reduction of amplification factor seems to also depend on the shaprness of the response curve; the sharper the response curve is, the more the amplification factor is reduced. Since the response curve becomes sharper as the entrance is narrowed down, the response curve becomes more sensitive to the presence of energy dissipation and may even show a decrease of resonant amplification factor. Even if the resonant amplification factor does not decrease but is merely slowed down in its rate of increase with a narrowing of the entrance, such a slowing down is enough to decrease the root-mean-square response factor except for the fundamental mode.

However, it should be noted that a scale model of long period oscillation has a large amount of energy dissipation compared to the prototype. If a harbor is surrounded with vertical walls, the energy dissipation will take place in two regions: the wake zone near the entrance and the boundary layer at the bottom. Although it is difficult to evaluate the intensity of turbulence in the wake zone, the frictional damping on the bottom may be estimated with equation (4.1). For the shallow water waves, equation (4.1) is simplified in terms of a transmission coefficient as:

$$1 - \mathbb{K}_T = \frac{kx}{4h}\sqrt{\frac{\nu T}{\pi}} \qquad (5.7)$$

For a model with a depth of 0.1 ft. and period of 5 sec., equation (5.7) gives the following attenuation rate for $kx = 3.2$ (second mode):

$$1 - (\mathbb{K}_T)_m = \frac{3.2}{4 \times 0.1}\sqrt{\frac{10^{-5} \times 5}{3.14}} = 0.032$$

Since the attenuation rate of a standing wave is approximately twice the above value, the total attenuation rate is 6.4 per cent which is a considerable amount of energy dissipation for resonant oscillation. If equation (5.7) is applied for a prototype harbor with a depth of 40 ft. and period of 100 sec. (length scale of 1/400), the attenuation rate is calculated as:

$$1 - (\mathbb{K}_T)_p = \frac{3.2}{4 \times 40}\sqrt{\frac{10^{-5} \times 100}{3.14}} = 0.00036$$

Although the boundary layer in the prototype is turbulent and has a larger rate of amplitude attenuation than the above value, it will be still far less than the attenuation rate in a model.

Hence, if a test is conducted on the effect of a narrowing of the harbor on a resonant amplification factor, a scale model may possibly show a marked decrease of resonant amplification factor because of large energy dissipation, even if the prototype harbor may show an increase. (Resonant periods will not be affected as discussed in Section 2.2.) In this sense, the results of model experiments concerning resonant amplification factor should be discussed with reservation.

5.4 Possibility of Harbor Paradox

Summing up the discussion of the harbor paradox, it may be concluded that it has little reality because:

i) the resonant amplification factor at the second mode does not increase as fast as the sharpness of the response curve increases,

ii) the response to waves with a continuous power spectrum increases only slightly with a narrowing of the entrance,

iii) the presence of energy dissipation will eventually decrease the root-mean-square response factor,

iv) the only possible case of the fundamental resonance mode does not produce a serious problem for moored ships.

However, emphasis must be placed on the importance of the energy dissipation mechanism. If there is no energy dissipation, a narrowing of the entrance does not reduce the root-mean-square amplitude of the resonant oscillations. The narrowing of the entrance can reduce the amplitude only when there exists some amount of energy dissipation. Although a sloping beach is said to reflect long period waves totally without breaking, it does dissipate some wave energy through frictional loss along the bottom. Permeable moles of multi-piles arranged at strategical locations are also considered to be effective to produce a good amount of energy dissipation. Engineers are advised to explore every feasible mechanism of energy dissipation in order to reduce the magnitude of resonant oscillation or to avoid its occurrence in harbors under their design.

VI. CONCLUSIONS

As shown in the preceding sections, this study has revealed several important characteristics of resonant oscillations in a rectangular harbor excited by incident waves, theoretically and experimentally. They are:

1. The present theory can predict the complete response curve of any rectangular harbor connected to the open-sea.

2. For a fully open harbor, only the fundamental and the second modes of resonance are important, but for a partially open harbor any resonant mode may be crucial for the excitation of "long period oscillation" in harbors.

3. A widening of a fully open harbor shifts the resonant periods of the harbor to the longer ones and decreases the amplification factors at resonance.

4. A narrowing of the harbor entrance results in the increase of the resonant amplification factors with a shift of the resonant periods toward those of an enclosed basin.

5. The harbor entrance is recommended to be located at the center, because it produces smaller amplification factors at resonance than at other locations.

6. The presence of energy dissipation inside the harbor causes large decreases in resonant amplification factors, but produces little change in the resonant periods or lengths.

7. In model studies, the reflection coefficient of wave filters and absorbers should be less than 0.2 for the simulation of the open-sea conditions in a wave basin. A consideration should also be taken on a proper basin size for the better simulation.

8. Although a narrowing of the harbor entrance increases the resonant amplification factor, the amplitude of actual oscillations in harbors will be decreased except for the fundamental mode because of increasing sharpness of response curve and presence of energy dissipation in actual harbors. Hence, the harbor paradox is most unlikely.

VII. RECOMMENDATIONS FOR FURTHER STUDY

The present study suggests the following for the subjects of the further study on the long period oscillations in harbors.

1. Analysis of Wave Induced Oscillations in a Harbor of Arbitrary Shape

   As mentioned in Section 1.2, the problem is to solve the Helmholtz equation (equation (1.3)) for given boundary conditions. The wave pattern function outside a harbor has been solved and given by equation (2.19). If the wave pattern function inside a harbor of given geometry is found by some methods, the entire wave motion is solved by matching outside and inside water surface elevations at the entrance. For a harbor of relatively simple planform, the inside wave pattern function may be obtained by a direct calculation or by the use of conformal mapping technique. In general, the inside wave pattern function will be obtained by rewriting equation (1.3) into a form of difference equation and by solving it numerically.

2. Effect of the Direction of Incident Waves on the Response of a Rectangular Harbor

   The present study has dealt only with incident waves normal to the coast line. Although Miles and Munk [1961] have shown that the response of a harbor is independent of the direction of incident waves as long as the entrance opening is very small compared to the wave length, experimental studies by Iribarren, et al., [1957] and Wilson [1960] have shown some effects of the directions of incident waves.

3. Effect of the Coast Line Arrangement on the Response of a Rectangular Harbor

   If the harbor in question is located in the depth of a bay or at the edge of a small island, the assumption of the aligned coast line extending to infinity does not hold; the slanted coast line will be a better approximation. The resonant period of a rectangular bay is known to be affected by the angle between the coast line and the axis of the bay (see Defant [1961]).

4. Analysis of a Rectangular Harbor with Moles

   The moles or jetties constructed in a harbor affect the response of the harbor in two ways. First, they change the resonant periods of the harbor. Second, they produce additional energy dissipation and reduce the resonant amplification factors. If the moles are long and the harbor is regarded as divided into compartments, the wave motion at the entrance to each compartment may be considered uniform. Then, an artificial boundary may be set up at each entrance and the wave motion may be solved in a similar manner as the analysis of

multi-harbors in Ippen and Raichlen [1962]. The energy dissipation caused by moles will be a subject of experimental study. Hensen [1959] has conducted an extensive study on a square harbor with various arrangements of moles.

5. Study of Energy Dissipation Mechanisms in Harbors and their Effect on Resonant Oscillations

To increase the magnitude of energy dissipation in a harbor is an important task assigned to harbor engineers. Constructions of impermeable moles, erections of multi-pile piers, provision of sloping beach, and the division of the harbor into several compartments are some examples of possible measures for the increase of energy dissipation. Since the energy dissipation is due to the viscosity of water and cannot be combined with the velocity potential, the effect of energy dissipation on resonant oscillation will be best studied experimentally. In the experiment, however, the problem of scale effect discussed in Section 5.3 should be paid a due regard.

VIII. REFERENCES

Abecasis, F. M., Castanho, J. R., and Neves, A. B. [1957]: XIXth International Navigation Congress, Section II, Communication I, London 1957, pp. 177 - 204.

Barrillon [1938]: "Mouvement de Seiche dans une Baie," Revue Générale de l'Hydraulique, Janvier - Fevrier.

Biesel, F. [1954]: "The Similitude of Scale Models for the Study of Seiche in Harbors," Proceedings of the Fifth Conference on Coastal Engineering, Grenoble, pp. 95 - 118.

Defant, A. [1961]: "Physical Oceanography," Pergamon Press, New York, Vol. II.

Hensen, W. [1959]: "Effects of Long Period Waves in Harbors," Hannoversche Versuchsanstalt für Grundbau und Wasserbau, Franzius Institut der Technischen Hochschule, June.

Honda, K., Terada, T., and Ishitani, D. [1908]: "On the Secondary Undulations of Oceanic Tides," Philosophical Magazine, Vol. 15, pp. 88 - 126.

Howard, L. N. [1959]: "Note on Resonant Oscillations in Harbors," Unpublished Paper, Massachusetts Institute of Technology, Hydrodynamics Laboratory.

Hudson, R. Y. [1947]: "Model Study of Wave and Surge Action, Naval Operating Base, Terminal Island, San Pedro, California," Tech. Memo. No. 2-237, Waterways Experiment Station, Corps of Engineers, U. S. Army, September.

Hunt, J. N. [1952]: "Viscous Damping of Waves over an Inclined Bed in a Channel of Finite Width," La Houile Blanche, Vol. 7, No. 6, pp. 836-842.

Ippen, A. T. and Raichlen, F. [1962]: "Wave Induced Oscillations in Harbors: the Problem of Coupling of Highly Reflective Basins," Massachusetts Institute of Technology, Hydrodynamics Laboratory, Report No. 49.

Ippen, A. T., Raichlen, F., and Sullivan, R. K., Jr. [1962]: "Wave Induced Oscillations in Harbors: Effect of Energy Dissipators in Coupled Basin System," Massachusetts Institute of Technology, Hydrodynamics Laboratory, Report No.52.

Ippen, A. T. and Goda, Y. [1963]: "Study of Wave Energy Dissipators Composed of Wire Mesh Screens," Massachusetts Institute of Technology, Hydrodynamics Laboratory, Technical Note (under preparation).

Iribarren Cavanilles, R., Nogales Olano, C., and Fernandez Fernandez, P. [1957]: "Backlash or Long Period Waves in Ports - Resonance Experiments Using Scale Models," Bulletin of International Navigational Congress, 1957 - Vol. II, No. 46, pp. 83 - 94.

Joosting, W. C. Q. [1957]: XIXth International Navigation Congress, Section II, Communication I, London 1957, pp. 205 - 227.

Knapp, R. T. and Vanoni, V. A. [1945]: "Wave and Surge Study for the Naval Operating Base, Terminal Island, California," Report of Hydraulic Structure Laboratory, California Institute of Technology, January.

Knapp, R. T. [1949]: "Model Studies of Apra Harbor, Guam, M. I.," Hydrodynamics Laboratory, California Institute of Technology, Report No. N-63, June.

Kravtchenko, J and McNown, J. S. [1955]: "Seiche in Rectangular Ports," Quarterly of Applied Mathematics, Vol. XIII, pp. 19 - 26.

Lamb, H. [1932]: "Hydrodynamics (6th edition)," Dover, New York

Larras, M. [1957]: XIXth International Navigation Congress, Section II, Communication I, London 1957, pp. 63 - 74.

LeMéhauté, B. [1954]: "Two-Dimensional Seiche in a Basin Subject to Incident Waves," Proceedings of the Fifth Conference on Coastal Engineering, Grenoble, pp. 119 - 149.

LeMéhauté, B. [1961]: "Theory of Wave Agitation in a Harbor," ASCE Journal of Hydraulics Division No. 2765, March.

McNown, J. S. [1952]: "Waves and Seiche in Idealized Ports," Gravity Waves Symposium, National Bureau of Standards, Circular 521.

Miles, J. and Munk, W. [1961]: "Harbor Paradox," ASCE Journal of Waterways and Harbors Division No. 2888. August.

Moriguchi, S., Udagawa, K., and Hitotsumatsu, S. [1956]: "Table of Mathematical Formulae, I," Iwanami, Tokyo, Japan.

Wilson, B. W. [1957]: XIXth International Navigation Congress, Section II, Communication I, London 1957, pp. 13 - 61.

Wilson, B. W. [1960]: "Model Study of Surge Action in a Port," The A. and M. College of Texas, Department of Oceanography and Meteorology, Tech. Report No. 24-(57), December.

Wilson, B. W. [1962]: ASCE Journal of Waterways and Harbors Division, Discussion to Paper No. 2888, Vol. 88, W.W. 2, pp. 185 - 194.

APPENDIX

A. Evaluations of Radiation Functions ψ_1 and ψ_2

The analytical evaluation of the radiation functions ψ_1 and ψ_2 for small values of kd was first accomplished by Howard [1959]. The first radiation function ψ_1 is defined in equation (2.34.1) as:

$$\psi_1 = \psi_1(kd) = \frac{2}{\pi} kd \int_0^{kd} \frac{\sin^2\alpha}{\alpha^2 \sqrt{(kd)^2 - \alpha^2}} \, d\alpha \qquad (A.1)$$

The term of $\sin^2\alpha/\alpha^2$ can be expanded into a Taylor series as:

$$\frac{1}{\alpha^2} \sin^2\alpha = \frac{1}{2\alpha^2} (1 - \cos 2\alpha)$$

$$= \frac{1}{2\alpha^2} \left[1 - \sum_{n=0}^{\infty} (-1)^n \frac{(2\alpha)^{2n}}{(2n)!} \right]$$

$$= 2 \sum_{m=0}^{\infty} (-1)^m \frac{(2\alpha)^{2m}}{(2m+2)!}$$

With a change of variable from α to θ where $\alpha = kd \sin\theta$, equation (A.1) is rewritten as:

$$\psi_1 = \frac{4}{\pi} kd \int_0^{\pi/2} \left[\sum_{m=0}^{\infty} (-1)^m \frac{(2kd)^{2m}}{(2m+2)!} (\sin\theta)^{2m} \right] d\theta$$

Since the above series converges uniformly, the integration can be applied to each term:

$$\psi_1 = \frac{4}{\pi} \text{ kd } \sum_{m=0}^{\infty} (-1)^m \frac{(2kd)^{2m}}{(2m+2)!} \int_0^{\pi/2} (\sin\theta)^{2m} d\theta$$

$$= \frac{4}{\pi} kd \frac{\pi}{2} \left[\frac{1}{2} + \sum_{m=1}^{\infty} (-1)^m \frac{(2kd)^{2m}}{(2m+2)!} \frac{1 \cdot 3 \cdots (2m-3)(2m-1)}{2 \cdot 4 \cdots (2m-2)(2m)} \right]^*$$

hence,

$$\psi_1 = kd \left[1 + 2 \sum_{m=1}^{\infty} (-1)^m \frac{(2kd)^{2m}}{(2m+2)!} \frac{1 \cdot 3 \cdots (2m-1)}{2 \cdot 4 \cdots (2m)} \right] \qquad (A.2)$$

For a small value of kd, ψ_1 is approximated with the first term only:

$$\psi_1 = kd + O(k^3 d^3)$$

which has been presented as equation (2.49.1).

The computer program, however, includes up to the seventh term (m = 6) of equation A-2 to cover a wide range of kd. The function ψ_1 is programmed as a subprogram, FUNCTION PSI1 (A), as shown in Figure A-1. The argument A stands for kd.

The second radiation function ψ_2 is defined in equation (2.34.2) as:

$$\psi_2 = \psi_2 (kd) = \frac{2}{\pi} kd \int_{kd}^{\infty} \frac{\sin^2\alpha}{\alpha^2 \sqrt{\alpha^2 - (kd)^2}} \, d\alpha \qquad (A.3)$$

This integral cannot be transformed into a series because of the infinity at its upper limit. However, the following transformations are possible for a small value of kd.

---

*See Moriguchi, et al., [1956], pp. 242.

FIG. A-1. FORTRAN PROGRAMS FOR RADIATION FUNCTIONS ψ_1 AND ψ_2

```
*       LIST
*       LABEL

        FUNCTION PSI1(A)

     1  AA = A*A
     2  PSI1 = A*(1. - AA/6. + AA**2/60. - AA**3/1008.)
     3  IF(A-1.) 90,90,4
     4  PSI1 = PSI1 + A*(AA**4/25920. - AA**5/950400. + AA**6/47174400.)
    90  RETURN
        END


*       LIST
*       LABEL

        FUNCTION PSI2(A)

     1  AA = A*A
     2  SUM = 0.04472*SINF(A)**2/AA
     3  X = 1.001*A
   104  IF(A-0.03) 5,107,107
     5  H = 0.004*A
     6  GO TO 14
   107  IF(A-0.1) 8,110,110
     8  H = 0.002*A
     9  GO TO 14
   110  IF(A-0.3) 11,13,13
    11  H = 0.001*A
    12  GO TO 14
    13  H = 0.0005*A
    14  SUM = SUM + 0.5*H*SINF(X)**2/(X**2*SQRTF(X**2-AA))
    15  DO 118 I=1,1000
    16  X = X+H
    17  SUM = SUM + H*SINF(X)**2/(X**2*SQRTF(X**2-AA))
   118  CONTINUE
   119  IF(X-3.) 20,20,22
    20  H = (3.14159-X)*0.001
    21  GO TO 15
    22  H = 0.06283
    23  DO 126 I=1,100
    24  X = X+H
    25  SUM = SUM + H*SINF(X)**2/(X**2*SQRTF(X**2-AA))
   126  CONTINUE
    27  SUM = SUM + 0.25/X**2
    28  PSI2 = 2.*A*SUM/3.14159
        RETURN
        END
```

Fig. A-1. FORTRAN Program for Computation of Frequency Response of Asymmetric Harbor

Let the integral be denoted by I. Then, it is rewritten as:

$$I = \int_{kd}^{\infty} \frac{\sin^2\alpha}{\alpha^2\sqrt{\alpha^2 - (kd)^2}}\, d\alpha$$

$$= \int_{kd}^{\infty} \frac{\sin^2\alpha}{\alpha^3}\, d\alpha + \int_{kd}^{\infty} \left(\frac{1}{\sqrt{\alpha^2 - (kd)^2}} - \frac{1}{\alpha}\right) \frac{\sin^2\alpha}{\alpha^2}\, d\alpha$$

The first integration is carried out as:

$$\int_{kd}^{\infty} \frac{\sin^2\alpha}{\alpha^3}\, d\alpha = \left[-\frac{1}{2}\frac{\sin^2\alpha}{\alpha^2}\right]_{kd}^{\infty} + \frac{1}{2}\int_{kd}^{\infty} \frac{\sin 2\alpha}{\alpha^2}\, d\alpha$$

$$= \frac{1}{2}\left(\frac{\sin kd}{kd}\right)^2 + \frac{1}{2}\left[-\frac{\sin 2\alpha}{\alpha}\right]_{kd}^{\infty} + \int_{kd}^{\infty} \frac{\cos 2\alpha}{\alpha}\, d\alpha$$

$$= \frac{1}{2} + 1 + O(k^2d^2) + \int_{2kd}^{\infty} \frac{\cos t}{t}\, dt$$

The last term is a cosine integral, $-C_i(2kd)$, which is evaluated as:

$$-C_i(2kd) = \int_{2kd}^{\infty} \frac{\cos t}{t}\, dt$$

$$= -\gamma - \ln 2kd + \int_{0}^{2kd} \frac{1 - \cos t}{t}\, dt$$

$$= -\gamma - \ln 2kd + O(k^2d^2)$$

where: γ = Euler's constant = 0.5772....

In order to evaluate the second integral in the expression for I, the sine function is expanded into a Taylor's series with a remainder:

$$\sin^2 \alpha = \alpha^2 - \frac{2}{3} \alpha^3 \sin 2\theta\alpha \qquad 0 < \theta < 1$$

The second integral is then evaluated with this expression as:

$$\int_{kd}^{\infty} \left[\frac{1}{\sqrt{\alpha^2 - (kd)^2}} - \frac{1}{\alpha}\right] \frac{\sin^2 \alpha}{\alpha^2} \, d\alpha$$

$$= \int_{kd}^{\infty} \left[\frac{1}{\sqrt{\alpha^2 - (kd)^2}} - \frac{1}{\alpha}\right] d\alpha - \frac{2}{3} \int_{kd}^{\infty} \left[\frac{\alpha}{\sqrt{\alpha^2 - (kd)^2}} - 1\right] \sin 2\theta\alpha \, d\alpha$$

The first term is simply

$$\left[\ln \frac{\alpha + \sqrt{\alpha^2 - (kd)^2}}{\alpha}\right]_{kd}^{\infty} = \ln 2$$

The second term is estimated as:

$$\left| \frac{2}{3} \int_{kd}^{\infty} \left[\frac{\alpha}{\sqrt{\alpha^2 - (kd)^2}} - 1\right] \sin 2\theta\alpha \, d\alpha \right|$$

$$\leq \frac{2}{3} \int_{kd}^{\infty} \left[\frac{\alpha}{\sqrt{\alpha^2 - (kd)^2}} - 1\right] d\alpha$$

$$= \frac{2}{3} \left[\sqrt{\alpha^2 - (kd)^2} - \alpha\right]_{kd}^{\infty} = \frac{2}{3} kd \ll 1$$

Adding all these terms, the integral I is finally expressed as:

$$I = [\frac{3}{2} + O(k^2d^2)] + [-\gamma - \ln (2kd) + O (k^2d^2)]$$

$$+ [\ln 2 + O(kd)]$$

$$= \frac{3}{2} - \gamma - \ln kd + O(kd)$$

Hence,

$$\psi_2 = \frac{2}{\pi} kd(\frac{3}{2} - \gamma - \ln kd) + O (k^2d^2) \qquad (A.4)$$

In the numerical evaluation, the integral was carried out for the five regions of α, shown in Figure A-2. The region I was provided in order to avoid the divergence of the integrand. The integral was approximated with:

$$\int_{kd}^{kd + h} \frac{\sin^2 \alpha}{\alpha^2\sqrt{\alpha^2 - (kd)^2}} d\alpha = \int_o^h \frac{\sin^2(kd + t)}{(kd + t)^2 \sqrt{t(t + 2kd)}} dt$$

$$\simeq \frac{\sin^2 kd}{(kd)^2\sqrt{2kd}} \int_o^h \frac{1}{\sqrt{t}} dt = \frac{2 \sin^2 kd}{(kd)^2} \sqrt{\frac{h}{2kd}}$$

$$= 0.04472 \frac{\sin^2 kd}{(kd)^2} \quad \text{for } h = 0.001 kd$$

The integral in the region V was also approximated with:

$$\int_{3\pi}^{\infty} \frac{\sin^2 \alpha}{\alpha^2\sqrt{\alpha^2 - (kd)^2}} d\alpha = \frac{1}{2} \int_{3\pi}^{\infty} \frac{1 - \cos 2d}{\alpha^2\sqrt{\alpha^2 - (kd)^2}} d\alpha$$

$$\simeq \frac{1}{2} \int_{3\pi}^{\infty} \frac{1}{\alpha^2\sqrt{\alpha^2 - (kd)^2}} d\alpha \simeq \frac{1}{4} (\frac{1}{3\pi})^2$$

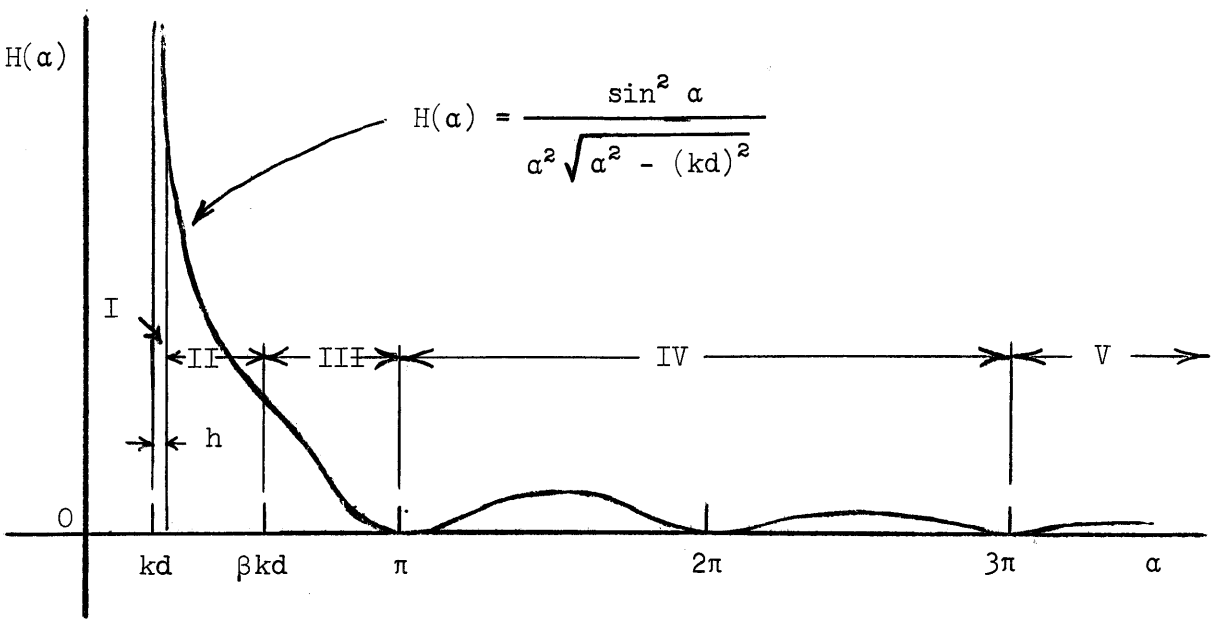

Note: h = 0.001 kd

$\beta = 4$ for $kd < 0.03$

$= 2$ for $0.03 \leq kd < 0.1$

$= 1$ for $0.1 \leq kd < 0.3$

$= 0.5$ for $0.3 \leq kd < 2\pi/3$

Figure A-2. Definition Sketch of Integration Range for ψ_2

Although this was a crude approximation, the resultant error was negligible because the integral for this region itself was very small compared to those for other regions. As for the regions II, III, and IV, simple summation methods were employed with divisions of 1,000, 1,000, and 100 respectively. These numbers of divisions and the range of the region II were so chosen after several trials to get maximum efficiency of computation with adequate accuracy. The program for this numerical integration is shown in Figure A-1 as FUNCTION PSI2 (A).

This program was rather slow, however. It took the IBM 7090 computer 1.58 sec. to compute one value of ψ_2 (kd). Hence, the computation of ψ_2 with this program was conducted for only 174 values of kd from 0.01 through 1.74 with increment of 0.01. With these data, a new program for ψ_2 was constructed, based on the method of linear interpolation. This new program was then used for the computation of the amplification factor.

B. FORTRAN Program for Computation of Amplification Factor

In the course of numerical analysis, several computer programs have been constructed and utilized: programs for frequency responses of fully open harbors with and without energy dissipation, frequency responses of symmetrical and asymmetric harbors with partial openings, responses of symmetrical harbors at arbitrary point, root-mean-square response factor of symmetrical harbors, etc. However, they had common frameworks because they were some simplified cases of the computation of general amplification factor defined in equation (2.41). For this reason, the program for the frequency response of asymmetric harbors is illustrated in Figure B-1. The program shown is complete with the DATA for the computation of frequency response curves presented in Figure 25, except FUNCTIONs PSI1 (A) and PSI2 (A) which are shown in Figure A-1. As it might be expected from the form of equation (2.41), the use of FUNCTION subprograms was a great help for the numerical analysis.

Table B-1 is a conversion table of major FORTRAN names employed to the symbols appearing in the text. The table will be a guide for the reader to read the program. Since the program is constructed just in the same manner as the equations are written, no explanation on programming logics will be necessary. As for the truncation of the series S_1 and S_2, the upper limits of summations are set at $n = 10(q + 1)$ and $2(q + 1)$ respectively, where q is the largest integer not exceeding $(2kb)/\pi$. The maximum error of summation due to the truncation is estimated as 1 per cent for both series.

TABLE B-1

Conversion Table of Major FORTRAN Names to Symbols in Text

FORTRAN Name	Text Symbol	Note
ABETAZ	β_n' (equation (2.28.1))	FUNCTION
AKD	kd	
ALPHA	d/b	opening ratio
AMPFAC	$\mathbb{R}$ (equation (2.42))	
BETAZ	β_n (equation (2.28))	FUNCTION
DELKL	Δ ($k\ell$)	increment of $k\ell$
EPSLON	ε	
HARKB	kb	
HARKL	$k\ell$	
N	q ($\leq 2kb/\pi$)	integer
P	n (in equations (2.37) and (2.43))	
PALPHA	$2\pi d/b$	
PSI1	ψ_1(equation (A.2))	FUNCTION
PSI2	ψ_2(equation (A.3))	FUNCTION
SINH	sinh	FUNCTION
SUMAZ	S_1 (equation (2.37))	FUNCTION
SUMBZ	S_2(equation (2.43))	FUNCTION
WIDNES	$2b/\ell$	Aspect ratio

```
*     LIST
*     LABEL

C  ASYM

    1 READ 1105, WIDNES, ALPHA, EPSLON, HARKL, DELKL, N
    2 IF(WIDNES) 900,900,5
    5 PRINT 2002, WIDNES, ALPHA, EPSLON
    6 PRINT 2003
    7 PALPHA = 6.2831853*ALPHA
  108 DO 120 I = 1,N
    9 HARKB = HARKL*WIDNES/2.
   10 AKD = ALPHA*HARKB
   11 SA = SUMAZ(EPSLON, PALPHA, HARKB, HARKL)
   12 SB = SUMBZ(EPSLON, PALPHA, HARKB, HARKL)
   13 PA = PSI2(AKD)/ALPHA
   14 PB = PSI1(AKD)/ALPHA
   15 SPA = SA + PA
   16 PAB = (SPA**2 + PB**2)/2.
   17 AMPFAC = (1.-SB)/SQRTF((0.5 + PAB) + (0.5 - PAB)*COSF(2.*HARKL)
     1                                   - SPA*SINF(2.*HARKL))
   18 PRINT 1005,HARKL, HARKB, SA, SB, AMPFAC
   19 HARKL = HARKL + DELKL
  120 CONTINUE
   22 GO TO 1
  900 CALL EXIT
 1005 FORMAT(5F20.5)
 1105 FORMAT(5F10.5, I10)
 2002 FORMAT(76H1  RESONANCE SPECTRUM OF ASYMMETRIC HARBOR WITH A PARTIA
     1L OPENING.    2B/L = F8.5, 10H     D/B = F8.5, 8H     E =F8.5////)
 2003 FORMAT(104H          REL. LENGTH(KL)      REL. WIDTH(KB)          SU
     1M.1               SUM.2              AMP. FACTOR(R) ///)
      END


*     LIST
*     LABEL

      FUNCTION BETAZ(P,HARKB)

      BETAZ = SQRTF((P*1.570796/HARKB)**2 - 1.)
      RETURN
      END


*     LIST
*     LABEL

      FUNCTION ABETAZ(P,HARKB)

      ABETAZ = SQRTF(1. - (P*1.570796/HARKB)**2)
      RETURN
      END



*     LIST
*     LABEL

      FUNCTION SINH(X)

    1 IF(X - 70.)  2,2,4
    2 SINH = 0.5*(EXPF(X) - EXPF(-X))
    3 GO TO 90
    4 SINH = 1.0E+30
   90 RETURN
      END
```

```
*     LIST
*     LABEL

      FUNCTION SUMAZ(EPSLON, PALPHA, HARKB, HARKL)

    1 N = XINTF(HARKB/1.570796)
    2 P = 1.
    3 S = 0.
    4 IF(N) 112,112,105
  105 DO 111 I=1,N
    6 ABT = ABETAZ(P,HARKB)
    7 IF(ABT) 8,8,9
    8 ABT = 1.0E-18
    9 S = S - ( SINF(P*PALPHA/4.)*COSF(EPSLON*P*3.1415927))**2
     1        /(P**2*ABT*TANF(ABT*HARKL))
   10 P = P + 1.
  111 CONTINUE
  112 NP = N + 1
   13 NNP = 10*(N+1)
  114 DO 118 I=NP,NNP
   15 BT = BETAZ(P,HARKB)
   16 S = S + (SINF(P*PALPHA/4.)*COSF(EPSLON*P*3.1415927))**2
     1        /(P**2*BT*TANHF(BT*HARKL))
   17 P = P + 1.
  118 CONTINUE
  200 SUMAZ = 32.*S/PALPHA**2
      RETURN
      END


*     LIST
*     LABEL

      FUNCTION SUMBZ(EPSLON, PALPHA, HARKB, HARKL)

    1 N = XINTF(HARKB/1.570796)
    2 P = 1.
    3 S = 0.
    4 IF(N) 112,112,105
  105 DO 111 I=1,N
    6 ABT = ABETAZ(P,HARKB)
    7 IF(ABT) 8,8,9
    8 ABT = 1.0E-18
    9 S = S - SINF(P*PALPHA/4.)*COSF(EPSLON*P*3.1415927)
     1        /(P*ABT*SINF(ABT*HARKL))
   10 P = P + 1.
  111 CONTINUE
  112 NP = N + 1
   13 NNP = 2*N + 4
  114 DO 118 I=NP,NNP
   15 BT = BETAZ(P,HARKB)
   16 S = S + SINF(P*PALPHA/4.)*COSF(EPSLON*P*3.1415927)
     1        /(P*BT*SINH(BT*HARKL))
   17 P = P + 1.
  118 CONTINUE
  200 SUMBZ = 8./PALPHA*S*SINF(HARKL)
      RETURN
      END


*     DATA

1.0       0.1       0.5       0.05      0.05            126
1.0       0.1       0.75      0.05      0.05            126
1.0       0.1       0.95      0.05      0.05            126
2.0       0.1       0.5       0.05      0.05            126
2.0       0.1       0.75      0.05      0.05            126
2.0       0.1       0.95      0.05      0.05            126
0.        0.        0.        0.        0.               0
```

Figure B-1

FORTRAN Program for Computation of Frequency Response of Asymmetric Harbor